Ministry of Higher Education and Scientific Research

Hassiba Benbouali, University of Chlef

Faculty of Civil Engineering and Architecture

Department of Civil Engineering

THESIS

Submitted to obtain the diploma of

DOCTORATE 3RD CYCLE LMD

Speciality: **Civil Engineering**
Option: **Structure**

By

OUISSAM YESSAD

Topic:

Study of the Behaviour of Steel Angle Tension Connections in Fire

Defended on 16 / 04 / 2026, in front of the jury composed of:

HARICHANE Zamila	Professor	UHBC Chlef	President
BOURAHLA Nouredine	Professor	ENP Algiers	Examiner
ABIDELAH Anis	Professor	USTO-MB	Examiner
GHRICI Mohamed	Professor	UHBC Chlef	Examiner
KADA Abdelhak	Professor	UHBC Chlef	Supervisor
LAMRI Belkacem	Professor	UHBC Chlef	Co-Supervisor

I would like to honor the memory of Prof. Lamri, who supervised this work with dedication and kindness. He passed away before the defense of this thesis. I remain deeply grateful for his guidance.

On a more personal level, I want to take a moment to honour the memory of my lost father and my sister. Their presence in my life shaped who I am today, and their love and support remain with me in spirit. I devoted this work to them, as a reflection of the strength and values they instilled in me. I miss them deeply, and their legacy continues to inspire me every day.

ACKNOWLEDGMENT

بسم الله الرحمان الرحيم

First of all, I wish to express my deepest gratitude to Almighty Allah for granting me the strength, health, and time to complete this research. Without this divine assistance, reaching this milestone would not have been possible.

I wish to express my deepest appreciation to my supervisors, Prof. Abdelhak KADA & Prof. LAMRI Belkacem (رحمه الله), for their constant support, expert guidance, and thoughtful advice throughout my PhD journey. Their mentorship, patience, and encouragement have been a source of strength and inspiration at every stage of this work. I am grateful for their patience and understanding as I navigated my way through the research world. Special thanks to Prof. Khalifa AL-JABRI, Prof. Mohummed Bilel Waris and Prof Franštik WALD for not only welcoming me as a visitor researcher at Sultan Qaboos University & the Czech Technical University. but also, for constantly pushing me to achieve more during our endless discussions and spirited debates. I am truly indebted to them for their encouragement and dedication, especially during the final stages of manuscript writing.

I am deeply grateful to the members of my PhD committee namely Prof. Zamila HARICHANE, Prof. Nouredine BOURAHLA, Prof. Anis ABIDELAH, and Prof. Mohamed GHRICI, whose valuable insights, thoughtful critiques, and unwavering commitment have significantly enriched the quality of this research. I sincerely appreciate the time, effort, and expertise they have so generously devoted to reviewing my work and contributing to its academic rigor and integrity.

I would also like to express my sincere gratitude to the Ministry of Higher Education and Scientific Research (MESRS) of Algeria for their invaluable and generous support, which enabled me to pursue and complete my PhD studies. Their commitment to advancing academic research and higher education has played a crucial role in supporting my academic journey and professional development.

DEDICATIONS

My primary dedication for this thesis is to myself.

I am deeply indebted to my mother, my sisters, and my brother. You are my greatest inspiration. Your tremendous support and encouragement are the foundation of my success. I would not have been able to achieve my success today without your leadership and belief in me. I dedicate this work to you because it means so much to me. Thank you for supporting me on this journey. I love you.

To my good friends, I would like to extend my sincere appreciation. In times of need, your friendship has consistently shone brightly, providing warmth and comfort. I am very grateful to have such wonderful friends as you, and you will always have a special spot in my heart. I am immensely grateful to each of you for the sheer amount of comfort and happiness you bring into my life.

I would especially like to thank my dear friends Aicha from India, Farzana from Brunei, Amira and Maouza from Oman. During my brief internship in Oman, I had an amazing time working with you. We had a lot of amazing adventures and formed deep friendships. Along with pursuing scientific interests, we engaged in rich cultural discussions that deepened my appreciation for and comprehension of our varied backgrounds. I'm thankful that we were able to laugh together and make beautiful memories.

My special gratitude goes to all my friends in Algeria, France, and the Czech Republic, I sincerely thank you for your unwavering support and friendship throughout my journey. Thank you for being such wonderful friends.

This entire work is dedicated to my supervisors, Prof. Abdelhak KADA, Prof. Belkacem LAMRI(رحمه الله), Prof. Khalifa AL-JABRI, Prof František WALD, and Prof. Abdelhamid BOUCHAIR, for their encouragement, wisdom, and guidance, which have been invaluable. I deeply appreciate your helpful advice, comments, and suggestions. Thank you for your time and direction.

To every one of you, I want to express my gratitude for making this journey incredibly unforgettable and distinctive. I sincerely appreciate your contribution to this journey.

ABSTRACT

Steel braced frames are considered one of the most effective strategies for ensuring structural resilience in earthquake zones such us Chlef (Algeria). However, structural safety under fire conditions remains a critical concern in civil engineering, particularly for steel structures, whose mechanical properties deteriorate significantly at elevated temperatures. This doctoral research focuses on the behaviour of bolted angle steel assemblies commonly used in braced steel frame systems under high temperature conditions.

The primary objective of this study is to investigate the mechanical response and failure mechanisms of these connections through advanced numerical modelling, supported by standard design approaches under current structural codes. To achieve this, detailed finite element models were developed using ANSYS APDL (Ansys Parametric Design Language), which offers robust capabilities for nonlinear, temperature-dependent simulations. The FE models account for geometric nonlinearity, contact interactions, and temperature-sensitive material degradation, enabling accurate prediction of connection behaviour under fire loading conditions.

A theoretical component-based model is developed to represent the mechanical behaviour of bolted connections in a more physically interpretable way, accounting for temperature-dependent material degradation, geometry, and contact behaviour. The model decomposes the connection into individual elements such as bolts, angle legs, and connected plates, each represented by spring-like components with stiffness and strength calibrated through numerical simulations.

The proposed model is validated through a comparative study against results obtained from the Component-Based Finite Element Method (CBFEM), which has recently gained popularity in the structural fire engineering community for its accuracy and balance between complexity and usability. The comparison demonstrates that the theoretical model provides reliable predictions of connection behaviour under elevated temperatures, capturing essential features such as stiffness reduction, load redistribution, and failure mechanisms.

This research contributes to a more accurate understanding of bolted connection behaviour in fire conditions. It proposes a simplified modelling strategy that could be implemented in design practice. It lays the groundwork for safer and more efficient design of braced steel structures subjected to fire. It opens up new research directions for experimental validation and extension

to other types of connections and boundary conditions and above all it provides substantial data for future analysis.

Keywords: Angle connections, Finite element analysis, Tensile force, Component-based model, Component-based Finite Element Model (CBFEM), Elevated temperature.

RESUME

Les palées de stabilité en acier sont considérées comme l'une des stratégies les plus efficaces pour assurer la résilience des structures dans les zones sismiques telles que Chlef (Algérie). Cependant, la sécurité structurelle dans des conditions d'incendie reste une préoccupation essentielle dans le domaine du génie civil, en particulier pour les structures en acier, dont les propriétés mécaniques se détériorent de manière significative à des températures élevées. Cette recherche doctorale se concentre sur le comportement des assemblages d'acier d'angle boulonnés couramment utilisés dans les systèmes de charpente métallique contreventée dans des conditions de température élevée.

L'objectif principal de cette étude est d'étudier la réponse mécanique et les mécanismes de déformation de ces connexions par une modélisation numérique avancée, soutenue par des approches de conception standard dans le cadre des codes structurels actuels. Pour ce faire, des modèles détaillés d'éléments finis ont été développés à l'aide d'ANSYS APDL (Ansys Parametric Design Language), qui offre des capacités robustes pour les simulations non linéaires et dépendantes de la température. Les modèles d'éléments finis tiennent compte de la non-linéarité géométrique, des interactions de contact et de la dégradation des matériaux sensible à la température, ce qui permet de prédire avec précision le comportement des connexions dans des conditions de charge d'incendie.

Un modèle théorique basé sur les composants est développé pour représenter le comportement mécanique des assemblages boulonnés d'une manière plus physiquement interprétable, en tenant compte de la dégradation des matériaux en fonction de la température, de la géométrie et du comportement du contact. Le modèle décompose la connexion en éléments individuels tels que les boulons, les cornières et les plaques connectées, chacun étant représenté par des composants semblables à des ressorts dont la rigidité et la résistance sont calibrées par des simulations numériques.

Le modèle proposé est validé par une étude comparative avec les résultats obtenus à partir de la méthode des éléments finis basée sur les composants (CBFEM), qui a récemment gagné en popularité dans le domaine de l'ingénierie structurelle incendie pour sa précision et son équilibre entre complexité et facilité d'utilisation. La comparaison démontre que le modèle théorique fournit des prévisions fiables du comportement des assemblages à des températures élevées, en

capturant des caractéristiques essentielles telles que la réduction de la rigidité, la redistribution des charges et les mécanismes de rupture.

Cette recherche contribue à une compréhension plus précise du comportement des assemblages boulonnés dans des conditions d'incendie. Elle propose une stratégie de modélisation simplifiée qui pourrait être mise en œuvre dans la pratique de la conception. Cela ouvre de nouvelles perspectives de recherche pour la validation expérimentale et l'extension à d'autres types de connexions et de conditions aux limites, et surtout, cela fournit des données substantielles pour des analyses futures.

Mots-clés : Connexions avec cornière, Analyse par éléments finis, Effort de traction, Modèle basé sur les composants, Modèle par éléments finis basé sur les composants (CBFEM), Température élevée.

ملخص

تعتبر النهايز الفولاذية من أكثر الاستراتيجيات فعالية لضمان مرونة الهياكل في المناطق الزلزالية مثل شلف (الجزائر). ومع ذلك، تظل السلامة الإنشائية في ظل ظروف الحريق مصدر قلق رئيسي في الهندسة المدنية، خاصةً بالنسبة للهياكل الفولاذية التي تتدهور خواصها الميكانيكية بشكل كبير في درجات الحرارة المرتفعة. يركِّز بحث الدكتوراه هذا على سلوك الوصلات الفولاذية ذات الزوايا المثبتة بمسامير والمستخدمة عادةً في أنظمة الصلب الإنشائية ذات الدعامات تحت ظروف درجات الحرارة المرتفعة.

الهدف الأساسي من هذه الدراسة هو فحص الاستجابة الميكانيكية وآليات الفشل لهذه الوصلات من خلال النمذجة العددية المتقدمة، مدعومة بمناهج التصميم القياسية في ظل القوانين الهيكلية الحالية. ولتحقيق ذلك، تم تطوير نماذج تفصيلية للعناصر المحدودة باستخدام ANSYS APDL (لغة التصميم البارامترية من أنسيز)، والتي توفر قدرات قوية للمحاكاة غير الخطية المعتمدة على درجة الحرارة. تأخذ نماذج العناصر المحدودة في الحسبان عدم الخطية الهندسية والتفاعلات التلامسية وتدهور المواد الحساسة للحرارة، مما يتيح التنبؤ الدقيق بسلوك التوصيلات في ظل ظروف تحميل الحرائق.

تم إعداد نموذج نظري قائم على المكونات لتمثيل السلوك الميكانيكي للوصلات المثبتة بالبراغي بطريقة أكثر قابلية للتفسير الفيزيائي، مع مراعاة تدهور المواد المعتمد على درجة الحرارة والهندسة وسلوك التلامس. يقوم النموذج بتحليل الوصلة إلى عناصر فردية مثل البراغي والأرجل ذات الزوايا والألواح المتصلة، ويتم تمثيل كل منها بمكونات تشبه الزنبرك مع صلابة وقوة تمت معايرتها من خلال المحاكاة العددية.

تم التحقق من صحة النموذج المقترح من خلال دراسة مقارنة مع النتائج التي تم الحصول عليها من طريقة العناصر المحدودة القائمة على المكونات (CBFEM)، والتي اكتسبت مؤخرًا شعبية في مجتمع هندسة الحرائق الهيكلية لدقتها وتوازنها بين التعقيد وسهولة الاستخدام. توضح المقارنة أن النموذج النظري يوفر تنبؤات موثوقة لسلوك الوصلات في درجات الحرارة المرتفعة، حيث يلتقط السمات الأساسية مثل انخفاض الصلابة وإعادة توزيع الحمل وآليات الفشل.

يساهم هذا البحث في فهم أكثر دقة لسلوك الوصلات المثبتة بمسامير في ظروف الحريق. ويقترح استراتيجية مبسطة ولكن نموذجية يمكن تنفيذها في ممارسة التصميم. يرسي الأساس لتصميم أكثر أماناً وفعالية للهياكل الفولاذية المسندة المعرضة للحريق. وهو يفتح آفاقًا جديدة للبحث من أجل التحقق التجريبي والتوسع إلى أنواع أخرى من التوصيلات والظروف الحدودية، وقبل كل شيء يوفر بيانات مهمة للتحليل في المستقبل.

الكلمات المفتاحية: الوصلات ذات الزوايا، تحليل العناصر المحدودة، قوة الشد، النموذج القائم على المكونات، نموذج العناصر المنتهية القائم على المكونات(CBFEM) ، درجة الحرارة المرتفعة.

PUBLICATIONS

This doctoral research has produced the following journal article and conference papers presented at both international and national levels.

Journal Paper

1. Ouissam Yessad, Abdelhak Kada, Belkacem Lamri, Khalifa Al-Jabri, Muhammad Bilal Waris and Abdelhamid Bouchair. "Modified Component-based Model for Single and Double-angle Bolted Connections Used in Braced Steel Frames at Elevated Temperature". Periodica Polytechnica Civil Engineering, 69(3), pp. 1046–1061, 2025.https://doi.org/10.3311/PPci.40269

International Conferences Paper

1. Ouissam Yessad, Abdelhak Kada, and Belkacem Lamri. "Behaviour of Shear Bolted Connections in Bracing Steel Frames at Elevated Temperature". 20th International Conference on Experimental Mechanics Applications in Materials Science, Engineering and Biomechanics. Porto, Portugal.2-7 July 2023.
2. Ouissam Yessad, Abdelhak Kada, and Belkacem Lamri. "Numerical Investigation of the Resistance of Bolted Angle-Gusset Connections at Elevated Temperatures". 3rd ICMM 2024 International Conference on Materials and Mechanics. Boumerdes; Algeria 20-21 November 2024.
3. Ouissam Yessad, Abdelhak Kada, and Belkacem Lamri. "Component-Based Finite Element Model for Single Angle Connections under Hydrocarbon Fire Situation ". The First International Conference on Civil Engineering and Materials Innovation 1st ICCEMI'24. Mascara, Algeria.09-10 December 2024.
4. Ouissam Yessad, Abdelhak Kada, Belkacem Lamri, and František Wald. "Fire design of bolted braced steel connections using component-based finite element method". International Fire Safety Symposium (IFireSS 2025) - 5TH Edition. Ulster University Belfast, Northern Ireland, UK 25-27 June 2025.
5. Ouissam Yessad, Abdelhak Kada, Belkacem Lamri, and František Wald. "ADVANCED DESIGN OF BOLTED STEEL BRACED CONNECTIONS AT ELEVATED TEMPERATURES". 4eme Conférence Internationale de Construction Métallique et Mixte. ENP Algiers, Algeria, 26-28 October 2025.

National Conferences Paper

1. Ouissam Yessad, Abdelhak Kada, and Belkacem Lamri. "Étude des connexions de structures en acier sous l'effet de températures élevées". 4eme Rencontre des doctorants de la Faculté de génie civil et l'architecture de. Université Hassiba Ben Bouali de Chlef, Algérie.15 décembre 2021.

2. Ouissam Yessad, Abdelhak Kada, and Belkacem Lamri. "Étude des connexions de structures en acier sous l'effet de températures élevées". 5eme Rencontre des doctorants de la Faculté de génie civil et l'architecture de. Université Hassiba Ben Bouali de Chlef, Algérie.19 décembre 2022.

3. Ouissam Yessad, Abdelhak Kada, and Belkacem Lamri. "Transient finite element analysis for the thermal response of braced steel connections under fire situation". Study Day on Building Engineering and Sustainability ' SDBES 24'. Medea, Alegia.25 June 2024.

4. Ouissam Yessad, Abdelhak Kada, and Belkacem Lamri. "Finite element model for temperature evolution on steel bolted shear connection type subjected to fire". 1er Colloque National sur l'Hydraulique et le Génie Civil CNHGC-2024. Bouira, Algeria.30-31 Octobre 2024.

5. Ouissam Yessad, Abdelhak Kada, and Belkacem Lamri. "Numerical modelling of steel welded top-seat angle connections exposed to ISO 834 standard fire". National Conference of Applied Sciences and Engineering, NCASE'24. Algiers, Algeria.17-18 November 2024.

6. Ouissam Yessad, Abdelhak Kada, and Belkacem Lamri. "Modelling the Thermal Performance of Steel Bolted Braced Connections in Fire Scenarios". 3rd NATIONAL CONFERENCE ON MATERIALS SCIENCES AND ENGINEERING (MSE'25). Chlef, Algeria.11-12 June 2025.

CONTENTS

LIST OF FIGURES

LIST OF TABLES

LIST OF SYMBOLS

Geometric Parameters

T	Angle, gusset thickness
d_0	Bolt hole diameter
d_b	Bolt diameter
e_1	End distance
e_2	Edge distance
A_{nt}	Net area subjected to tension
A_{nv}	Net area subjected to shear
N	Number of forces transferring through friction surfaces
A_s	Tensile area of the bolt
K_1	Geometrical parameter

Material Properties

G	Shear modulus of the gusset plate
f_u	Ultimate strength of the angle/gusset
f_{ub}	Ultimate strength of the bolt
f_y	Yield stress
E	Young modulus

Bolt Forces and Resistances

F_{pc}	Bolt pre-tightening forces
F_b	Shear loads
F_v	Bearing load
$F_{v,Rd}$	Ultimate shear load of the bolt
$F_{v,Rd}$	Bearing resistance of the plate

Plate, angle and Connection Resistances

$N_{t,Rd}$	Plate resistance subjected to tension
$N_{pl,Rd}$	Plastic resistance

$N_{u,Rd}$	Net section resistance
$V_{eff,1,Rd}$	Block shear resistance

Stiffness Parameters

$K_{\upsilon,b}$	Shear stiffness of the bolt
K_b	Bending stiffness
K_{br}	Bearing stiffness of bolt holes
K_{fi}	Initial anti-slip stiffness
K_{fp}	Degradation stiffness
K_s	Groove factor (K_s= 1.0 for the standard hole)
K_v	Shear stiffness

Temperature-Related

$R_{f,v,b}$	Reduction factors of shear strength exposed to fire
Δt	Time interval
$\Delta\theta_{a,t}$	Increase of temperature during the time interval Δt

Bolt Deformations

$\overline{\Delta}$	Nominal deformation of bolt holes
Δ_b	Total deformation of bolt holes
Δ_v	Shear deformation of the bolt

Greek Letters

α_v	0.60
B	Reduction factor dependent on the pitch p_1 and number of bolts
γ_{M0}	Partial safety factor equal to 1
γ_{M2}	Partial safety factor equal to 1.25
M	The anti-slip factor of friction surfaces
Ψ	Influential factor of fire temperatures
Φ	Configuration factor / influential factor of fire temperatures
ε_f	The emissivity of the fire

ε_m	The surface emissivity of the member
$\varepsilon_{t,\theta}$	Limiting strain for yield strength
$\varepsilon_{u,\theta}$	Ultimate strain
$\varepsilon_{y,\theta}$	Yield strain
Ω	Influential factors of fire temperatures
θ	The temperature
θ_a	The steel temperature [°C]
θ_g	Gas temperature in the fire compartment
θ_m	The surface temperature of the member
P	Unit mass of steel

LIST OF ACRONYMS

CBFEM	Component Based Finite Element Method
CBM	Component-Based Method
CEN	European Committee for Standardization
EC3	Eurocode 3
EXP	Experimental
EN	European Norm
FE	Finite Element
FEA	Finite Element Analysis
FEM	Finite Element Method
ISO 834	Conventional fire curve

GENERAL INTRODUCTION

1.1 Motivation and Background

Nowadays, structural steel is a prevalent building material used in skyscrapers, parking lots, schools, and residential buildings. The primary advantages of structural steel is its strength, durability, ease of use for large spans, light weight, ease of installation and speed of construction, flexibility, ductility, and ease of fabrication in various sizes, for this reason developers aimed to create modern, resilient, and sustainable building designs [1-3].

Steel connections play a necessary role in structural engineering because they assist individual structural elements to transfer forces and moments to one another. The applied loads can be evenly distributed across the entire structure when there is effective load transfer. The behaviour of steel connections has a significant impact on the integrity of a steel structure. Failure of a steel connection can lead to the gradual collapse of the entire structure. Increased temperatures can significantly affect the performance of steel connections in a structure. The increase in steel temperature depends on the severity of the fire, the area of steel exposed to the fire, and the extent of fire protection measures used [4]. High temperatures lead to changes in material properties, loss of strength and stiffness, and can cause failure of steel connections. As the temperature increases, the yield strength and tensile strength of steel, screws and welds decrease. As a result, the reduction in strength can seriously impair the load-bearing capacity of steel connections.

Accurate simulation of steel connections and components at elevated temperatures is important to ensure the safety and structural integrity of steel structures in the event of a fire. Finite element models can predict the temperature distribution within steel joints during a fire, accounting for radiation, convection, and heat conduction. Also, FEM allows detailed modelling of connection components such as bolts, welds and plates to study their behaviour at elevated temperatures. Designers can predict the fire behaviour of steel connections under the influence of elevated temperatures, including deformations, stresses and strains.

The component-based model (CBM) offers a robust analytical framework. This approach models the connection as an assembly of deformable components, allowing accurate prediction of stiffness and resistance. At high temperatures, the CBM incorporates temperature-dependent material properties and reduction factors to capture strength degradation. Previous studies have shown its effectiveness in representing the thermal and mechanical response of isolated

connections. Hence, the CBM is well adapted for assessing bolted connections under fire and normal design conditions [5, 6].

The principal goal of this dissertation is to understand to behaviour of bolted angle steel connections, force-displacement relationships, ultimate strength, initial stiffness and the different failure modes of such type of connections and comparing the proposed model CBM with the findings from the finite element analysis and the CBFEM model.

1.2 Objectives & Research Questions

Further research is required to understand the behaviour of angle braced steel connections especially when the failure mode transitions between ambient to elevated temperature conditions.

This thesis aims to establish advanced numerical models to predict the behaviour of bolted angle steel braced connections especially the force-displacement relationships, the ultimate resistance and the initial stiffness. For this purpose, the simulations will be carried out with the finite element software ANSYS APDL [7] including the geometric and material non linearities, the contact sliding and the boundary conditions.

To determine the most appropriate failure mode of the modelled angle braced steel connections the European design code [8] was chosen as the basis for calculating the structural resistance of these assemblies, ensuring consistency with recognized engineering practices.

A parametric analysis is carried out considering bolt type, bolt numbers, single /double angle, and angle size on the fire resistance and the failure load of bolted angle braced steel connections. The adequacy of the calculation of these assemblies resistance by the simplified rules of Eurocode 3 part 1-1 [9], Eurocode 3 part 1-2 [10], Eurocode 3 part 1-8 [8], will be verified by the numerical models.

As a result of this research work, a component-based model is proposed to determine the ultimate load-displacement curves of at ambient and elevated temperatures using limit plastic strain. Also, the proposed CBM model will be verified by the CBFEM model.

This study addresses the following research questions:

- How does the elevated temperature influence the type of failure mode of simple shear connections in angle braced steel frame?

- What effect do the number of bolts have on the behaviour angle braced steel connections under the shear failure mode at ambient and at elevated temperatures?
- Which geometric parameters can lead to changes in the failure modes or structural response of bolted angle connections at elevated temperatures?

1.3 Thesis outline summary

The thesis is divided into 5 main chapters. At first, a general introduction is presented, which offers an overall generalization of the issue and sets out the foundation and the aims of the study.

Chapter 1 is a comprehensive literature review on the effect of elevated temperature on steel structures, material properties of steel, bolts, and welds, and the experimental and numerical studies on the steel joints and members at high temperatures. The numerical modelling techniques are presented for bolts and welds in addition to solid models. The reduction factors proposed in different code designs are summarised. Several experimental studies on the isolated parts and full-scale tests at elevated temperatures exist. Previous numerical models for the modelling of steel joints and steel members at elevated temperatures are described.

In Chapter 2, we explore the role of angle steel in structural applications and address the phenomenon of shear lag fracture. The chapter also provides an overview of the key definitions related to the characteristics and behaviour of bolted angle steel connections under tension, both at ambient and elevated temperatures. Furthermore, it examines the design methodologies for these connections under varying temperature conditions, in line with Eurocode 3, Parts 1-2 and 1-8.

Chapter 3 focuses on the numerical methodology used to simulate the behaviour of bolted steel connections under tension loading subjected to ambient and elevated temperatures. This includes a description of the cases studied, as well as the modelling of steel solids in ANSYS software. We also address the challenges encountered during simulation convergence and explain how these issues were resolved. Furthermore, this chapter discusses the results of the influence of bolt type, number of bolts, angle size, and single/double angle on the displacement and the ultimate tensile force.

In Chapter 4, based on the findings of the numerical models in Chapter 3, the component-based model developed by Sarraj for the fin-plate under the axial load slip relationship was modified

and utilized for the single and double-angle steel connections at ambient and elevated temperatures. The proposed model defines the mechanical properties and characteristics of each component at any given temperature, allowing for more accurate predictions of the connections' performance. The results have shown reliable estimates of both the initial stiffness and the ultimate strength of the connections, ensuring a more precise evaluation of their behaviour under tension loading and temperature conditions.

In Chapter 5, CBFEM (Component-Based Finite Element Method) models for bolted connections in angle steel are discussed in detail for both ambient and elevated temperatures. The chapter covers various aspects of the models, including the type of models used, the contact interactions between components, the convergence study, and the overall analysis process. Furthermore, the newly developed software design demonstrates impressive accuracy and reliability when applied to evaluate the CBFEM models, providing excellent results in assessing the performance of these connections under different temperature conditions.

At the end, a general conclusion summarizes the main conclusions that can be drawn from the whole thesis and gives recommendations for future research work to better comprehend the behaviour of this type of connection.

CHAPTER 1. LITERATURE REVIEW

1.1 Introduction to steel connections

Steel connections are an essential part of every steel construction [11], serving as the vital link between various major structural elements. These connections are responsible for transferring loads and forces between beams, columns, and other members, ultimately ensuring the overall integrity and stability of the building or infrastructure. The primary methods for creating steel connections today include bolting and welding, each offering distinct advantages in terms of strength, efficiency, and ease of construction. However, the behaviour of the structural frame, particularly at the connection points, is highly complex. The performance of these connections is influenced by a variety of factors, including material properties, load distribution, joint geometry, and the type of connection used. As a result, the analysis and design of steel connections require careful consideration of these parameters to ensure safety and optimal performance. The complexity of steel connection behaviour has made it a significant area of research within structural engineering. Over the years, extensive studies have been conducted to improve the understanding of the different variables that affect connection performance, as well as to develop more efficient and reliable construction methods. These research efforts continue to evolve, driven by advances in material science, computational modelling, and experimental techniques. As new challenges emerge, particularly in the context of modern design requirements such as sustainability, high-performance materials, and seismic resilience, the study of steel connections remains a critical field of inquiry.

1.2 Steel structures in fire phenomenon

Fire is a critical event characterized by significant uncertainty. The performance of steel structures during a fire is influenced by several key factors, including the temperature increase of steel components, the structure's fire resistance limit, the mechanical properties of steel, and the design and construction of the steel structure.

In fire engineering design, it is essential to consider steel's mechanical and thermal properties, as changes in these properties can lead to complex structural behaviour. Steel buildings are particularly susceptible to fire due to steel's high thermal conductivity and low specific heat. One of the main vulnerabilities of steel in a fire is the significant reduction in its strength and stiffness at elevated temperatures [12].To reduce the risks associated with fire, structural steel elements are often protected with fireproofing materials. However, the cost of fireproofing is a

significant disadvantage. Fire safety measures are essential to reduce the loss of life and economic impact caused by fire. To prevent structural failure caused by high temperatures, passive fire protection is required. For galvanized steel, zinc coating can improve the fire protection system. Hot-dip galvanized steel has several advantages over uncoated steel, including lower emission factors, slower heating rates, and delayed critical temperature onset [13, 14]. Gernay [15] explored the Performance-Based Design (PBD) approach for structural fire safety, emphasizing its goal-oriented process and key components reviewing case studies to demonstrate its value and outlining the role of structural fire engineers and discussed recent research on fire performance evaluation, including thermal-structural modelling, material behaviour at high temperatures, and probabilistic risk assessments addressed the challenges and future directions for advancing performance-based structural fire design.

1.3 Thermal actions

1.3.1 Temperature in Unprotected steel members

In an unprotected steel member with a uniform temperature distribution across its cross section [10, 16], the temperature increase, $\Delta\theta_{a,t}$, within a short time interval Δ_t (up to 5 seconds) is determined by the total heat the section absorbs during that time. This temperature change is described by the following equation (1):

$$\Delta\theta_{a,t} = K_{sh}.\frac{A_m/V}{C_a.\rho_a}.h_{net,d}.\Delta t \quad (1)$$

Where: K_{sh} is correction factor for the shadow effect and is set to unity for conservative results. For sections under normal fire conditions, it is given by equation (2), and for all other cases it is given as in equation (3):

$$k_{sh} = 0.9\,[A_m/V]_b/[A_m/V] \quad (2)$$

$$k_{sh} = [A_m/V]_b/[A_m/V] \quad (3)$$

$[A_m/V]_b$ denotes the box value of the section factor. $[A_m/V]$ is the section factor for unprotected steel members (1/m), it represents the effect of the geometry of the steel section

and the condition of its exposure to fire A_m is the surface area of the member per unit length (m^2/m), V is the volume of the member per unit length (m^3/m).

1.3.2 Total heat transfer

Heat transfer is the movement of heat across the system boundary due to a temperature difference between the system and its environment. It is interesting to note that the temperature difference is considered a "potential" that causes heat transfer from one point to another [17]. Heat is also known as flux, which is received by the steel element during exposure to fire. It is defined as the sum of two distinct flows: convection and radiation as indicated in equation (4). Heat can move from one place to another in many ways. The different heat transfer modes are:

$$h_{net,d} = h_{net,r} + h_{net,c} \quad (4)$$

Where $h_{net,r}$ is the net radiative heat flux component per unit surface area and is given by equation (5):

$$h_{net,r} = 5.67.10^{-8}.\Phi.\varepsilon_m.\varepsilon_f[(\theta_g + 273)^4 - (\theta_g + 273)^4 \quad (5)$$

Where

$5.67.10^{-8}$ the Stephan Boltzmann constant (W/m^2K^4); Φ the configuration factor; ε_m the surface emissivity of the member; ε_f the emissivity of the fire; θ_g the effective radiation temperature of the fire environment (°C).

$h_{net,c}$ is the net convective heat flux component and is given by equation (6):

$$h_{net,c} = \alpha_c(\theta_g - \theta_m) \quad (6)$$

θ_m the surface temperature of the member (°C).

1.4 Thermal properties

The initial step in ensuring a structure can withstand fire risks is to determine the fire temperatures that the structural components and materials will experience in the case of a fire. The thermal effect corresponds to the temperature increase of the hot gases in the place and is determined by the heat transfer conditions on the surface of the components. The temperature

of the structure increases under the influence of the thermal effect. This phenomenon is called "heat transfer" and causes thermal expansion and deterioration of the mechanical properties of the heated parts of the structure.

1.4.1 Temperature in steel

Determining the temperature distribution in steel joints requires consideration of the thermal characteristics of structural steel, including density, thermal expansion, thermal conductivity, and specific heat. According to EN-1993-1-2 [18], steel has a 7850 kg/m³ density, which is thought to be unchanged by temperature increases.

a. Thermal elongation

The thermal elongation ($\Delta L/L$) that structural and reinforcing steels undergo when subjected to elevated temperatures is determined by equation (7):

$$\frac{\Delta L}{L} = \begin{cases} -2.416 \times 10^{-4} + 1.2 \times 10^{-5}\theta_a + 0.4 \times 10^{-8}\theta_a^2 & 20℃ \leq \theta \leq 750℃ \\ 11 \times 10^{-3} & 750℃ \leq \theta \leq 860℃ \\ -6.2 \times 10^{-3} + 2 \times 10^{-5}\theta_a & 860℃ \leq \theta \leq 1200℃ \end{cases} \quad (7)$$

This behaviour is illustrated below in Figure 1-1. If the expansion of the steel structure is limited, it can introduce very high forces into the elements, which must be taken into account.

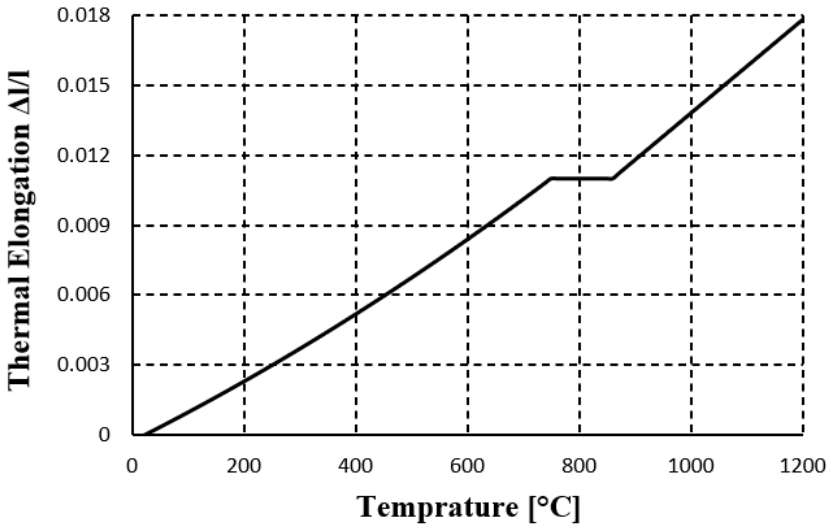

Figure 1-1. Thermal Elongation

b. Specific heat

The specific heat of steel, C_a, is the amount of energy needed to heat 1 kg of material by one degree Kelvin or Celsius. It is important because it greatly influences the rate at which steel heats up. The equations (8) for determining specific heat are as follows:

$$C_a = \begin{cases} 425 + 0.773\theta - 1.69 \times 10^{-3}\theta^2 + 2.22 \times 10^{-8}\theta^3 & 20℃ \le \theta \le 600℃ \\ 666 + \frac{13002}{738-\theta} & 600℃ \le \theta \le 735℃ \\ 545 + \frac{17820}{\theta-731} & 735℃ \le \theta \le 900℃ \\ 650 & 900℃ \le \theta \le 1200℃ \end{cases} \quad (8)$$

In simple models, the value can be taken as $C_a = 600\,J/kg.K$ .The specific heat graph is shown in Figure 1-2. The point in the middle is due to a phase change in the metal frame, which absorbs additional energy without increasing the temperature of the frame. This explains the non-linear graphs often observed for metal structures.

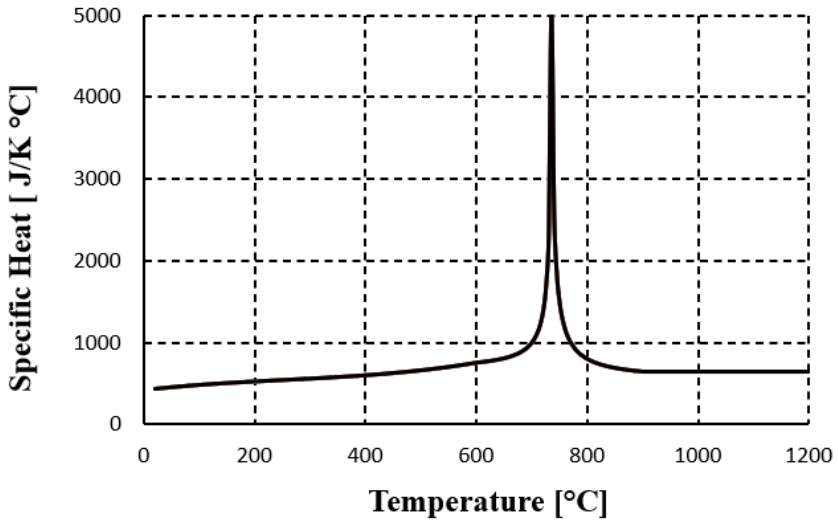

Figure 1-2. Specific Heat

c. Thermal conductivity

The thermal conductivity of the metal structure, λ_a is the rate at which it transmits heat. This property also influences the rate at which metal structures heat up during a fire. It is given by equation (9):

$$\lambda_a = \begin{cases} 54 - 3.33 \times 10^{-2}\theta_a & 20℃ \leq \theta_a \leq 800℃ \\ 27.3 & 800℃ \leq \theta_a \leq 1200℃ \end{cases} \quad (9)$$

In simple calculation models, a constant value of $\lambda_a = 45\, W/mK$ can be used. The temperature-dependent thermal conductivity graph is shown in Figure 1-3. After the phase change, the thermal conductivity remains constant.

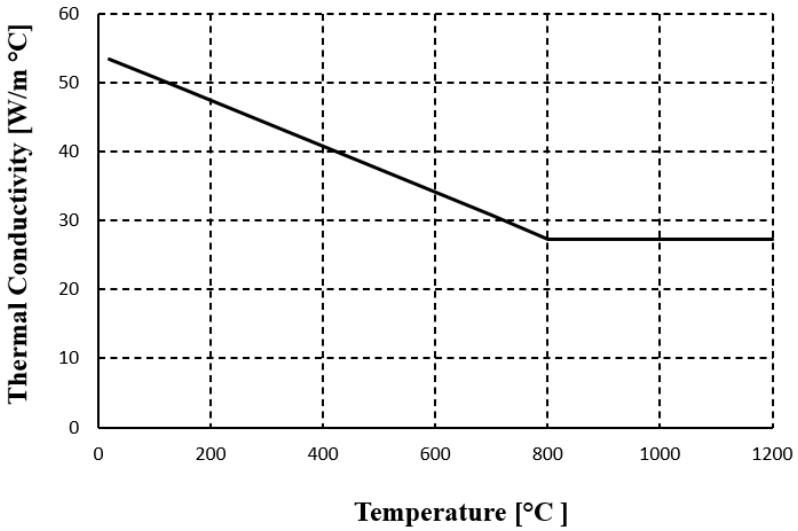

Figure 1-3. Thermal Conductivity

1.5 Mechanical material properties at high temperatures

The steady-state test and the transient heating test are two distinct approaches in material testing. In a steady-state test, the coupon is first heated to a desired temperature and then subjected to a constant tensile load until it fractures. This method simulates prolonged exposure to steady thermal conditions and assesses the material's performance under sustained heat and mechanical stress. In contrast, the transient heating test involves gradually increasing the temperature while maintaining a constant load on the coupon. The temperature continues to rise until the material fractures. This test is useful for understanding the material's behaviour when exposed to rapid temperature changes. While the steady-state test focuses on long-term behaviour at a fixed temperature, the transient test examines responses to dynamic thermal conditions [19], helping researchers evaluate materials under different thermal stress scenarios.

1.5.1 Structural steel

The strength and stiffness of structural steel decrease with increasing temperature as indicated in Table 1-1. The yield strength of structural steel at around 550°C is only about half of the yield strength at room temperature. The determination of the strength reduction factor for hot rolled steel depends not only on the material but also on the test method used to determine the strength of the steel, the heating rate, and the elongation limit. It is obvious that between 400°C and 700°C, structural steel will experience a significant loss in strength and stiffness.

Table 1-1. Reduction factors for steel in EN 1993-1-2 [18]

Steel Temperature (°C)	**Yield Strength Reduction Factor**	**Young Modulus Reduction Factor**
20	1	1
100	1	1
200	1	0.9
300	1	0.8
400	1	0.7
500	0.78	0.6
600	0.47	0.31
700	0.23	0.13
800	0.11	0.09
900	0.06	0.068
1000	0.04	0.045
1100	0.02	0.023
1200	0	0

According to EN 1993-1-2 [18], the stress-strain relationship of steel at high temperatures is composed of two straight lines joined by an elliptical curve. The first linear section of the elastic material behaviour continues until the proportional limit ($f_{p;\theta}$)is reached. Figure 1-4 shows the general stress-strain relationship. Table 1-2 contains the equations required to create the stress-strain relationship for carbon steel. The degradation of steel is represented using Eurocode 3 stress-strain relationshipsas commonly adopted in previous studies [20].

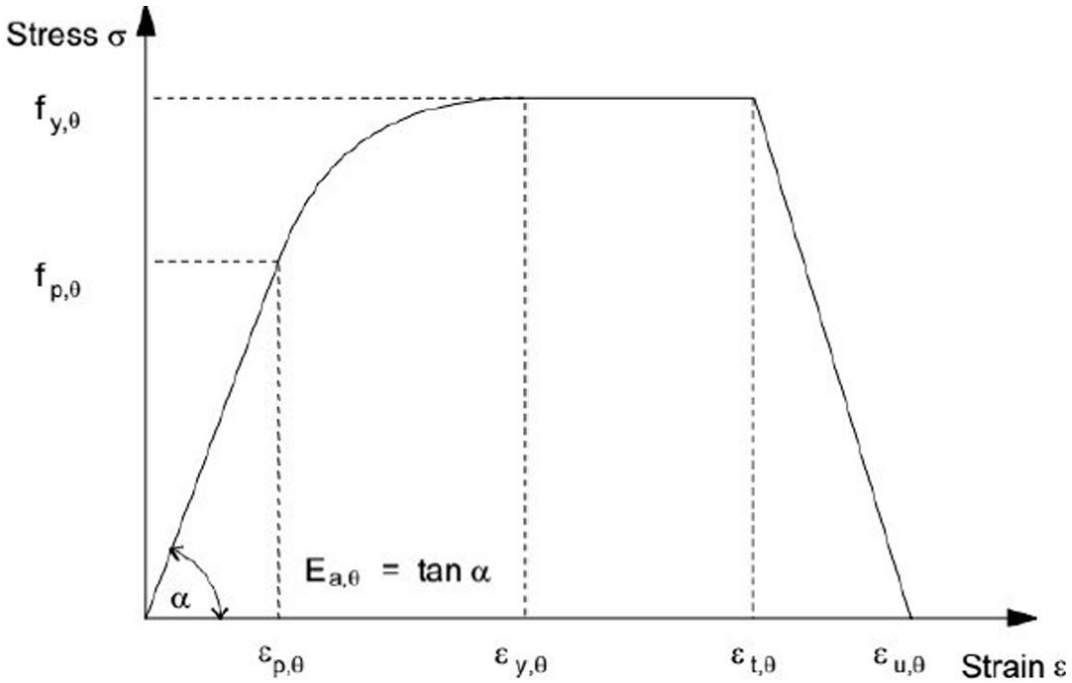

Figure 1-4. Stress-strain relationship for carbon steel at elevated temperature [18]

Table 1-2. Stress-strain curve equations (EN 1993-1-2, 2005)

Strain (e)	**Stress (s)**
$\varepsilon \le \varepsilon_{p;\theta}$	$\varepsilon E_{a;\theta}$
$\varepsilon_{p;\theta} < \varepsilon < \varepsilon_{y;\theta}$	$f_{p;\theta} - c + (b/a)[a^2 - (\varepsilon_{y;\theta} - \varepsilon)^2]^{0.5}$
$\varepsilon_{y;\theta} < \varepsilon < \varepsilon_{t;\theta}$	$f_{y;\theta}$
$\varepsilon_{t;\theta} < \varepsilon < \varepsilon_{u;\theta}$	$f_{p;\theta}[1 - (\varepsilon - \varepsilon_{t;\theta})/(\varepsilon_{u;\theta} - \varepsilon_{t;\theta})]$
$\varepsilon = \varepsilon_{u;\theta}$	0

Where a, b, and c in the above table are parameter functions which are defined as:

$$a^2 = (\varepsilon_{y;\theta} - \varepsilon_{p;\theta})(\varepsilon_{y;\theta} - \varepsilon_{p;\theta} + c/E_{a;\theta}) \quad (10)$$

$$b^2 = c(\varepsilon_{y;\theta} - \varepsilon_{p;\theta})E_{a;\theta} + c^2 \quad (11)$$

$$c^2 = \frac{(f_{y;\theta} - f_{p;\theta})^2}{(\varepsilon_{y;\theta} - \varepsilon_{p;\theta})E_{a;\theta} - 2(f_{y;\theta} - f_{p;\theta})} \quad (12)$$

1.5.2 Bolts

The mechanical characteristics of bolts at high temperatures are not well documented. In addition to proposing reduction factors for the elastic modulus of tested bolts; Sakumoto et al. [21] reported an experimental study on the mechanical properties of some high-strength fire-resistant screws (F10T torque control screws) at high temperatures and proposed a reduction factor for the elastic modulus of the tested screws. Experimental studies have shown that the strength of screws decreases significantly between 300°C and 700°C. Li et al. [22] established mathematical formulas for yield strength, ultimate tensile strength, Young's modulus, and elongation were developed by testing 30 material coupons subjected to the same heat treatment used in the actual bolt manufacturing process. The selected bolt type for testing was high-strength steel 20MnTib. The mechanical response of ASTM A325 and A490 bolts under double shear loading was studied at temperatures up to 800°C [23]. The tests showed that at ambient temperature, A325 bolts have strength comparable to Grade 8.8 bolts. However, at elevated temperatures, A325 bolts do not exhibit the same behaviour as Grade 8.8 bolts. In contrast, A490 bolts display a similar decrease in strength with temperature, similar to Grade 8.8 bolts A series of tests were conducted by Hu [24] on Grade 8.8 high-strength bolts by the latest British and European standards (BS 4190:2000 and EN ISO 4014, 4017, respectively). Kodur. V et al. [25] conducted steady-state single shear and tension tests within a temperature range of 20–800°C to evaluate the high-temperature thermal and mechanical properties of Grade A325 and A490 high-strength steel bolts. The study found that the strength reduction in A325 and A490 bolts was more significant compared to conventional steel. Additionally, A325 steel showed slightly lower strength and stiffness than A490 bolts across the 20–800°C range**.** Peixoto et al. [26] conducted experiments on high-strength structural A325 and A490 bolts subjected to double shear loading at elevated temperatures. Cai et al. [27] presented a numerical analysis approach to predict high-strength steel connections' fracture behaviour at elevated temperatures, focusing on material properties and fracture parameters for ASTM A325 bolts and A572 Grade 50 steel. It highlights the significant impact of bolt shear failure mode on the degradation of load and deformation capacities under high temperatures, especially for connections with large end distances. Pang et al. [14] conducted an experimental program to examine the elevated-temperature material properties of three types of high-strength bolts with property classes 8.8, 10.9, and 12.9. Rezaeian et al. [28] studied the effect of temperature on the mechanical properties of Grade 10.9 steel bolts. Their findings showed that Grade 10.9 bolts undergo a rapid reduction

in strength at temperatures above 400°C, with strength dropping to 40% and 5% of the original value when heated to 600°C and 800°C, respectively. Ban et al. [29] carried out standard tensile coupon tests on high-performance (HP) bolts across temperatures from 20 to 900°C. They also introduced constitutive models and predictive equations to describe the material properties of the HP bolts at different temperatures. Shaheen et al. [30] studied and examined high-strength and stainless-steel bolts, which exhibited a notably ductile response during stripping failure. This behaviour is undesirable as it leads to premature bolt failure. At ambient temperature, stripping occurred at specific Lt lengths, which varied depending on the nut's deviation from the basic profile. The stripping failure threshold (Lt) decreased with temperature for high-strength bolt assemblies, whereas for stainless steel bolts, the threshold fluctuated without a clear pattern. In EN-1993-1-2 [18], there is no consideration for the elastic modulus of bolts and welds, therefore, only the strength reduction factor can be found for tension and shear. Table 1-3 illustrated the reduction factors from the code design.

Table 1-3. Reduction factors for Bolts in EN 1993-1-2; 2005 [18]

Temperature (°C)	$k_{b;\theta}$
20	1.000
100	0.968
150	0.952
200	0.935
300	0.903
400	0.775
500	0.550
600	0.220
700	0.100
800	0.067
900	0.033
1000	0

1.5.3 Welds

The behaviour of welds at high temperatures plays a crucial role in predicting the response of a welded joint. Welds are designed to carry a combination of axial and shear forces at elevated temperatures. As a result, a longitudinal weld, which is aligned parallel to the applied load, may experience a component of loading that is perpendicular to its length, potentially causing it to

behave like a transverse weld. A fillet weld's reduced strength per unit length at elevated temperatures can be assessed using the reduction factors provided in Table 1-4.

Yu [31] reported on a series of experiments examining the ultimate strength and fracture performance of structural steel welds at elevated temperatures. Rezaeian et al. [28] presented the findings of an experimental investigation into the high-temperature mechanical properties of steel welds made using the shielded metal arc welding (SMAW) process with E6013 and E7018 electrodes. The ultimate strength of the welds increased up to 400°C. Additionally, the results showed that the yield stress of the steel welds decreased more quickly than that of structural steel between 450°C and 800°C.

Table 1-4. Reduction factors for Welds in the Eurocode

Temperatures (°C)	**Reduction factors for the weld's strength**
20	1
100	1
150	1
200	1
300	1
400	0.876
500	0.627
600	0.378
700	0.13
800	0.074
900	0.018
1000	0

1.6 Behaviour of steel members and joints at elevated temperatures

Research on how steel structures behave in the event of a fire has gained a lot of attention in recent years [32, 33]. Steel structures' structural reaction to fire action is influenced by heat gradient, material deterioration, loss of stiffness and strength, and expansion constraints**.** It is not well known or adequately standardized how thermally induced stresses and deformations affect steel constructions' fire response. The majority of studies examined how semi-rigid joints responded to ascertain their stiffness and resistance properties. According to Simões da Silva et al. [34], the following phenomena make predicting the fire response of a steel connection far

more difficult than ambient design: changes in steel material properties with rising temperatures, precise time-temperature variation prediction within the various joint components, elongation difference between the various joint components due to rising temperatures, and appropriate definition of fire development models within the building. The moment-rotation behaviour of steel joints can only be predicted by the first three occurrences.

The joints are typically thought of as being hard or pinned in design. In reality, though, the joints behave in a semi-rigid manner rather than being completely rigid or pinned. When considering strength, stiffness, and rotational capacity, the mechanical behaviour of steel joints is a complicated phenomenon. Based on isolated member tests under typical fire conditions, the current design codes forecast a structure's resistance to high temperatures. Because thermal expansion is restricted, interactions between elements in real structures cause stresses, deformations, and either local or global failure of the structure. The solitary member tests are unable to observe or anticipate these events. Natural fire curves, which are divided into three phases growth, full maturity, and decay cannot be represented by standard fire curves [35]. Experimental findings on how steel joints react to fire conditions are somewhat limited because of the expensive cost of the fire tests and the small furnace size. Full-scale testing and fire incidents demonstrated the significance of collaborative reaction on the structure's overall performance. Due to their lower temperatures and a slower rate of heating than the linked parts, which is caused by the connection's high concentration of thermal mass, beam-to-column joints are typically thought to have adequate fire resistance. However, the collapse of the World Trade Center on September 11, 2001 [36], Cardington's large-scale fire tests [37], and subsequent investigations have shown that the assumption that beam-to-column connections have adequate fire resistance is incorrect. This is because in the early and middle stages of a fire, due to the restraint of the thermal expansion of the beams, the internal forces change from moments and shear at ambient temperature to moments, shear and compression, and finally to shear and stresses in the later stages when the chain reaction begins, resulting in a large concentration of thermal mass at the joints. Experiments on individual joints and substructures are unable to produce these realistic loading conditions. Large-scale furnace testing has revealed the true reaction of joints at high temperatures. [36, 38, 39]. In 2012, Burgess et al. [40] reviewed research on the behaviour of structural connections in fire, highlighting their crucial role in preventing progressive collapse. Early studies focused on moment-rotation behaviour, but full-scale fire tests revealed the importance of connections' tying capacity for structural stability. The

component-based approach, initially used for ambient temperature design, is adapted to model connection behaviour under fire conditions. Furnace tests at various temperatures help characterize the model, which is integrated into global structural fire analysis to prevent progressive collapse in fire scenarios.

1.6.1 Experimental studies on steel joints at both temperatures

The first experimental fire tests on joints were conducted by CTICM [41] and British Steel [42] on six different types of joints, ranging from flexible to rigid, using the ISO 834 fire curve. The purpose of the testing was to examine how well high-strength bolts functioned at higher temperatures. The findings showed that at high temperatures, the bolts and the components they are linked to may experience significant deformations. Lawson [43] performed the first fire tests on steel and composite joints by subjecting them to a typical fire while maintaining varying major-axis junctions under continuous stress. Flush endplate, extended endplate, and web cleat joints are the three types of bolted junctions that have been the subject of research. The tests were conducted to create a design strategy for steel beams that considers joint rotational restraint. The ductility and capacity of common steel joint types under fire pressures were investigated by the universities of Manchester and Sheffield [44-48]. The joints were subjected to substantial deformation and breakage during the test program, as well as combinations of shear and tying forces. The tying and rotational capacities of web cleat joints under tying force at high temperatures were investigated by [49]. Al-Jabri et al. [50] conducted five series of experimental tests in a cruciform arrangement, testing twenty end-plate connections under two conditions: flush (partially restrained) and flexible (simple). These tests were carried out in a furnace and followed the testing program by Leston-Jones LC [51], which examined smaller sections (UB254×102×22 beams and UC152×152×23 columns) using full-depth end-plate connections. Liu et al. [52] carried out experimental tests to study the behaviour of a one-bay gravity frame under varying levels of axial restraint. Axial restraint was applied to the adjacent bays of the frame using braces with different axial stiffness values. Both end-plate and double-angle connections were evaluated. The tests were conducted without a slab, using UB178×102×19 beams. Point loads were applied to the beam by two actuators at approximately one-third of the span, resulting in four-point bending. These loads were applied at load ratios of 0.3, 0.5, and 0.7, based on the beam's flexural capacity at ambient temperature. The furnace's time-temperature curve was closely aligned with the ISO 834 [53] curve.

Yu et al. [47] conducted a series of experiments to investigate the moment-rotation behaviour of simple shear connections. Stub beams (UB305×165×40) were connected to stub columns (UC254×89) using fin plate (shear tab) connections. The specimens were tested in a furnace with an inclined tensile force applied to the beam. The angle at which the load was applied corresponded to a predetermined ratio of shear to tying force demand on the connection. Fourteen specimens were tested, with variations in bolt diameter (20 mm and 24 mm), bolt grade (Grade 8.8 and 10.9), and the number of bolts in the connection (single column with three bolts or two columns, each with three bolts). No composite slab was included in the test setup, and the specimens were tested at steady-state temperatures of 20°C, 450°C, 550°C, and 650°C, ensuring no thermal gradient through the connection. The results showed that fin plate (shear tab) connections maintain moment capacity during a fire, potentially increasing the survival time of a building. All tested fin plate connections failed due to bolt shear fracture at elevated temperatures. Yu et al. [47] concluded that the reduction in connection strength with increasing temperature was largely influenced by the temperature-dependent retention factors of bolt shear strength, regardless of the ambient temperature design. When bolt strength was increased, the ambient temperature controlling limit state shifted to block shear, while the elevated temperature limit state remained bolt shear fracture. Hu et al. [54] presented the results of computational and experimental studies on the behaviour of steel simple beam end framing connections under fire conditions. These connections are vital for maintaining structural integrity during a fire, as fire can significantly impact their strength and stiffness. The study focuses on single plate connections, which are commonly used in the US. Computational studies examined the connection's behaviour during both the heating and cooling phases of a fire, along with its force and deformation demands. Experimental tests at elevated temperatures were carried out to validate the computational predictions and provide insights into failure modes. Selden et al. [55] reported experimental studies of the thermal and structural behaviour of composite beams with shear connections exposed to fire conditions. The beams, designed with flat, lightweight concrete slabs, were subjected to vertical loading and heated using high-temperature ceramic radiant heaters. Findings revealed a reduction in load capacity due to heating, with concrete compression failure occurring at steel temperatures of 350–500°C. Notably, the shear-tab connection fractured during the cooling phase, highlighting the significance of considering both heating and cooling in fire scenarios. Faralli et al. [56] examined the second-order effects caused by geometric and material non-linearities in T-stubs bolted to rigid support using experimental, numerical, and analytical methods. Experimental data is presented for various T-stub geometries to ensure that significant second-order effects develop, expanding the existing test data. Finite element models are developed to study how geometric and material parameters

affect the resistance and ductility of T-stubs under large displacements. The study reveals that bolt restraint is key to activating catenary action in the flange and the development of a second hardening branch in the tensile response, identifying two new failure modes not considered in classical theory or EC3 (Part 1.8). A mechanical model is proposed to identify the parameters influencing second hardening, and a criterion is suggested to estimate when second-order effects become active. Qiang et al. [57] explored the behaviour and failure mechanisms of high-strength steel endplate connections under fire conditions through an experimental study. Full-scale tests were performed on beam-to-column high-strength steel endplate connections at both 550°C under steady-state fire conditions and at ambient temperature for comparison. The results were also compared to mild steel endplate connections. The study validated Eurocode 3 provisions with the test data. It was found that a thinner high-strength steel endplate enhances the rotation capacity of the connection, both in fire and at ambient temperature, ensuring safety and achieving nearly the same moment resistance as mild steel endplate connections. Wang et al. [58] examined the fire behaviour of high-strength steel shear connections (Q690 and Q960) through experiments and numerical modelling. It finds that slip load decreases faster than the ultimate load at elevated temperatures, with a shift in failure mode around 500 °C. The research highlights the importance of friction coefficient and bolt load in shear connection performance and compares results to design codes, showing that AISC 360-16 provides the most accurate predictions. Qiang et al. [59] investigated the performance of extended endplate connections by treating T-stubs as equivalent components. Ambient- and elevated-temperature tensile tests were conducted on High Strength Steel (HSS) T-stubs to examine the effects of various factors, including temperature, flange thickness and strength, bolt location, bolt diameter, and bolt strength. A total of 28 T-stubs were tested, and their failure modes were analysed experimentally. Additionally, the applicability of Eurocode 3 Part 1–8, using elevated-temperature reduction coefficients for HSS, was assessed through theoretical calculations. The study provides design recommendations for improved connection performance under elevated temperatures based on the findings. Abdoh [60] examined steel plates' deformation and fracture behaviour in bolted connections using a 3D peridynamic model to simulate excessive deformation and fracture under shear, moment, and torsion. The model is validated against experimental data and offers a novel approach to overcome the limitations of mesh-based methods in modelling ductile materials. It reveals a shift in fracture behaviour from ductile to brittle under high moment and torsion values. The 3D peridynamic model helps optimize steel plate designs for improved structural integrity. Khonsari et al. [61] studied the behaviour and failure mechanisms of a half-scale 3D frame with moment-resisting and braced

frames under fire conditions, using 6 mm thick flush end-plate connections. Exposed to a scaled ISO 834 fire curve, the frame reached temperatures up to 1100°C. The study assessed the influence of connection ductility by comparing results with a previous study using less ductile connections. The results showed that flexible connections allowed the frame to endure large rotations (up to 0.7 radians) and significantly improved the frame's robustness, withstanding 65 minutes under fire. Wang et al. [62] examined the behaviour of web angle cleat connections using austenitic high-strength bolts (A4L-80) at ambient and elevated temperatures, comparing them with connections using carbon steel bolts (Grade 8.8). Experimental results show that austenitic bolts outperform carbon steel bolts in fire resistance at elevated temperatures, maintaining structural integrity at 650°C, whereas carbon steel bolts fail prematurely.

1.6.2 Experimental research on construction structures under real fire

A full structure consists of the structural components and the walls, floor slabs, and other non-structural components. Even though they are quite costly, fire tests on entire buildings are necessary to determine how a building will react in the event of a fire.

The two most thorough studies to forecast the structural behaviour of a whole structure at high temperatures are the Broadgate fire catastrophe [63] and the Cardington full-scale fire testing [64]. As seen in Figure 1-5, six full-scale fire tests were carried out inside the structure at different sites during 1995 and 1996. These tests have been extensively documented in previous studies [65, 66]. The fire event at the World Trade Center in New York [67] was a tragic incident that highlighted the real-life consequences of connection failure under high temperatures as illustrated in Figure 1-6. Orabi et al. [68] revisited the collapse of WTC7, examining its investigation and exploring the hypothesis that a possible hydrocarbon fire may have weakened the large transfer structure within the building's mechanical space. The fire tests conducted at the Cardington laboratory [69] revealed that during the heating phase of a fire, the temperature of the joints was lower than that of the beams. However, in the cooling phase, the joints cooled more slowly than the beams and reached higher temperatures. Additionally, the shear tabs experienced higher temperatures than the bolts, with the lower bolts being hotter than the upper ones. The tests also observed elongations in the holes of the beam webs and shear tabs, which were caused by the significant connection rotations. Wang [70] presented the findings of an analysis on the global structural behaviour of the 8-story steel-framed building at Cardington, based on the two large-scale fire tests conducted by BRE. These tests were carried out to

examine the behaviour of entire building structures under realistic fire conditions and to provide reliable test data for validating numerical models. Wang et al. [71] conducted full-scale fire experiments on steel composite frames under furnace loading. The results indicated that fire-resistance design should not rely solely on the performance of individual elements tested in isolation. It is crucial to consider the interactions between members within the entire structure.

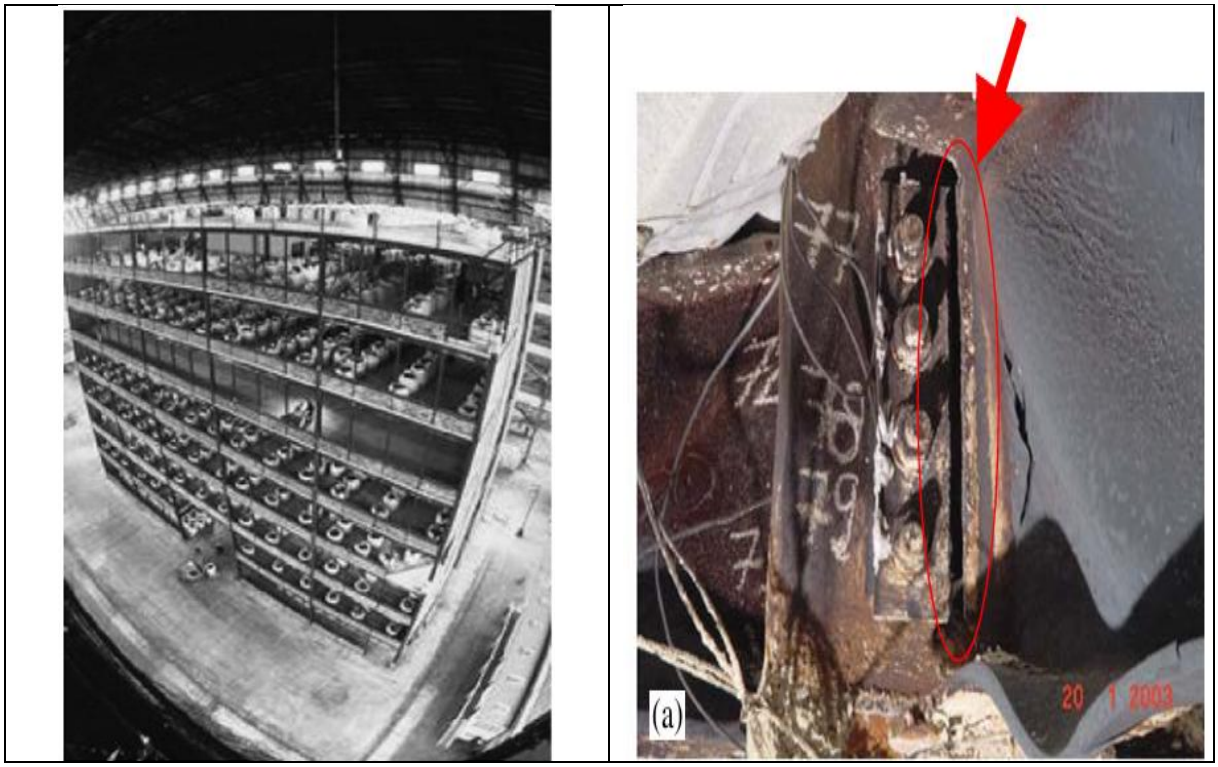

Figure 1-5. Full-scale structure fire test at Cardington Laboratory [69]

Figure 1-6. Failure of truss beam connections in the WTC towers due to fire Exposure (2001) [72]

1.7 Methods of analysis of steel connections at elevated temperatures

Joints are often exposed to a range of forces, such as moments, shear forces, and axial forces, due to their interactions with neighbouring structural members. Consequently, the mechanical behaviour of a joint can be defined by its rotational stiffness (the initial slope of its moment-rotation curve), strength, and rotation capacity. However, experimental fire tests are expensive and may not adequately represent the behaviour of all types of joints.
The moment-rotation curve is typically characterized through different simulation methods:

- Component Method
- Finite Element Analysis
- Component-Based Finite Element Method

1.7.1 Component method

The component method involves dividing a joint into compression, tension, and shear zones, with each zone's behaviour being represented by several fundamental components. The overall behaviour of the joint can be determined by combining the contributions of individual components, which consist of rigid links and translational springs with a nonlinear force-displacement response. These components can be arranged in parallel or series, depending on the situation. This approach is referred to as the spring stiffness method. For end-plate connections, the component method involves assembling spring elements across the tension, compression, and shear zones, as illustrated in Figure 1-7.

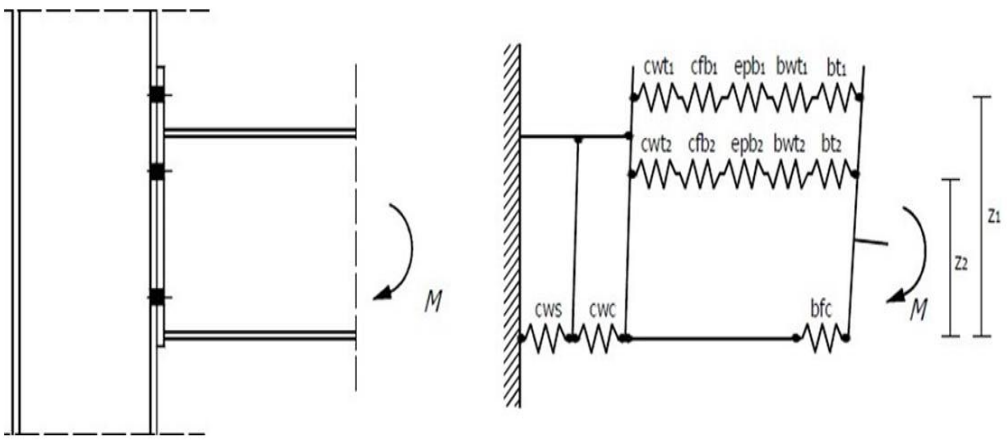

Figure 1-7. Component model adopted by EN 1993-1-8 [73]

The component-based method involves three key steps [74]:

1. Identifying the active components within the joint;
2. Assessing the stiffness and resistance properties of each individual component;
3. Combining all the individual components to determine the overall stiffness and resistance characteristics of the entire connection.

The component-based method has been standardized for analysing semi-rigid joints at ambient temperatures in EN 1993-1-8 [73] which identifies various joint components, along with their stiffness and strength, based on a literature review. For a bolted extended end-plate joint subjected to a simple bending moment, the active joint components specified in EN 1993-1-8 include: column web under shear (cws), column web in compression (cwc), column web in tension (cwt), column flange in bending (cfb), end-plate in bending (epb), bolts in tension (bt), weld (w), beam web and flange in compression (bwc, bfc), and beam web in tension (bwt). Eurocode also accounts for the effect of temperature on these components by applying reduction factors to the material properties, as outlined in EN 1993-1-2 [18].

Leston-Jones [38] developed a component model for elevated temperatures to predict the behaviour of bare-steel and composite flush end-plate joints with two bolt rows. In this model, the fundamental components include the column flange in bending, bolts in tension, end-plate in bending, and column web in compression, as illustrated in Figure 1-8. The validation results reveal a high level of consistency with the experimental data [38].

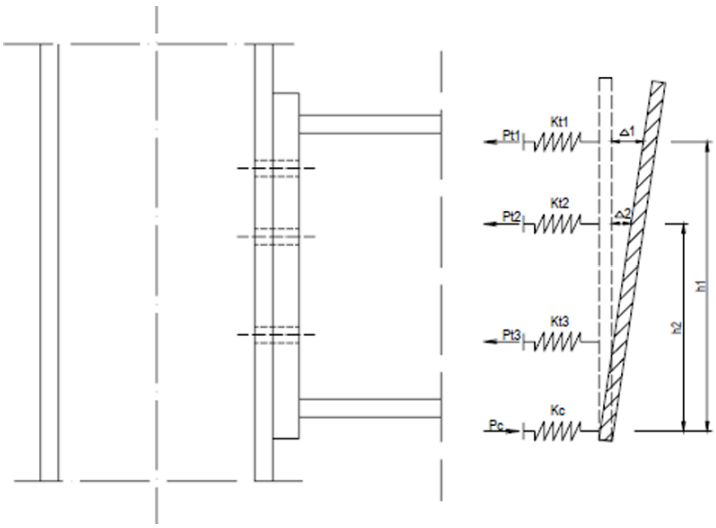

Figure 1-8. Spring Stiffness Model for Bare-Steel Flush End-plate Joint [38]

Al-Jabri [75] expanded on the work of Leston-Jones [38] to model the fire behaviour of bare steel and composite flexible end-plate joints , the model is presented in Figure 1-9. The active components in this model include the bolts, the column flange end-plate in the tension zone, and the column web panel in the compression zone.

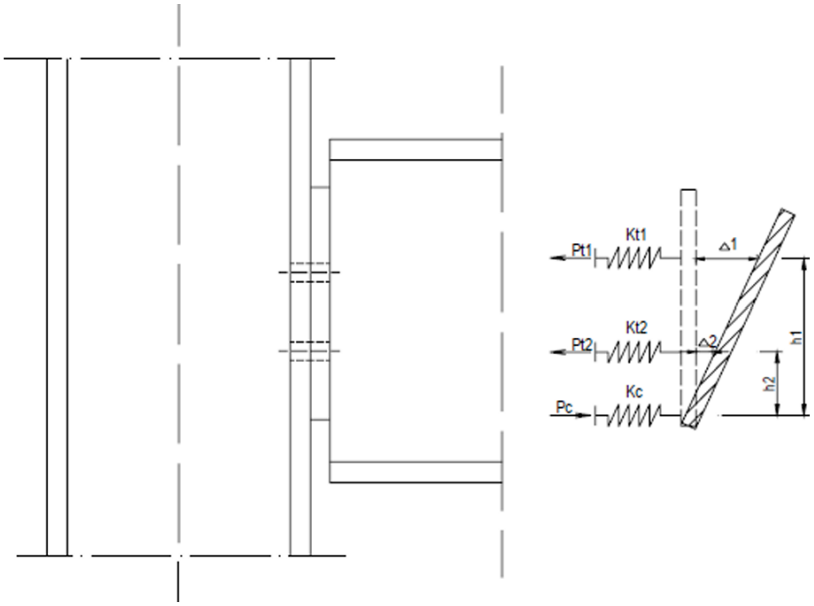

Figure 1-9. Spring model for flash plate [75]

Simões da Silva et al. [6] aimed to expand the component method to evaluate the fire response of steel joints. They introduced an analytical approach to predict the moment-rotation behaviour, incorporating the changes in yield stress and elastic modulus of the components as the temperature rises. The model was validated using fire tests on flush end-plate joints carried out by [75].

Simões da Silva et al. [6] aimed to extend the component method for evaluating the fire response of steel joints. They proposed an analytical procedure to predict moment-rotation behaviour, accounting for the changes in yield stress and elastic modulus of the components as the temperature rises. The model was validated using fire tests on flush end-plate joints performed by Al-Jabri [75]. Furthermore, Spyrou [76] developed a component-based method to study the behaviour of components in the tension and compression zones of flush end-plate joints at both ambient and elevated temperatures. The active components needed to model a real end-plate joint include the end-plate in bending, column flange in bending, bolts in tension, and column web in compression. Weigand et al. [77] used the component-based modelling approach to derive

the ultimate tensile strength and modulus of elasticity for grade A325 and A490 bolts from double-shear tests at elevated temperatures. These properties are then used to model the temperature-dependent degradation of shear strength and stiffness for bolts of various diameters. The model also accounts for load reversal effects. It accurately predicts bolt behaviour under high-temperature and varying load conditions. Yu et al. [78] created a mechanical model to predict the behaviour of web cleat connections under tying forces, building on test results showing their strong tying resistance and rotational capacity at elevated temperatures. The model includes plastic hinge formation and the effect of angle opening on resistance, alongside existing algorithms for bolts and other components. Failure criteria from tests are integrated to predict the occurrence and sequence of connection failure. Block et al. [60] developed a component-based element for end-plate joints in the fire to predict the moment-rotation curves of connection experiments at both ambient and elevated temperatures, as shown in Figure 1-10. Their study details the derivation of the stiffness matrix for this new element and its integration into the non-linear finite element program Vulcan. However, the presented connection element does not account for certain factors, including group effects in the bolt rows, shear deformation in the column web, shear deformation in the beam-end zone, local buckling of the beam's bottom flange, and bolt behaviour during cooling. Despite these omissions, the new element successfully combines the component method with a detailed representation of overall connection behaviour.

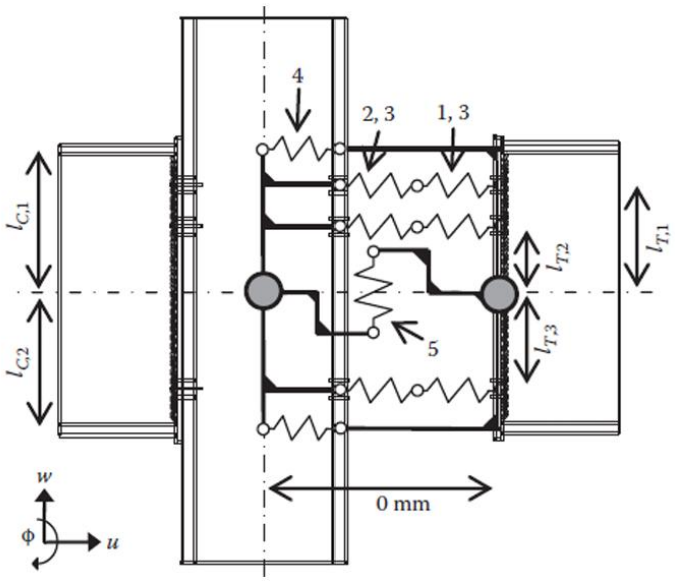

Figure 1-10. Block Component Model [79]

Sarraj [80] applied the component-based method to model the behaviour and robustness of steel fin plate joints under elevated temperatures. They proposed a simplified mechanical model made up of three components: plate bearing, bolt shearing, and web-to-plate friction. Santiago [81] developed a comprehensive model divided into four partial models for flush end-plate and extended end-plate joints. Each partial model applies to a specific combination of axial force (tension or compression) and bending moment (hogging or sagging). Taib [82] developed a component-based model to examine the behaviour of fin-plate joints under fire conditions. Sana et al. [83] proposed a component model that offers insights into fire-induced axial forces and rotations in steel bolted top and seat angle connections. It stands out for its low computational effort while maintaining accuracy. Quan et al. [84] developed a component-based model for the buckling zone, which accounted for both beam-web shear buckling and bottom-flange buckling. The model offered a reasonably accurate and conservative prediction of the force-deflection relationship for Class 1 and 2 beams. Xie et al. [85] focused on the behaviour of connections in structures exposed to fire, particularly the plate in bearing components using fully threaded bolts. Since fire testing full structures are costly and time-consuming, a component-based model simulates connection behaviour under fire conditions. The key to this model is determining temperature-dependent force-deflection relationships, which have not been extensively studied. The behaviour of the plate in the bearing component was investigated at both ambient and elevated temperatures using 3-D finite element analysis (FEA) with ABAQUS. Parameters such as edge distance, bolt pitch, end distance, plate thickness, bolt-hole diameter, bolt bearing angle, and temperature were analysed for their effects on the component's behaviour. The study identified failure modes, resistance, stiffness, and force-deflection relationships and proposed prediction models for the component's resistance and stiffness.

Liu et al. [86] proposed a component-based model for a novel steel connection design, illustrated in Figure 1-11, to enhance fire resistance. The new design's performance was compared to the previous version using a sub-frame model, showing increased ductility. Five case studies applying the novel connection to sub-frames with different beam spans revealed that axial forces in the beams were significantly reduced compared to beams with rigid connections. Analytical models for key components (web-cleat and WCSC) of the novel connection were developed using simple plastic theory, and two component-based model schemes were proposed, considering both loading and unloading behaviour. The result curves from these models were validated against Abaqus simulations and experiments. Finally, the component-

based model was applied to simple examples, demonstrating how various spring rows behave during connection deformation.

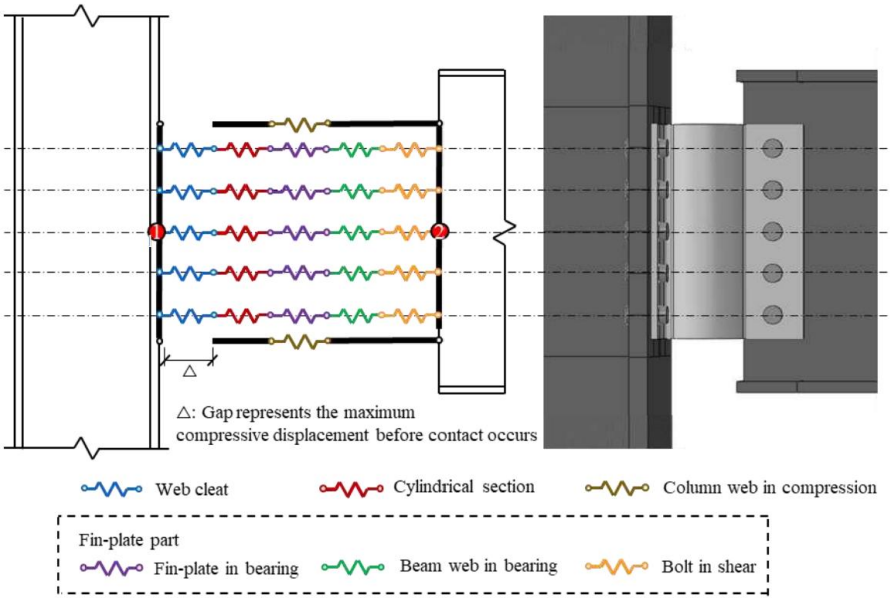

Figure 1-11. Novel scheme of component-based model [86]

Quan et al. [87] generated a component-based model for composite fin-plate connections at beam-column interfaces, incorporating the effect of slab continuity. The model simulates connection failure using fracture criteria for the plates and bolts and is validated using experimental data, including tests under elevated temperatures. Implemented in Vulcan software, it provides accurate predictions for composite beams with fin-plate connections under fire conditions. Parametric studies are conducted to explore the impact of axial restraint stiffness and reinforcement ratio on beam behaviour and connection force distribution.

Zhao et al. [88] introduced a component-based model to analyse the nonlinear behaviour of semi-rigid connections, implemented in a finite element package for structural analysis. The model's accuracy is validated by comparing numerical results with experimental data. Additionally, the contribution of bolt slip and OBTID connections' semi-rigidity are compared to Eurocode 3 provisions. Guo et al. [89] developed and validated component-based models (CBMs) for beam-column joints exposed to fire, incorporating welded and bolted joint configurations. The CBMs are integrated into ABAQUS software to simulate collapse responses in multi-story steel structures. Analysis reveals that joint configurations significantly affect collapse behaviour and force redistribution. For structures with higher loading ratios, reinforcing columns or adding fire protection is recommended to prevent progressive collapse.

Wang et al. [90] proposed a high-temperature component-based method for top-and-seat-with-web-angle (TSWA) beam-to-column connections, focusing on fire scenarios. It introduces coefficients for accuracy and incorporates temperature-dependent material properties. A universal spring stiffness model is developed and validated with a 3% error margin. The method's simplicity and generalization make it suitable for fire-resistant structural design. Guo et al. [91] presented a generalized component-based model (CBM) for extended endplate (EP) joints, aimed at simulating progressive collapse scenarios induced by fire. The model captures the nonlinear behaviour of EP joints from initial yielding to failure under fire-induced column removal. It incorporates trilinear force-deformation for fire-exposed panel zones and detailed spring parameters for connecting zones. The simplified CBM is implemented in ABAQUS and validated against experimental and refined FE models. Results show that the CBM accurately predicts collapse responses with high computational efficiency at elevated temperatures. Wang et al. [62] developed a modified component-based model to replicate the M-θ response of web angle cleat connections with either austenitic or carbon steel bolts. The model also considers the prying action of the column flange, addressing limitations in previous models for web cleat connections. This modified model provides a conservative yet reliable prediction of connection performance in fire conditions, ensuring safety without overly conservative estimations at the joint level. Zhan et al. [92] presented a generalized component-based model (CBM) for extended endplate (EP) joints to evaluate their performance in fire-induced progressive collapse scenarios. The model captures the full-range nonlinear behaviour of EP joints, using simplified methods and trilinear force-deformation models for the panel and connecting zone.

The primary elements in a bolted end-plate connection can be modelled using equivalent T-stubs [73, 93], which have historically been used to represent components in the tension zone. Thus, the end-plate connection can be viewed as a combination of the column flange T-stub and the end-plate T-stub. Previous studies have identified three distinct failure modes [76] for a T-stub assembly, which are influenced by the ratio between the flange resistance and the bolt resistance. T-stub assemblies can fail in one of three possible modes:

1. Yielding of the T-stub flange, followed by yielding and fracture of the bolts.
2. A complete yielding mechanism in the T-stub flange.
3. The T-stub flange remains elastic until the bolts fracture.

The T-stub model serves as an effective, simplified approach to simulate the response of the tension zone in bolted joints, which significantly influences the overall deformability of the joint. The equivalent T-stubs consist of two T-shaped components connected by one or more rows of bolts through their flanges. Figure 1-12 depicts the possible failure modes of a T-stub specimen.

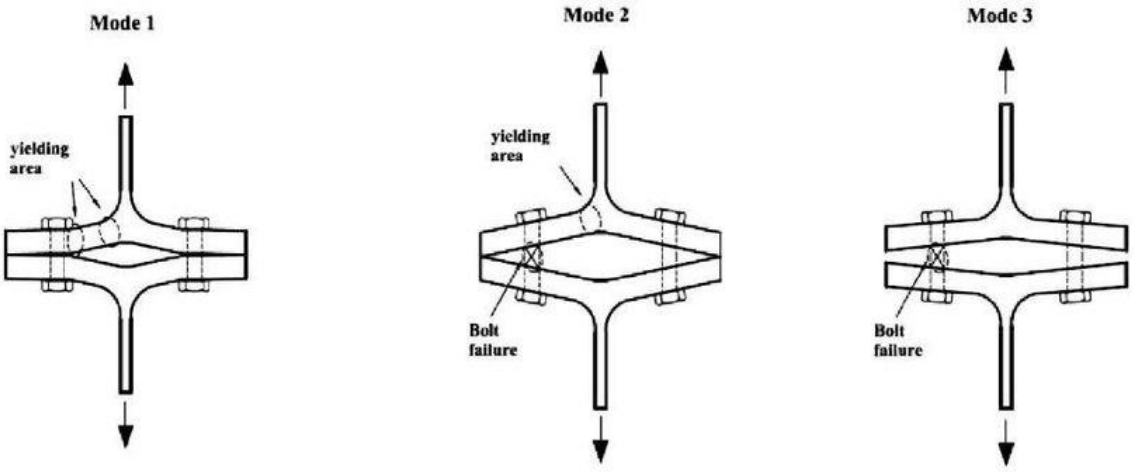

Figure 1-12. Three Failure Modes of T-Stub [94]

Analytical models were presented for predicting the moment-rotation curve of steel beam-to-column endplate connections, focusing on the T-stub component at ambient temperatures and under fire condition Heidarpour et al. [95] , Ribeiro et al. [96], Saberi et al. [97], Lyu et al. [98] , Zhang et al. [99], Barata et al. [100], Li et al. [101], Johan et al. [102], Li et al. [103], Gao et al. [104], Roy et al. [105] and Wang et al. [106]. The models accurately capture the force-deformation response of T-stubs and were validated against experimental and finite element results. While it reliably predicts initial stiffness and moment resistance.

1.7.2 Finite element method

For many years, considerable effort has been focused on modelling steel joints using finite element models. The finite element method is a robust tool that can precisely predict the mechanical behaviour of joints [107] . It is capable of addressing nonlinear material properties, large deformations, and the interactions between bolts and plates. Crucial factors influencing the accuracy of finite element modelling include the optimal mesh size, bolt simulation, element choice, material behaviour, and, most importantly, the modelling of contact and gap elements [108]. Numerical modelling of joints at elevated temperatures offers an alternative to

experimental testing for investigating joint behaviour. Various approaches can be used to model bolted and welded joints using finite element methods. Plates can be represented using solid or shell elements. However, modelling bolts are more complex in bolted connections. Several methods have been proposed by different authors in previous studies. Spyrou [76], [109] utilized a finite element model to predict joint behaviour under high temperatures by modelling the elements as 3D T-stubs. Kevin et al. [110] employed Abaqus software to recreate the fire event for the World Trade Center 5 building and analyse the fire behaviour of steel beam-to-column shear tab connections. The model did not simulate the fracture of connection components, with the plastic strain being used to indicate when the failure occurred in the connections. Schaumann et al. [111] introduced a detailed 3D numerical model of a bolted steel endplate connection, designed to simulate the structural behaviour under fire conditions by considering the interaction of all structural members. It incorporates nonlinear factors such as temperature-dependent material properties and is validated through experimental tests from the University of Sheffield in 2008, which included large deformations and fractures. Al-Jabri et al. [109] modelled steel flush endplate joints in the fire to generate their moment-rotation characteristics. Sarraj et al. [112] simulated the behaviour of fin-plate joints at elevated temperatures. Qiang et al. [113] modelled the beam-to-column high-strength steel endplate connections under fire conditions. Selamet et al. [114] investigated the behaviour of three types of shear joints (single-plate, single-angle, and double-angle joints) under fire conditions. Seif et al. [115] presented a finite element modelling method to simulate fracture in structural steel and bolt connections, such as those with connection plates and bolts, under elevated temperatures. It combines stress-strain relationships with a plastic strain-based failure criterion for element erosion. The method was calibrated using high-temperature experimental data on tensile coupon elongation at fracture. Hantouche et al. [116] explored the fire performance of steel double angle connections through computational models developed in Abaqus and validated by experimental data. The study examines the impact of load ratio, initial temperature, and connection placement on their behaviour at elevated temperatures. Findings reveal that double angle connections perform better than shear tab connections in fire, providing insights for improved design methods. Fischer et al. [117] developed and benchmarked 3D finite element models to predict the behaviour and failure of composite beams with simple (shear) connections under gravity loads and fire conditions, including heating and cooling phases. The models simulate detailed structural components such as steel beams, concrete slabs, and connection elements at elevated temperatures and are validated against experimental data. Comparisons show that the models

accurately predict deformation histories and failure modes. The validated model is recommended for parametric studies to complement experimental research on composite beams and simple connections under fire. In 2017, Fischer et al. [118] presented analytical parametric studies on the structural response of composite beams with simple connections under combined gravity loads and fire scenarios. Using 3D finite element models, the study examines various factors like connection type, slab reinforcement, and fire resistance rating. Results show no premature fracture failure leading to collapse for beams with proper fire resistance. The continuity of the composite slab and steel reinforcement significantly influences the system's performance and resilience during a fire. Gernay et al. [119] conducted a numerical study using SAFIR to assess the impact of semi-rigid joints on the global structural response at elevated temperatures. A key aspect of modelling connections using finite element methods is how to accurately simulate the behaviour of connectors, such as bolts and welds. Akagwu [120] examined the behaviour of bolted web-flange steel splice connections when exposed to elevated temperatures using the numerical modelling method. The study identified the failure modes of these connections and analysed the key factors that influence their response under extreme temperature conditions. Zheng et al. [121] analyzed the failure mechanism and collapse resistance of partially restrained steel connections (angle steel-bolted) in fire-exposed frames. It reveals that thermal expansion causes all connection configurations to enter the compressive arching action (CAA) stage, and higher column load ratios shift damage from the connection to the column. The study highlights the importance of rotational constraints and the role of negative axial force in enhancing flexural resistance. A theoretical method is proposed to predict failure mechanisms, improving the identification of weak components and anti-collapse strategies in similar structures.Natesh et al. [122] investigated the performance of double-angle shear connections in composite floor systems under fire conditions using numerical analyses. It identifies two main failure triggers: excessive deformation from web buckling during heating and beam contraction during cooling. The study suggests design improvements, such as stiffened angles and slotted holes, to enhance fire performance and prevent premature connection failure. Huseyin et al. [123] emphasized the benefits of using explicit solvers in structural fire analysis to address challenges like convergence errors and large deflections. A comparison between implicit and explicit solvers using Abaqus is presented, along with validation for multi-bolted connections under fire conditions. The explicit solver simplifies modelling, especially for bolted connections, and the study offers optimal mesh density. It provides a helpful guide for researchers, reducing time spent on iterative debugging in fire

analysis. Rezaeian et al. [124] investigated the fire performance of welded top-seat angle connections in steel structures using a finite element model. Parametric studies show that adjusting gap size, top angle size, and thickness significantly impacts fire behaviour and beam deflection. The findings enhance the understanding of fire resistance for these connections, contributing to design improvements for fire conditions.

1.7.3 Component-based finite element method

The Component-Based Finite Element Model (CBFEM) is an advanced approach that integrates the component model with the finite element model analysis. It is implemented in several structural engineering software packages using SAFIR, VULCAN and IDEAStatiCa providing a powerful tool for analysing complex structures. This innovative method is beneficial for evaluating steel bolted assemblies, offering enhanced accuracy and flexibility in modelling their behaviour. CBFEM considers ambient [125, 126] and elevated temperatures [127-129], making it suitable for various real-world applications, especially in environments where thermal conditions play a crucial role. By combining the strengths of component modelling and finite element analysis, CBFEM enables more detailed and reliable predictions of the performance of bolted joints under different loading conditions. It simplifies the representation of structural components, facilitating the analysis of complex bolted connections. The model allows engineers to study the behaviour of steel structures with a high level of precision, offering insights into their strength, stability, and durability. CBFEM also provides a comprehensive framework for evaluating the effects of temperature variations, which is essential for the design of structures exposed to fire or high-heat conditions. This modelling approach has gained significant attention in the last decade due to its ability to address the limitations of conventional methods. CBFEM contributes to safer and more efficient designs in the construction and engineering industries by improving the understanding of bolted assemblies. As a result, it represents a major advancement in the field of structural analysis, particularly for bolted steel assemblies in challenging environments.

1.8 Conclusion

The literature review has analysed the current state of knowledge regarding the behaviour of bolted steel connections when subjected to elevated temperatures and fire events. This analysis has provided valuable insights into the complex interactions between temperature effects and

the mechanical properties of steel. A significant portion of the reviewed studies consistently emphasizes the critical role of temperature-dependent material properties in influencing the performance of bolted steel connections under fire conditions. These studies highlight the progressive degradation of steel's strength and stiffness as temperatures rise, with a marked reduction in load-carrying capacity occurring when temperatures exceed approximately 400°C. The loss of steel strength and stiffness at high temperatures is a key factor that leads to structural failure or compromised performance of bolted connections during fire events. Furthermore, the review identifies a gap in research were only restricted models for bolted connections under fire conditions have been studied. In this work, we focus on the behaviour and the characterisation of bolted angle connections used in braced steel frames which has not been tackled previously.

CHAPTER 2. ANGLE STEEL GUSSET CONNECTIONS

2.1 Introduction

Angle gusset steel connections are a fundamental type of joint that is generally used in steel structures to allow efficient load transfer between structural components. In the connection, the gusset plate serves as a central tie component, with angle sections in L-shaped steel sections bolted or welded into it to achieve a rigid or semi-rigid joint with resistance to axial and shear forces. Angle sections are simple to fabricate and connect to other members because of their geometry, and their structural efficiency can resist tension and compression forces. Such contacts can be engineered to accept load directions and magnitudes that may vary, so they are useful in the context of intricate structural systems where forces must be transferred in multiple directions.

2.2 Comprehensive overview of the usage of angles in steel structures

2.2.1 Common Applications in Buildings, Bridges, and Towers

In the field of building construction, angle steel is a fundamental component used for forming strong, reliable connections between structural elements [130]. It is commonly incorporated into truss assemblies [131], where it functions as a member that handles both tension and compression, depending on its location within the system. Angle sections are also widely used in floor framing, acting as connectors between primary and secondary framing members. This helps distribute vertical loads and enhances the overall stability of the floor system. Furthermore, angle steel plays a crucial role in connecting beams to columns [132, 133], where it is used to create moment-resisting or simple shear connections, depending on the structural demands. Also, angle connections play an essential component in braced stability systems, particularly in steel structures, where they provide a practical means of connecting bracing members to beams and columns. These connections typically use L-shaped steel angles Figure 2-1, which can be either bolted or welded, depending on the design requirements. Their primary function is to transfer axial forces from the bracing elements into the structural frame, helping to resist lateral loads such as wind or seismic forces. In addition to their strength, angle connections offer a certain level of flexibility, which is especially useful in seismic zones where energy dissipation and ductility are important [134].

Figure 2-1. Modern seismic brace connection [135]

In bridges [136], especially in truss and girder systems, steel angle members create crucial joints that play a vital role in the effective transfer of loads throughout the structure. These angle members are typically positioned at the intersections of structural elements, where they help distribute forces between vertical, diagonal, and horizontal components. The connections made using angle sections often experience significant axial forces, either in tension or compression, depending on the location and type of loading. Due to these demanding force conditions, the design and fabrication of such joints require high levels of precision to ensure proper alignment and performance. Accurate engineering is essential not only for strength but also to prevent premature failures caused by stress concentrations or fatigue. These joints must also be capable of withstanding dynamic loading conditions, including the constant movement and vibration from vehicular traffic. Environmental factors such as temperature fluctuations, wind, and moisture also impose additional stresses over time. Therefore, the materials and connection details must be selected and designed to ensure long-term durability and structural integrity. Overall, steel angle members in bridge systems are key components that contribute significantly to the reliability and safety of the structure.

Figure 2-2. Brace connections in the Bridges [137]

In towers Figure 2-3, especially lattice-type transmission towers and communication masts, angle steel is widely used due to its high strength-to-weight ratio, structural efficiency, and ease of fabrication. These towers rely on a network of interconnected angle sections arranged in triangular patterns, which provide excellent stability and resistance to wind and seismic forces. The lightweight of angle steel helps reduce foundation loads and simplifies transportation and handling. Bolted connections are the predominant method of joining members, allowing for quick assembly in the field without welding. This is particularly advantageous in remote or elevated locations with limited access and equipment. Bolted joints also make maintenance easier, enabling straightforward inspections, tightening, or part replacement. Standardized angle profiles support modular construction, reducing manufacturing and construction time. Additionally, angle members are typically hot-dip galvanized to enhance durability in outdoor environments. The result is a cost-effective, strong, and maintainable structure suited for critical infrastructure. Angle steel continues to be a preferred choice for tower applications worldwide.

Figure 2-3. Angle steel bolted connection in a transmission tower [138]

2.2.2 Types of Angle Sections: Equal vs. Unequal Angles

In structural steelwork, angle sections are categorized primarily into equal-leg angles and unequal-leg angles, based on the relative lengths of their legs. These profiles, commonly referred to as " L-sections " or " angle irons, " are hot-rolled steel elements widely used in construction and engineering applications due to their versatility and strength.

According to EN 10056-1:2017 [139], equal leg angles have both legs of the same length and are designated as L a × b × t, where a and b is the length of each leg and t represents the uniform thickness of the material as indicated in Figure 2-4. These sections are symmetrical, making them suitable for applications that require uniform stress distribution, such as bracing systems, trusses, and structural frameworks.

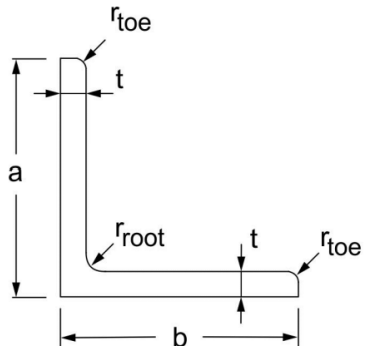

Figure 2-4. Equal leg angle [139]

On the other hand, unequal leg angles feature legs of different lengths and are denoted as L a × b × t, with *a* and *b* indicating the long and short leg lengths, respectively as illustrated in Figure 2-5. These asymmetrical sections are particularly useful in situations where design constraints, such as space limitations or directional loading, demand flexibility. For example, unequal angles are often used in composite beams, corner reinforcements, or as part of load-bearing frames where alignment with other structural elements is crucial.

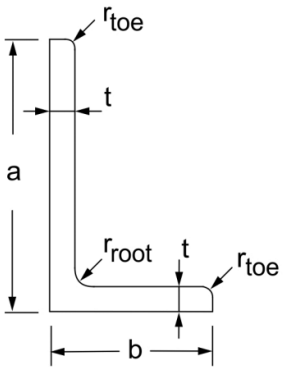

Figure 2-5. Unequal leg angle [139]

EN 10056-1-2017 [139] not only standardizes the geometrical dimensions of these profiles, including leg lengths, thicknesses, and internal corner radii, but also sets the permissible tolerances for manufacturing. These include straightness, squareness, and twist tolerances, which are essential for ensuring proper fit-up during assembly and reliable performance in structural applications. The internal radius (root radius) and optional toe radius (outer radius) are also specified to control stress concentration points and facilitate fabrication processes such as welding or bolting.

2.2.3 Connection methods and structural configuration

The performance of angle assembly members under tension loading is not only influenced by their cross-sectional properties, but also by the method of connection and the structural configuration used to transmit the axial force into the member. The two primary methods of connecting angle members are bolting and welding, each with its structural behaviour and implications for design.

Bolted angle members are typically connected using gusset plates, which serve as intermediate elements to transfer loads between members. The bolts are usually arranged in single-row or

staggered configurations, placed through one leg of the angle. This common practice leads to an eccentric connection, as the load is applied through the bolt group on one leg, while the centroid of the angle section is offset from this load path. This results in a combination of axial tension and secondary bending within the member, a condition known as eccentric loading.

Figure 2-6 Bolted angle steel in braced system [140]

Welding offers a more direct and often stiffer connection, which can eliminate or reduce the eccentricity commonly associated with bolted joints. Angle members can be welded along one or both legs directly to gusset plates or other structural elements Figure 2-7. When welded on both legs and along their full length, the axial force can be transmitted more evenly through the centroid, resulting in pure tension loading with minimal secondary effects.

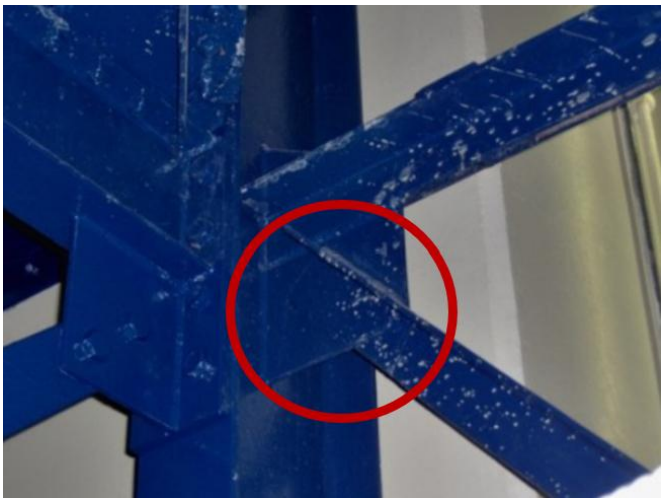

Figure 2-7. Welded Angle-to-Gusset Connection in a Steel Bracing System [141]

The structural configuration of angle tension members significantly affects their performance, particularly in terms of load distribution, eccentricity, and deformation. Single-angle members connected through one leg often experience eccentric loading, introducing secondary bending and stress concentrations. In contrast, double-angle members arranged back-to-back on either side of a gusset plate provide more centric loading, reducing bending effects and improving axial strength. The orientation of angles, whether toe-in or toe-out, also influences connection detailing, fabrication ease, and stress flow. Toe-in setups are more compact, while toe-out setups allow better access for welding or bolting. Symmetrical configurations help balance internal forces and minimize twisting. Proper alignment with the load path ensures effective force transfer. Overall, thoughtful structural configuration enhances strength, stability, and efficiency in tension applications.

2.3 Shear lag phenomenon

2.3.1 Definition and significance in steel design

Shear lag [142] in bolted steel connections occurs when an applied tension force utilizing bolts is not uniformly transmitted across the entire cross-section of the member being connected, especially in wide or asymmetrical sections. Since the load is transmitted at discrete points, normally via bolts or welds, only the portion of the cross-section in intimate contact with these fasteners immediately begins to resist the load. The other parts, particularly those farther from the row of bolts, are slower or "lag" in taking their share of the load. This produces a non-uniform stress distribution, with the connected parts being more highly stressed and the unconnected regions taking less of the overall resistance to tension. Thus, the effective net area of the cross-section to resist the tensile load is less than the total net area and results in a so-called loss in effective net area. In structural construction, this effect is particularly important because it can significantly reduce the tensile strength of members such as angles, channels, or wide plates, especially if the connection is unilateral or along a partial cross-section. Design specifications like AISC or Eurocode allow for shear lag by way of reduction factors or effective area formulas, such that the lesser capacity of the member is properly taken care of in proportioning economical and safe steel members.

2.3.2 Key research findings in shear lag effects

Since 1934, various studies have investigated the shear lag phenomenon in steel bolted assemblies in terms of stress distribution, effective net area, and tensile capacity of numerous structural members. Analytical models, experimental tests, and code-based provisions have been developed by researchers to better understand and compute the influence of shear lag, particularly for asymmetrical as well as partially connected sections such as angles, tees, and wide plates [142-151]

2.3.3 Parameters influencing shear lag

Shear lag of bolted connections refers to uneven stress distribution along the axis within joined members or plates, specifically where the transmission of forces may not be uniform, optimally for the entire cross-section. Shear lag holds immense significance when applied to tension members and can contribute significantly to reduced design strength. Multiple parameters establish this phenomenon in shear bolted connections:

2.3.3.1 Connection geometry

In bolted assemblies, shear lag results from an unequal distribution of stress caused by specific geometric and connection-related elements. One major factor is the eccentricity of the load path; when the applied force does not act through the centroid of the connected member, stress becomes concentrated in specific areas. The length and width of the connected plate also influence shear lag; wider or shorter plates have a reduced ability to distribute load evenly, intensifying the effect. Edge distance and bolt spacing are important. When bolts are too close to the edge or each other, the stress transfer becomes less efficient, leading to greater shear lag. Furthermore, the number and arrangement of bolts can increase the problem; if bolts are placed far from the member's centroid, this creates additional eccentricity. These factors combined can significantly impact structural performance and must be addressed in design to ensure uniform load transfer and prevent localized failures.

2.3.3.2 Members cross-section

The cross-sectional shape of a member plays a crucial role in influencing shear lag in bolted assemblies. Members with open or unsymmetrical shapes, such as angles, channels, and T-

sections, often experience more shear lag compared to flat plates, as the load path is not evenly distributed across the section. The shape of the cross-section determines how effectively the applied force can be transmitted through the member. Additionally, the thickness of the connected elements affects shear lag, as thicker plates are generally more resistant to deformation and can help distribute stress more uniformly. Thinner elements, on the other hand, may deform more easily, exacerbating the uneven stress distribution. Another important factor is the location of the connection within the member's cross-section.

2.4 Structural analysis of bolted-angle connections

Angle gusset bolted connections under tension transfer loads primarily through bolt shear and bearing, with the eccentric configuration of the angle introducing additional stresses. Their structural behaviour depends on gusset plate stiffness, bolt layout, and stress concentrations around bolt holes. Common failure modes include bolt shear, bearing failure, block shear, and net-section rupture of the angle [152].

2.4.1 Failure modes and mechanisms

To better understand the structural response of angle gusset bolted connections under tension, it is essential to examine the different ways in which these joints can fail. The applied tensile forces create complex stress interactions that may activate distinct resistance mechanisms. These mechanisms give rise to several potential failure modes, which are discussed in the following sections.

a. Bearing failure

Bearing failure occurs when the plate material around a bolt hole is crushed due to high compressive stresses from the bolt shank. It is characterized by local deformation or elongation of the hole rim rather than complete rupture. This mode is strongly influenced by plate thickness, bolt diameter, and edge distances. Design standards limit bearing stress through formulas based on bolt size and plate strength. Insufficient end or edge distances can lead to excessive deformation or tear-out. Figure 2-8 illustrates the bearing failure mechanism in an angle bolted connection.

Figure 2-8 Bearing failure in bolted angle steel connections [138]

b. Bolt shear failure

Bolt shear failure occurs when the shear force in a connection exceeds the bolt's shear capacity, leading to fracture along defined shear planes. It is frequently observed in tension connections where bolts resist the applied load directly. The resistance depends on bolt material, diameter, and whether the load is transferred through single or double shear planes. Figure 2-9 illustrates the bolt shear failure mechanism in angle connections.

Figure 2-9. Bolt in shear failure mode [138]

c. Block shear failure

Block shear failure is a mixed failure mode that combines tension rupture on one path and shear yielding or fracture on an adjacent path, forming a block of material torn out around the bolt group. It typically occurs when bolts are placed close to the plate edge, reducing the net shear area. The capacity depends on plate thickness, bolt arrangement, and material strength.

Figure 2-10 illustrates the block shear failure mechanism in angle connections.

Figure 2-10. Block shear failure in angle connection [153]

d. Net section tension failure

Figure 2-11 shows the net section tension failure in angle connections. This mode develops when the tensile force causes fracture across the reduced net area weakened by bolt holes. The crack typically propagates along the bolt line, perpendicular to the applied load, where stresses concentrate. Its occurrence is governed by hole diameter, bolt spacing, edge distance, and the tensile strength of the angle material.

Figure 2-11. Net section tension failure [154]

2.5 Design provisions for the load resistance of bolted angle steel assemblies

2.5.1 Design guidelines

The design approach presented in references [8, 10] and [155, 156] provides a comprehensive set of formulas and guidelines for determining the ultimate resistance of bolted assemblies, particularly those involving angle connections. This method consists of the specification of critical parameters such as bolt spacing, edge and end distances, and bolt hole diameter, all of which directly influence the strength and failure mode of the connection. Additionally, the number of angles used, whether a single-angle or double-angle configuration, is considered, as it affects load distribution and stiffness. The total number of bolts in the connection is also a key factor, playing a significant role in resisting applied forces and determining the overall capacity.

2.5.2 Design resistance at ambient temperature

Design guidelines for carbon steel single angles in tension connected by a single row in the direction of loading are provided by Eurocode 3 part 1- 8 [8]. The following equations:

- **Net section capacity of angles joined by one bolt:**

$$N_{u,Rd} = \frac{2(e_2 - 0.5d_0)tf_u}{\gamma_{M2}} \tag{13}$$

- **Net section capacity of angles joined by more than one bolt:**

$$N_{u,Rd} = \frac{\beta A_{net} f_u}{\gamma_{M2}} \tag{14}$$

Where:

γ_{M2} is the partial safety factor with a Eurocode recommended value of 1.25; t represents the angle thickness; f_u the ultimate resistance; d_0 is the bolt hole diameter; β is a reduction factor dependent on the pitch P1 and the number of bolts; it may be determined by linear interpolation.

- **Shear resistance of a bolt per shear plane:**

$$F_{v,Rd} = \frac{\alpha_v f_{ub} A}{\gamma_{M2}} \tag{15}$$

Where

α_v equal to 0.6 according to the Eurocode; f_{ub} is the ultimate strength of the bolt; A is the tensile stress area of the bolt.

- **Bearing resistance per bolt:**

$$F_{b,Rd} = \frac{K_1 \alpha_b f_u dt}{\gamma_{M2}} \tag{16}$$

Parameters α_b and $k1$ are determined considering mainly geometrical parameters as given below:

perpendicular to the direction of load transfer for edge and inner bolts, respectively

$$K_1 = \min\left(2.8\frac{e_2}{d_0} - 1.4\frac{P_2}{d_0}, 2.5\right) \tag{17}$$

$$K_1 = \min\left(1.4\frac{P_2}{d_0}, 2.5\right) \tag{18}$$

in the direction of load transfer

$$\alpha_b = \min\left(\alpha_d, \frac{f_{ub}}{f_u}, 1\right) \tag{19}$$

$$\alpha_d = \frac{e_1}{3d_0} \text{ for end bolts} \tag{20}$$

$$\alpha_d = \frac{P_1}{3d_0} - 0.25 \text{ for inner bolts} \tag{21}$$

The design equations for calculating the block shear resistance are as follows:

$$V_{eff,1,Rd} = \frac{f_u A_{nt}}{\gamma_{M2}} + \frac{f_y A_{nv}}{\sqrt{3}\gamma_{M0}} \text{ for centric load} \quad (22)$$

$$V_{eff,1,Rd} = 0.5\frac{f_u A_{nt}}{\gamma_{M2}} + \frac{f_y A_{nv}}{\sqrt{3}.\gamma_{M0}} \text{ for excentric load} \quad (23)$$

Where: A_{nt} is the net area subjected to tension, A_{nv} is the net area subjected to shear, γ_{M0} is the partial safety factor equal to 1.

The design equation for the gusset plate resistance in tension loading according to the Eurocode 3 part 1-1[9] is given by :

$$N_{t,Rd} = min\begin{cases} N_{pl,Rd} = \dfrac{Af_y}{\gamma_{M0}} \\ N_{u,Rd} = \dfrac{0.9A_{net}f_u}{\gamma_{M2}} \end{cases} \quad (24)$$

2.5.3 Design resistance at elevated temperature

Considering the mechanical properties of steel at elevated temperatures [10], the simplified design resistance under fire conditions is derived from the corresponding expressions at ambient temperature [8]. The resistance of the bolted angle gusset plate at a given temperature θ is obtained by reducing the 20 °C resistance values using appropriate temperature-dependent reduction factor $K_{b,\theta}$ for bolts and $K_{y,\theta}$ for steel, both evaluated at the temperature θ reached at time *t*. The values of these factors are presented in Table 2-1. Equations (25–29) define the bearing resistance, ultimate resistance, bolt shear resistance, and block shear resistance, while explicitly accounting for the influence of elevated temperature.

$$F_{b,t,Rd} = F_{b,Rd}.K_{b,\theta} \quad (25)$$

$$N_{u,Rd,\theta} = N_{u,Rd}.K_{y,\theta} \quad (26)$$

$$F_{v,t,Rd} = F_{v,Rd}.K_{y,\theta} \quad (27)$$

$$V_{eff,1,Rd} = V_{eff,1,Rd}.K_{y,\theta} \quad (28)$$

$$N_{t,Rd} = N_{t,Rd}.K_{y,\theta} \quad (29)$$

Table 2-1. Properties of structural steel at high temperatures

Steel temperature (°C)	Reduction factors for steel at temperature θ_a, $K_{y,\theta}$	Reduction factors for bolt at temperature θ_a, $K_{b,\theta}$
20	1.000	1.000
500	0.780	0.550
700	0.230	0.100

2.6 Case studies

Angle gusset connections are denoted as cases of study from 1 to 6, Figure 2-12 describes the connection according to the Eurocode 3 [8] configuration. The geometric characteristics of the investigated connection configurations are summarized in Table 2, which provides the detailed dimensions and parameters adopted in the analysis. In order to assess the structural response under both ambient and fire conditions, a uniform temperature distribution was assumed throughout the connection components. The reference ambient case was taken at θ = 20 °C, while elevated temperature scenarios were simulated at θ = 500 °C and θ = 700 °C, which are representative of typical ranges encountered in structural fire design studies. For the material properties, all gusset plates and angle members were assumed to be made of structural steel grade S235, characterized by a yield strength of f_y= 235 MPa. The connections were fastened using bolts with a diameter of 16 mm, considering two strength classes: grade 8.8 bolts with a yield strength of f_{yb}=640 MPa, and grade 6.8 bolts with a yield strength of f_{yb}=480 MPa. In addition, the elastic behaviour of both steel and bolts was defined by adopting a conventional modulus of elasticity equal to 210 GPa.

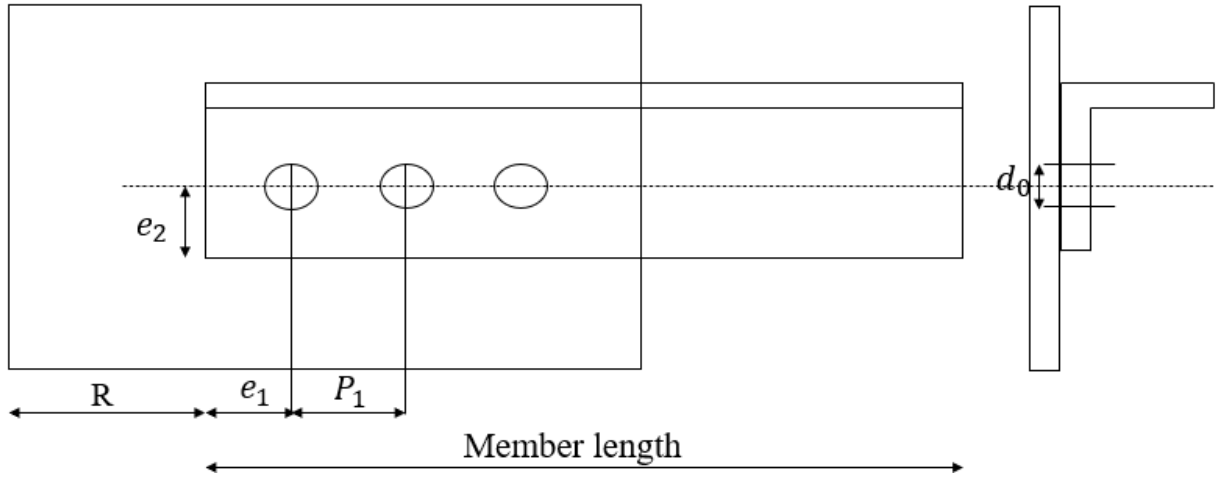

Figure 2-12. Definition of symbols for angles connections (Case with 3 bolts)

Table 2-2 presents the geometric parameters of the studied cases, offering a comprehensive description of their dimensional properties and structural specifications that serve as the basis for the subsequent analysis.

Table 2-2. Gusset angle connections description for all studied Cases

Case of study	Angle size (mm)	Gusset plate dimensions (mm)	No. of Bolt	End distance $'e_1'$ (mm)	Pitch, $'p_1'$ (mm)	R (mm)
1	UA 100X100X10	200X200X15	1	50	-	100
2	UA 100X100X10	240X200X15	2	30	60	115
3	UA 100X100X10	260X200X15	3	35	75	120
4	2 x UA 100X100X10	200X200X15	1	50	-	100
5	UA 70X70X7	240X100X10	2	30	60	120
6	UA 70X70X7	240X100X10	2	25	40	120

2.7 Preminaly design & checking according to Eurocode 3

Table 2-3 presents the shear strength values for both types of bolts without applying any safety factors, thereby allowing a direct comparison of their inherent load-carrying capacities. As the temperature increases, a significant reduction in strength is observed. At 500 °C, the shear strength of the bolts decreases to approximately 55% of their original room-temperature capacity, while at 700 °C this reduction becomes much more severe, dropping to only about 10% of the initial value. In parallel, the steel material used in the connections also undergoes

strength degradation under elevated temperatures. At 500 °C, the connections retain only about 78% of their ambient-temperature strength, corresponding to a 22% loss, whereas at 700 °C they maintain just 23% of their original capacity, which represents a reduction of about 77%. These results highlight the pronounced vulnerability of both bolts and steel connections to elevated temperatures, with bolts exhibiting a sharper decline in performance compared to the connection material itself. The cases were designed per Eurocode 3 to anticipate failure mechanisms, which are then observed in the FE model [157].

Table 2-3. Designed models at 20°C,500°C,700°C according to EC3

Studied Scenario	Shear résistance (kN)		Bearing resistance (kN)	Block shear Resistance (kN)	Gusset resistance (kN)	Angle resistance (kN)
	Bolt 8.8	Bolt 6.8				
T=20°C						
Case (1)	75	64	320	199	705	575
Case (2)	150	128	160	238	705	276
Case (3)	225	191	240	398	705	244
Case (4)	150	128	320	199	705	1150
Case (5)	150	128	143	181	235	93
Case (6)	150	128	93	56	235	93
T=500°C						
Case (1)	41	35	250	155	550	449
Case (2)	83	70	125	185	550	215
Case (3)	124	105	188	310	550	190
Case (4)	83	70	250	155	550	898
Case (5)	83	70	111	141	184	73
Case (6)	83	70	111	37	184	73
T=700°C						
Case (1)	8	6	74	46	163	133
Case (2)	15	13	38	55	163	64
Case (3)	23	19	56	91	163	70
Case (4)	15	13	74	46	163	265
Case (5)	15	13	33	41	54	21
Case (6)	15	13	33	15	54	21

2.8 Conclusion

This chapter established the scientific background for bolted single-angle connections to gusset plates under tensile loading and elevated temperatures. The literature review highlighted the complex behaviour of these connections, mainly governed by geometric eccentricity and non-uniform stress distribution. In particular, the shear lag phenomenon was identified as a key factor reducing the effective resistance of the angle, depending on the connection configuration and bolt arrangement. Based on this framework, the studied cases were designed using the Eurocode 3 guidelines (EN 1993-1-8 and EN 1993-1-2). This standard provides comprehensive methodologies for the analysis and design of such connections, accounting for performance under both ambient and elevated temperature conditions. The primary focus of the study was to evaluate the ultimate tensile strength of bolted angle steel assemblies subjected to axial tension, with an emphasis on the effects of varying geometric configurations and bolt types.

CHAPTER 3. FINITE ELEMENT MODELLING AND SIMULATION

3.1 Introduction

The finite element method (FEM) is a widely used numerical tool for analysing complex structural behaviour. In the modelling of steel connections, FEM enables detailed simulation of non-linearities, contact interactions, and temperature-dependent responses. K.S. Virdi's *Guidance on Good Practice in Simulation of Semi-Rigid Connections by the Finite Element Method* [158] outlines essential modelling practices for achieving reliable and accurate results, particularly in semi-rigid and bolted joints. By examining various connection parameters, the finite element model serves as an effective tool for extending research beyond the limitations of experimental programs and enhancing our understanding of connection behaviour. This chapter provides a detailed description of a comprehensive three-dimensional finite element model using Ansys APDL Software [7] to predict the behaviour of bolted steel angle gusset connections effectively. By contrasting the findings of the FE calculation with experimental data [159, 160] based on load-displacement curves, evaluations of this model have been provided.

3.2 Methodology

Finite element modelling presented in most numerical studies from the literature simulate the connections behaviour considering appropriate material representation, element type, contact definition, and mesh refinement to ensure reliable results.

3.2.1 Material properties

The material properties adopted for the connection model components are as follow: Young's modulus of 210,000 MPa and a Poisson's ratio (ν) of 0.3. The gusset plate and angle members were modelled using S235 structural steel. Two types of bolts were considered in the analysis: high-strength grade 8.8 bolts and ordinary grade 6.8 bolts. The yield stress and ultimate tensile strength of S235 steel, as well as those corresponding to the 8.8 high-strength bolts and 6.8 ordinary bolts, were assumed based on their nominal material characteristics. The values are listed in Table 3-1.

Table 3-1 Material Properties

Material type	S235	Bolt 8.8	Bolt 6.8
Yield strength [N/mm²]	235	640	480
Ultimate strength [N/mm²]	360	800	600

In this study, the stress–strain behaviour of steel was modelled in accordance with the provisions of Eurocode, as illustrated in Figure 3-1. The Young's modulus, proportional limit, and yield strength of carbon steel at elevated temperatures were reduced using the temperature-dependent reduction factors specified in Eurocode [10]. For simplification at the design stage, the constitutive material model adopted in the numerical simulations does not account for the linear material softening between 15% and 20% strain that is included in the Eurocode model for steel at both ambient and elevated temperatures. At elevated temperatures, the stress–strain relationship of steel undergoes significant modifications compared to its behaviour at room temperature. Instead of exhibiting a linear–perfectly plastic response as under ambient conditions, the model prescribed by EN 1993-1-2 [10] adopts an elastic–elliptic–perfectly plastic form. Furthermore, to ensure numerical stability in advanced calculation models, a linear descending branch is incorporated at large strain levels.

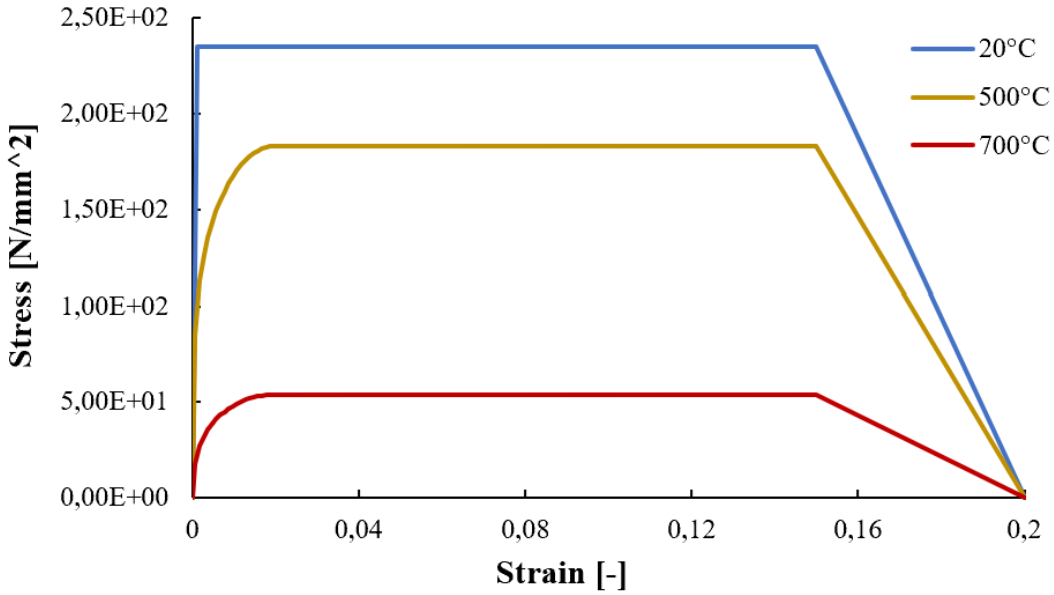

Figure 3-1. Material Behaviour of Plate and Angle Members

For structural bolts, a bilinear material model is adopted, where yielding begins at the strain εp corresponding to the yield strength. Beyond this point, the response is idealized as perfectly plastic until failure. In accordance with EN ISO 898-1 [161], the ultimate elongation of the bolt material is approximated as 25% of the nominal ultimate elongation specified for the bolt class. The same modelling approach is applied at elevated temperatures, with material properties reduced according to the Eurocode reduction factors. Figure 3-2 illustrates the material models

adopted for bolts in the solid finite element model under both ambient and elevated temperature conditions.

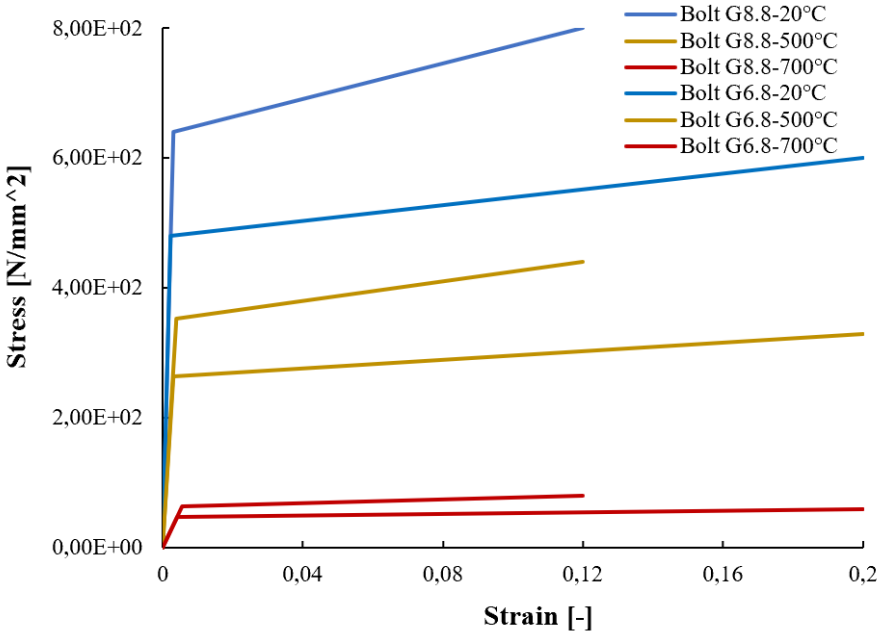

Figure 3-2. Material Behaviour of the bolts

3.2.2 Element type

Solid elements are widely adopted in finite element modelling of structural components due to their ability to capture three-dimensional stress states. In this study, the SOLID185 element was employed to represent all components of the connection assembly, including the gusset plate, angle sections, and bolts. This element type has eight nodes, each with three translational degrees of freedom in the x, y, and z directions. SOLID185 can account for material and geometric nonlinearities, including plasticity, hyperelasticity, stress stiffening, large deflection, and large strain behaviour, thereby ensuring its suitability for simulating the complex behaviour of connections under elevated temperatures, as illustrated in Figure 3-3.

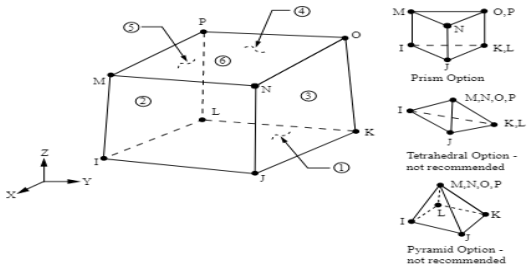

Figure 3-3. Solid 185 [162]

To ensure accurate representation of the connection assembly, an appropriate meshing strategy was adopted for each component, as illustrated in Figure 3-4. The gusset plate and angle sections were discretized using a relatively fine mesh to capture stress gradients, particularly in regions near bolt holes and connection interfaces. Bolts were meshed with higher refinement around the shank and threads to accurately simulate load transfer and local stress concentration. A coarser mesh was applied to regions away from critical stress zones in order to optimize computational efficiency without compromising accuracy. Transition meshing techniques were also used to provide smooth element size variation between refined and coarse zones, thereby improving convergence stability and ensuring reliable finite element results.

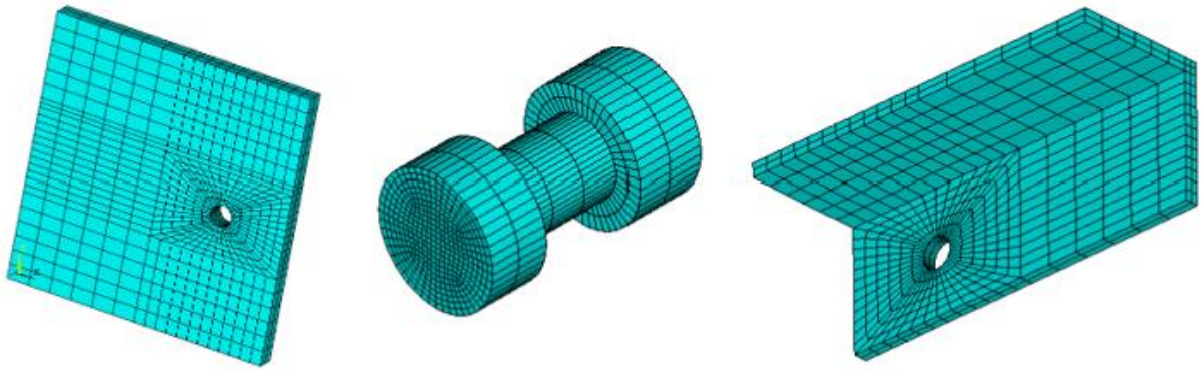

Figure 3-4. Mesh patterns for the bolt, plate and the angle used in solid model

3.2.3 Contact

Numerical modelling of bolted connections requires accurate representation of contact interactions between components. In this study, surface-to-surface contact was adopted to simulate the interfaces between bolt, plates, and gusset Figure 3-5.

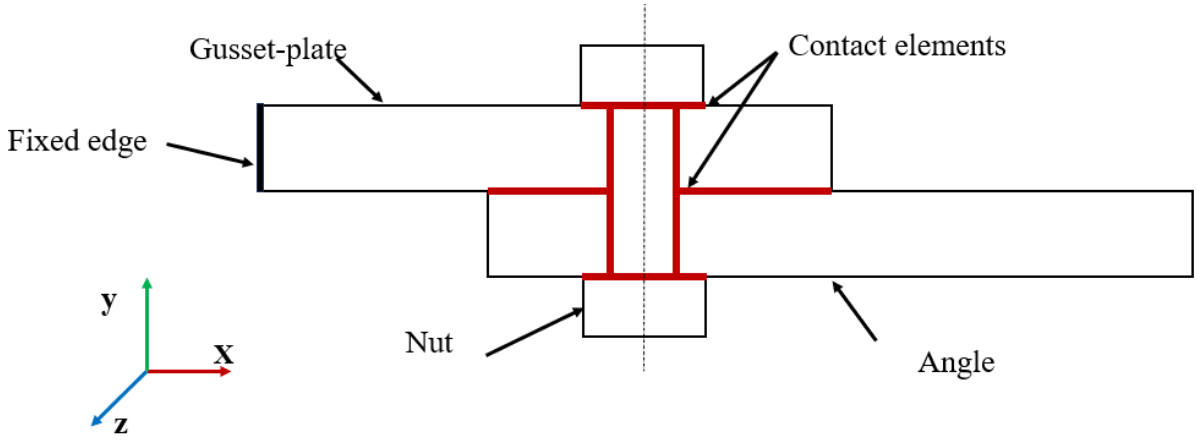

Figure 3-5. Contact surface distribution (Plan on angle gusset connection)

The 3D target element (TARGE170) defined the target surfaces, while the 3D contact element (CONTA174) represented the deformable regions, allowing simulation of sliding, separation, and frictional effects. Critical interfaces included bolt shank-to-hole, bolt head-to-plate, bolt nut-to-gusset, and angle-to-gusset surfaces, with the contact zones illustrated in the software simulation Figure 3-6. A Coulomb friction model with a coefficient of 0.2 was applied to capture sliding behaviour and ensure realistic load transfer. Simulating contact in ANSYS APDL is challenging but can achieve satisfactory accuracy with proper arrangements.

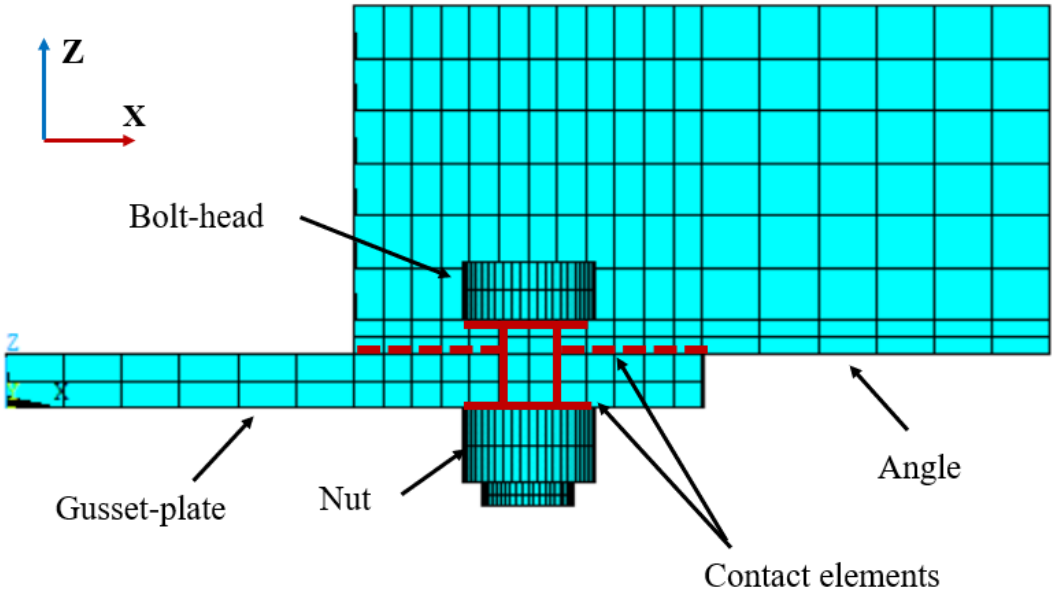

Figure 3-6. Contact regions

3.2.4 Boundary conditions

To ensure that the assembly remained within the load plane, appropriate boundary and loading conditions were defined in the numerical simulations as indicated in Figure 3-7. The support constraints were applied by restraining the degrees of freedom at selected nodes, where displacements were fixed in the three translational directions (Ux = 0, Uy = 0, Uz = 0). Additionally, the nodes along a reference line on the upper side of the gusset plate were restrained in the out-of-plane direction (Uz = 0) to prevent rigid body motion and maintain numerical stability. The external load was applied incrementally as a time-dependent function, ensuring gradual convergence of the nonlinear solution. This load was distributed to the nodes of the angle section in the horizontal direction, simulating the applied force on the connection in a realistic manner. The adopted loading strategy allowed the model to capture both the initiation and progression of nonlinear effects under increasing load.

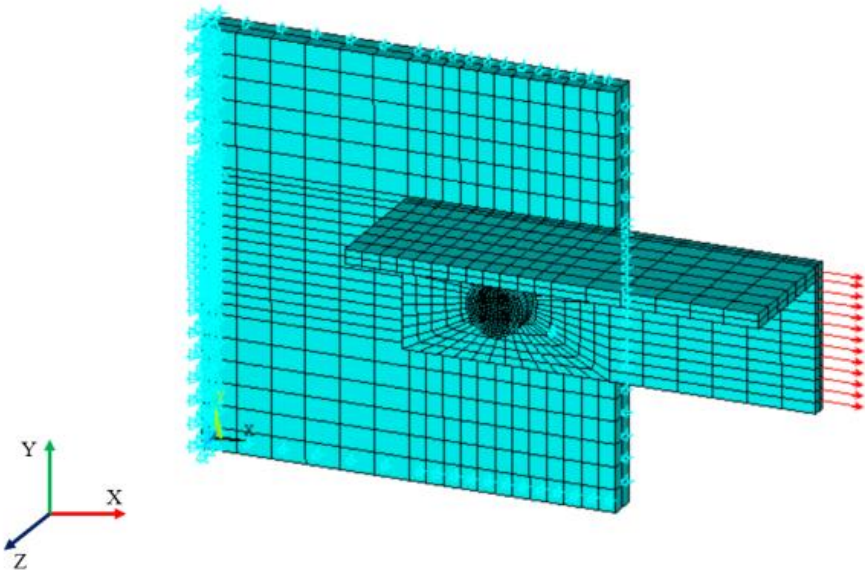

Figure 3-7. Details of the FE Model with applied load and boundary condition

3.2.5 Analysis method

In this study, material, geometric, and contact nonlinearities were modelled in ANSYS APDL using the PLASTIC, NLGEOM, and CONTACT PAIR commands. A static analysis with displacement control was performed, where the Newton–Raphson method solved the nonlinear problem through load increments and iterations. Contact algorithms, which check the state of slave nodes (open, closed, stuck, or sliding), make the analysis computationally demanding. Convergence difficulties often arise, requiring smaller increments and repeated iterations to achieve equilibrium.

The organigram Figure 3-8 presents the sequential steps of the ANSYS APDL analysis procedure. The process starts with the definition of the geometric model, followed by the development of the finite element model and the specification of contact elements. Subsequently, load and boundary conditions are introduced, which are divided into two parallel tasks: the generation of a load table and the assignment of boundary conditions. These stages converge in the application of load until failure at the limit plastic strain according to stress-strain behaviour, leading to the initiation of the model solution. This structured workflow ensures a systematic and accurate simulation of the structural behaviour.

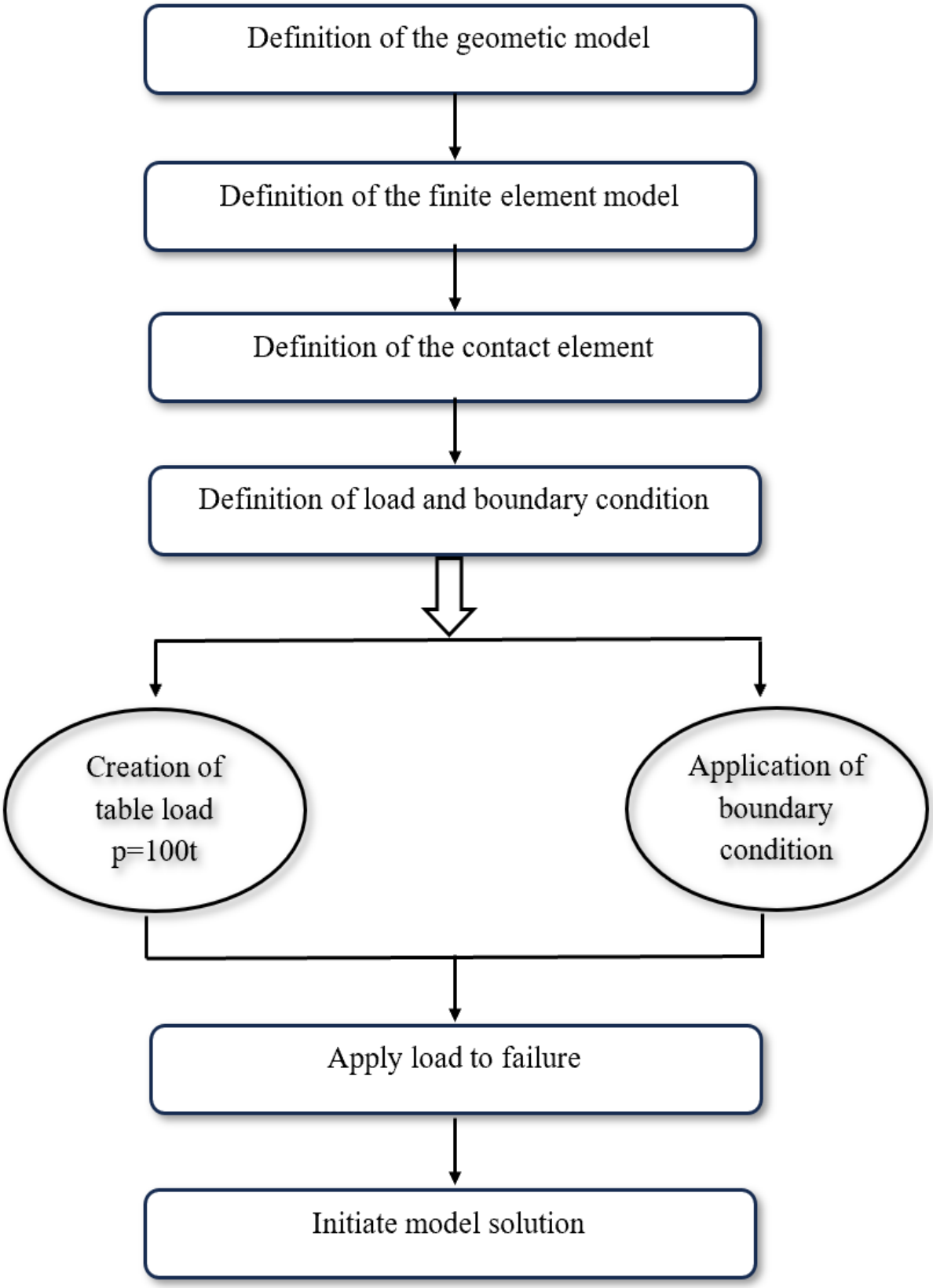

Figure 3-8. Sequential procedure of structural analysis using ANSYS APDL

3.3 FE Model Convergence Study

The connection assembly was discretized into several manageable regions in order to achieve an efficient and accurate meshing strategy. A refined mesh with an element size of 2 mm was applied to the bolts to ensure accurate stress distribution and smooth interaction at the bolt–hole interfaces. Since the bolts were defined as the master surfaces in the contact formulation, a comparatively coarser mesh of 4 mm was adopted in the surrounding regions of the bolt holes to optimize computational efficiency without compromising accuracy. Around the bolt holes, the mesh size was further refined to one-quarter of the angle thickness, allowing for precise capture of local stress concentrations. For the plate and angle members, the mesh was subdivided into elements of 8 mm in the contact zones, while in the non-contact regions a coarser mesh was implemented with an element size twice that of the fine mesh, with at least two elements distributed through the thickness to maintain accuracy in out-of-plane behaviour.

To validate the chosen mesh density, a mesh sensitivity study was conducted using bolt mesh sizes of 1 mm, 1.5 mm, 1.75 mm, and 2 mm, as summarized in Table 3-2. The results of this investigation indicated that the 2 mm mesh provided the most suitable balance between accuracy and computational cost. This mesh size (corresponding to Model No. 4) exhibited excellent agreement with the reference simulation results, confirming its adequacy for subsequent analyses.

Table 3-2 Mesh sensitivity study

Model No	No of elements	Force (kN)	Displacement (mm)
1	9641	87.13	3.51
2	9552	87.18	3.52
3	8665	87.12	3.51
4	8420	87.11	3.51

3.4 Validation of the FE model

To verify the accuracy and reliability of the Finite Element (FE) model under both ambient and elevated temperature conditions, experimental results from the literature were employed as benchmarks. The fire performance of bolted lap-joint connections was assessed using the test data reported by Fischer et al. [160], which focused on bolt shear failure at different elevated temperatures, and by Ungkurapinan [159], who investigated bolt bearing failure at ambient temperature. These two sets of experimental studies provided a comprehensive basis for

validation, as they covered the primary failure modes typically governing the response of bolted connections.

A direct comparison between the experimental load–displacement curves and those obtained from the FE simulations is presented in Figure 3-9. The displacements were recorded as axial deformations, measured from a fixed reference point at the constrained end of the specimen to a second reference point located at the load application point. The comparisons demonstrate that the FE model is capable of reproducing the connection behaviour with a high level of accuracy. Specifically, the shear failure mode at both ambient and elevated temperatures (Figure 3-9. a) exhibited excellent agreement in terms of initial stiffness and ultimate load-carrying capacity. Similarly, the bearing failure mode at ambient temperature (Figure 3-9. b) was well captured, reflecting the robustness of the numerical model in simulating localized deformation mechanisms.

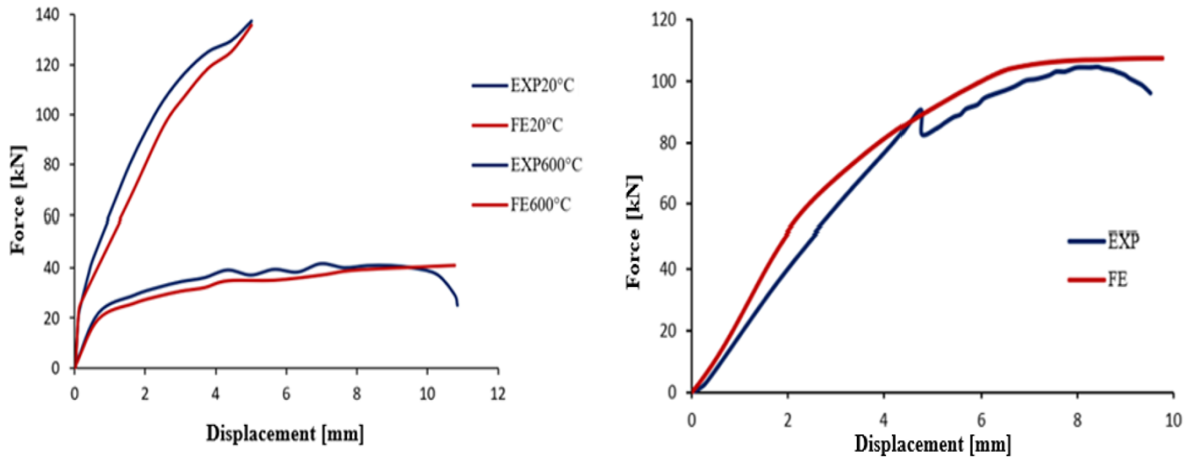

(a) (b)

Figure 3-9. Comparison of FE results with load-displacement curves from experimental tests:

(a): bolt shear mode (b): bearing failure mode

Table 3-3 further highlights the comparison of critical experimental peak loads with those predicted by the FE analysis. The close correlation between the two sets of results confirms that the developed FE model provides a reliable and predictive tool for evaluating the structural performance of bolted connections across a range of temperature conditions. This validation establishes confidence in the model's capability to be used in subsequent parametric and fire performance studies.

Table 3-3 Comparison of critical values from tests and FE analysis

Tests specimen N	Experimental results (kN)	FE results (kN)	FE to experimental results ratio
Ungkurapinan (20°C)	98	100	1.020
Fischer (20°C)	137.3	135.8	0.987
Fischer (600°C)	41	40	0.975

3.5 Case studies and discussions

Parametric investigations were carried out using the validated numerical model in order to systematically evaluate the influence of key connection parameters on the structural response of bolted steel angle connections exposed to elevated temperatures. The parameters considered in this study include the geometric characteristics of the angle sections (such as leg dimensions and thickness), the distinction between single- and double-angle configurations, the strength class of the bolts, and the total number of bolts employed in the connection. The primary focus of the analysis was to investigate how variations in these parameters affect the tension force–slip relationship, which governs the stiffness, ductility, and ultimate load-carrying capacity of both single- and double-leg angle connections. The combined numerical and analytical assessment (CHAPTER-2) enables a comprehensive understanding of the governing factors that influence connection behaviour, offering guidance for the design and performance evaluation of bolted angle connections in fire scenarios.

3.5.1 Effects of the bolt grade

Figure 3-10 (Case 1 to 4) depicts how bolt-type alterations influence angle connection responses. Within the comparison set, the model replaced the G8.8 bolts in the assemblies with G6.8 bolts. It can be seen that the change of the bolt grade from ordinary black bolt G6.8 with medium resistance to high strength G8.8 bolt shows the hardest resistance. However, in case 5 & Case 6, the failure was caused by the angle fracture, the effect of the bolt type on the ultimate resistance of the connections has no influence. The values derived from the finite element analysis differ significantly from those specified in **Table 2-3** of Eurocode 3 and they are 20% higher than those of the code rules under the same loading conditions because Eurocode 3 provides in its provisions a safety factor that ensures the reliability of the structure. This safety factor results in more conservative measurements based on established safety standards. For example, taking Case 1 as an example, the shear resistance value without considering the

safety factor is 75 kN. In comparison, the value provided by the software is 87 KN, a percentage difference of approximately 16%.

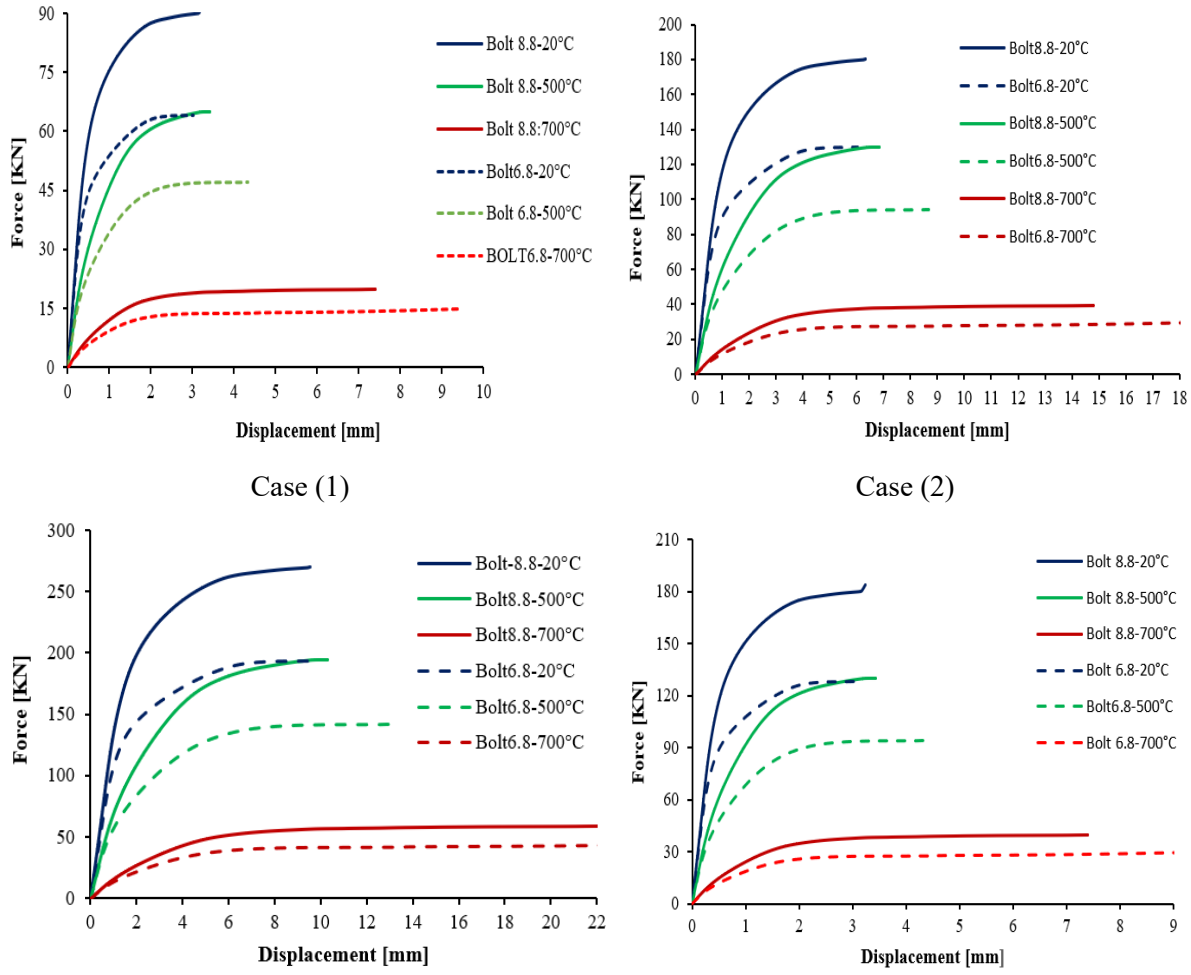

Figure 3-10. Effect of the variation of HR bolt and ordinary bolt

3.5.2 Effect of bolt and angle number

The effect of the number of bolts on the connection response was evaluated by considering assemblies with one, two, and three bolts. The results, presented in Figure 3-11, clearly show that the load capacity of the connection increases almost proportionally with the number of bolts. This demonstrates that each additional bolt contributes directly to resisting the applied tensile load. For all models with a UA 100 × 100 × 10 section (Cases 1–4), the governing failure mode was bolt fracture. Under the same temperature conditions, the assembly with two bolts sustained nearly double the load of the single-bolt case, while the three-bolt configuration carried approximately three times the load. This proportional trend confirms that, within the

tested range, the connection strength is strongly dependent on the total number of bolts. The results further highlight that increasing the bolt number not only enhances the maximum strength but also improves the connection stability by reducing localized deformation.

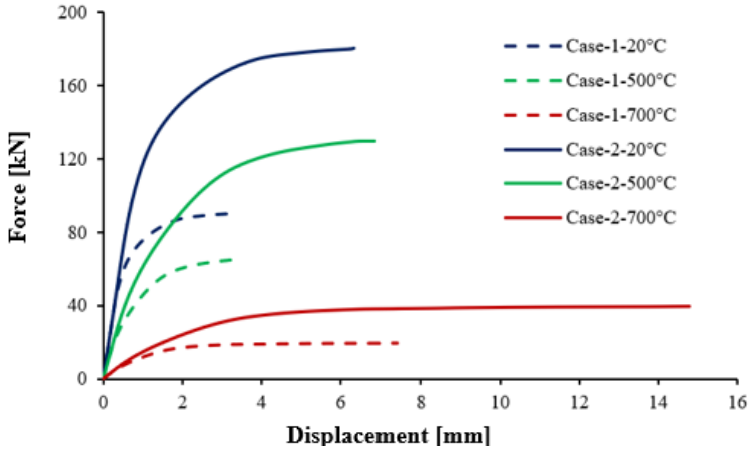

(a)

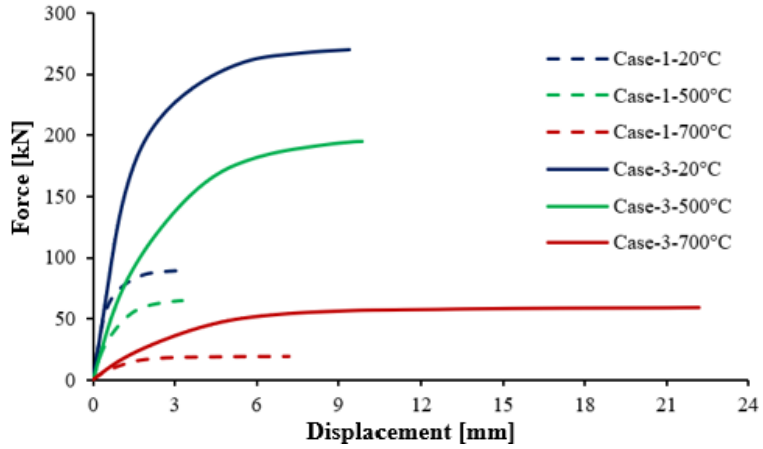

(b)

Figure 3-11. Effect of the variation of bolt number: (a): from two to one, (b) from three to one

Figure 3-12 shows the results of the numerical models, confirming that the deformation and stress distributions for Case 1 are well captured when using either HR bolts grade 8.8 or bolts grade 6.8 at all temperature levels. At ambient temperature, stresses remain relatively low in the plates and angles but become significant in the bolts where the load is directly applied. As the temperature increases, stresses gradually rise in the plates and angles, particularly for assemblies with two and three bolts (Cases 2 and 3), indicating that shear remains the dominant failure mode across all temperature ranges. It was also observed that in Cases 1 and 4, the connections experienced rotation after failure due to the eccentricity between the gusset plate and the angles. In contrast, for Cases 2 and 3, the degree of rotation was notably reduced

compared with the single-bolt configuration, consistent with the findings of Ungkurapinan [159]. A detailed presentation of the stress distributions for all the studied scenarios is provided in the **Appendix**.

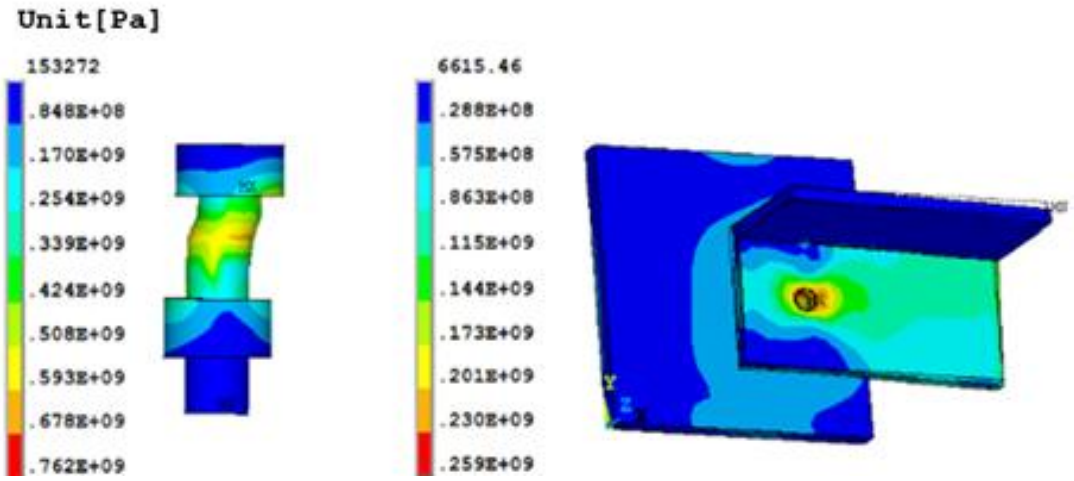

Figure 3-12. Equivalent stress of the connection (case 1) at 20°C and at the failure load

Figure 3-13 presents the load–displacement curves for Case 1 and Case 4, highlighting the influence of the double-shear plane introduced in the two-angle configuration. In the single-angle arrangement of Case 1, the connection is governed by a single shear plane, which limits its capacity and leads to higher stress concentration on the bolts. By contrast, Case 4 benefits from a double-shear mechanism, where the applied load is shared between two shear planes, resulting in a more uniform stress distribution and reduced local deformation. The comparison shows that the ultimate load resistance in Case 4 is more than twice that of Case 1, demonstrating not only a significant increase in strength but also an improvement in stiffness and overall structural stability. This clearly confirms the advantage of adopting a double-angle configuration, which enhances the performance of the connection under tensile loading conditions.

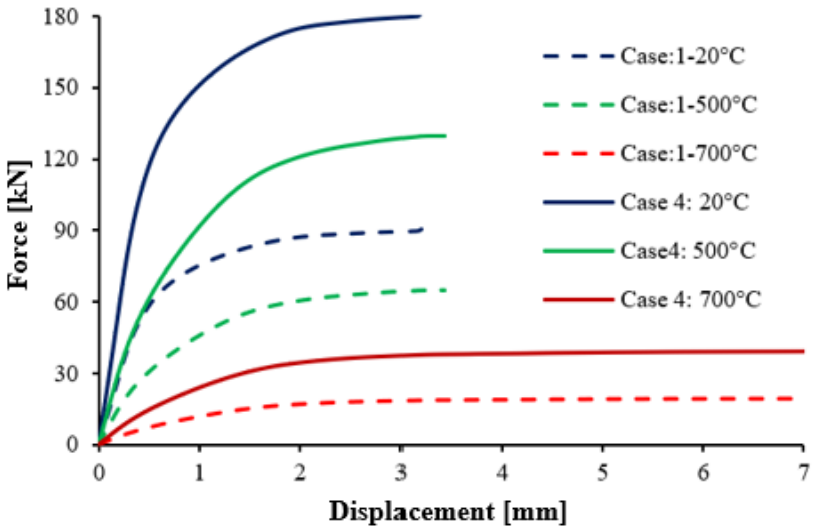

Figure 3-13. Effect of the variation of the angle number from two to one

3-5-3 Effect of angle size

The finite element analysis for Case 5 indicates that connections with relatively smaller angle sections primarily failed by tensile rupture of the steel angle when subjected to elevated temperatures. For the UA 70 angle section, the design capacity predicted by the code is 93 kN, whereas the numerical simulation yielded a higher value of 110 kN, representing a difference of approximately 18%, as previously discussed. This variation reflects the ability of the numerical model to capture local stress redistribution and deformation effects that are not fully accounted for in simplified code predictions.

Figure 3-14 illustrates the influence of elevated temperatures on the tensile response of single-angle bolted connections. As the temperature increases, the load-carrying capacity of the connection steadily decreases, highlighting the progressive deterioration of the mechanical properties of the steel components. In this case, comparable reductions in the peak load are observed at successive temperature levels, confirming the sensitivity of the connection to temperature effects. This correlation is directly associated with the reduction in yield strength and ultimate tensile strength of both the bolt and angle materials at high temperatures, which collectively govern the overall performance and ultimate failure mode of the connection.

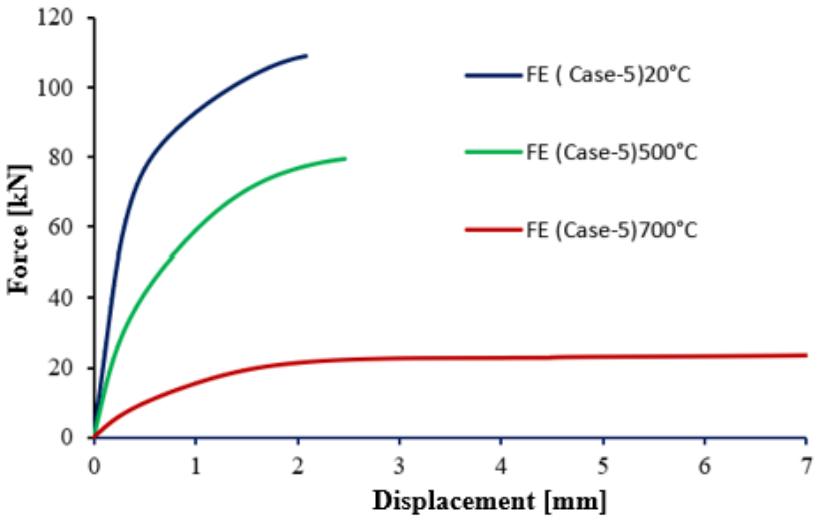

Figure 3-14. Effect of temperature on small size angle

Figure 3-15 presents the results of the finite element model, showing that the deformation is consistently concentrated within the angle section across all temperature levels, regardless of whether bolt grade 8.8 or bolt grade 6.8 is employed. The stress distribution reveals that stresses remain relatively low in the plate region, while significantly higher stresses are observed in the angle, particularly at the points of load application. This indicates that the plate primarily serves as a load transfer medium, whereas the angle itself is the critical component governing the connection behaviour. The concentration of stresses and deformations within the angle confirms that the dominant mode of failure is tensile rupture of the angle rather than shear failure of the bolts or yielding of the plate. This outcome highlights the sensitivity of smaller angle sections to tensile stresses under elevated temperatures and further validates the finite element model in capturing the actual failure mechanism of the connection. The complete set of stress contour plots for this case, along with the other studied scenarios, is provided in the **Appendix** for reference.

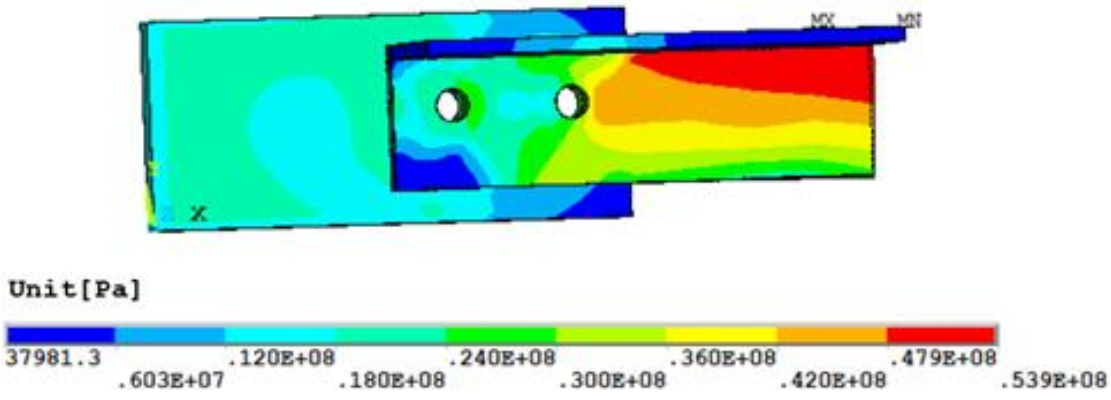

Figure 3-15. Equivalent stress of the angle at 700°C at the failure load

To investigate the influence of angle size on connection behaviour, modifications were introduced to both the edge distance and the load transfer path in Case 6. The edge distance was reduced to 25 mm (e_2=25 mm), which limited the available shear area and increased the likelihood of shear rupture along the expected failure plane. In addition, the load path was adjusted to concentrate the stress flow, promoting the development of a combined tension–shear failure mechanism characteristic of block shear [163].

The predicted connection capacity according to the design code was compared with the results obtained from the finite element model to evaluate the code's accuracy in representing the observed behaviour. In all cases, the FE model provided higher capacity predictions than those derived from the design code.

Figure 3-16 illustrates the results obtained from the finite element model, clearly showing the occurrence of block shear failure at ambient temperature. The figure highlights the typical stress concentration along the shear plane and the tension path around the bolt holes, which together govern the block shear mechanism. It also demonstrates how the reduced edge distance and the adjusted load transfer path contribute to the initiation and propagation of the combined tension–shear failure. The deformation and stress contours indicate that the angle section carries the majority of the load, while the plate primarily facilitates load transfer, confirming the expected block shear behaviour predicted for this configuration.

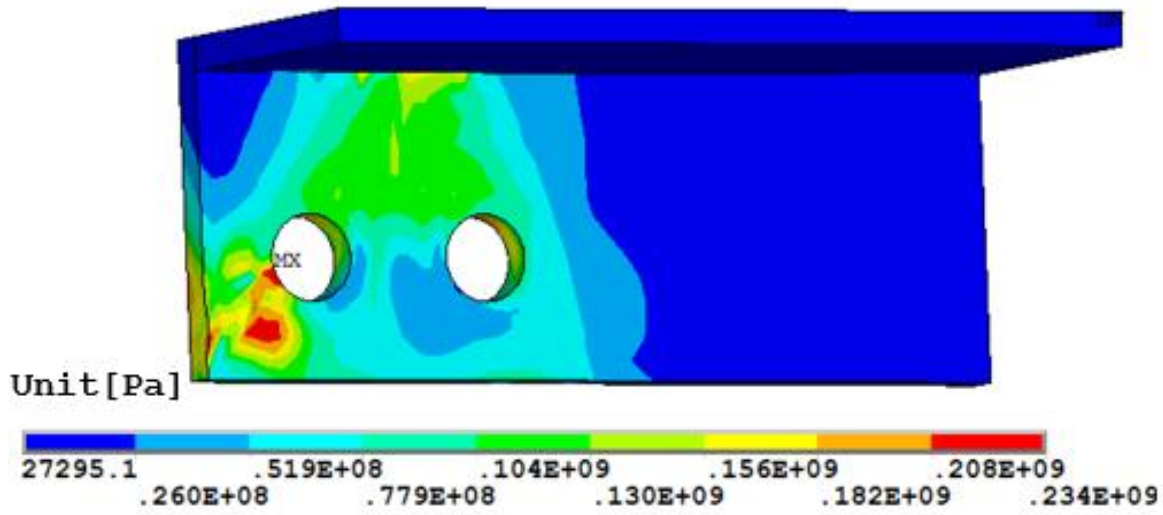

Figure 3-16. Block shear failure at 20°C (case 6)

At 500 °C, the failure mode of the connection begins to transition from the typical block shear mechanism toward tensile rupture of the angle section. This shift indicates that the elevated temperature reduces the shear strength of the material, making the angle more susceptible to

tension-induced failure. By 700 °C, this trend becomes more pronounced, and the dominant failure mode is entirely governed by tensile rupture of the angle, as illustrated in Figure 3-17. The progression highlights the strong influence of temperature on the mechanical behaviour of the steel components, where material softening at higher temperatures diminishes the contribution of shear resistance and emphasizes the tensile vulnerability of the angle section.

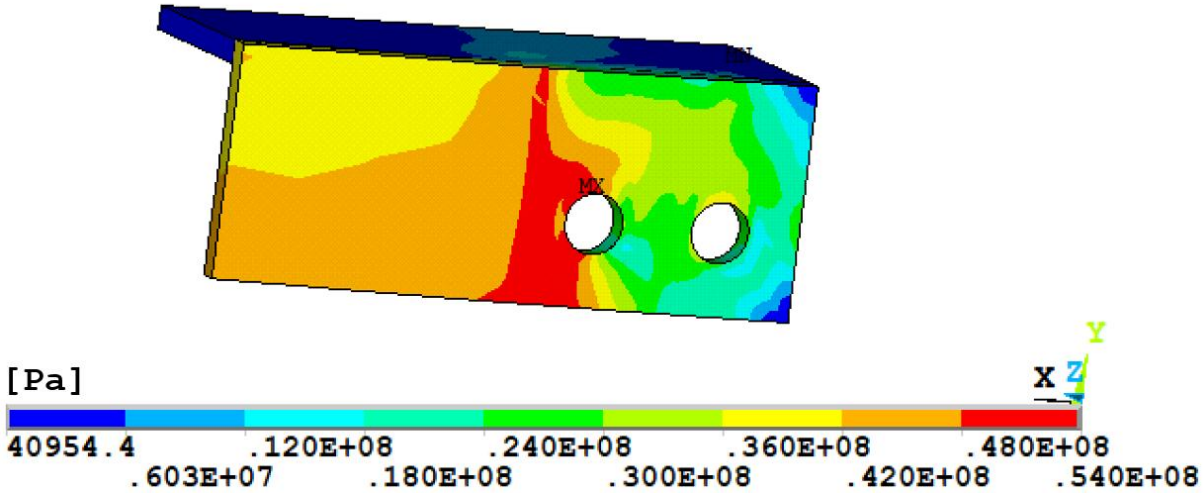

Figure 3-17. Equivalent stress of the angle at 700°C

3.6 Conclusion

In this chapter, finite element models of bolted angle gusset steel connections and bolted steel lap joints were developed using ANSYS APDL. The numerical analyses accounted for geometric and material non-linearities, as well as key characteristics of bolted joints, including element contact and friction. Experimental results and appropriate failure criteria were used for model validation across multiple failure modes, demonstrating excellent agreement. These findings confirm that the FE model is a reliable and effective tool for detailed investigations of bolted steel angle connections, enabling comprehensive parametric studies and performance assessments. Based on the parametric study, it was concluded that the connection behaviour is significantly influenced by the bolt grade, the number of bolts and angles, and the angle size. Higher bolt grades and an increased number of connection components enhance strength and stiffness, while larger angle sizes improve overall resistance.

CHAPTER 4. MODIFIED COMPONENT-BASED MODEL

4.1 Introduction

The design of beam-to-column connections in Eurocode 3 [8] is primarily based on the component method, developed through extensive experimental and analytical studies. While effective at ambient temperature, the code assumes the same provisions which are applyed at elevated temperatures, despite not explicitly accounting for complex phenomena such as bending-shear interaction, large deformations, and fracture. Originally proposed by Zoetemeijer [164] and subsequently refined by many researchers cited above , the component method has gained wide recognition for its adaptability and efficiency. By identifying the active components, defining their load–displacement behaviour, and assembling them into a mechanical joint model, it provides a practical framework for predicting connection performance under various conditions.

4.2 Modified component-based method

The objective of this study is to develop an adapted component-based model, building upon the framework introduced by [80], with key modifications tailored to better represent practical connection configurations. In this adapted model, the traditional second plate used in Serraj's [80] configuration is replaced by a steel angle, allowing for a more representative simulation of common structural connections. The model accounts for two types of bolted connections: high-strength bolts, which transfer forces primarily through friction as shown in Figure 4-1 (a) and ordinary bolts, which are designed to be twisted off easily and transfer loads without relying on friction, as illustrated in Figure 4-1(b). These configurations are analysed at both ambient and elevated temperatures to capture the effects of thermal degradation of the mechanical properties on connection behaviour. The component-based approach models the joint as a series of elementary components, with each component idealized as a spring whose mechanical response can be described mathematically. This spring-based abstraction allows for a systematic analysis of individual deformation mechanisms within the connection. The methodology presented in the following sections outlines the step-by-step process used to derive the ultimate displacement of the joint under applied loading.

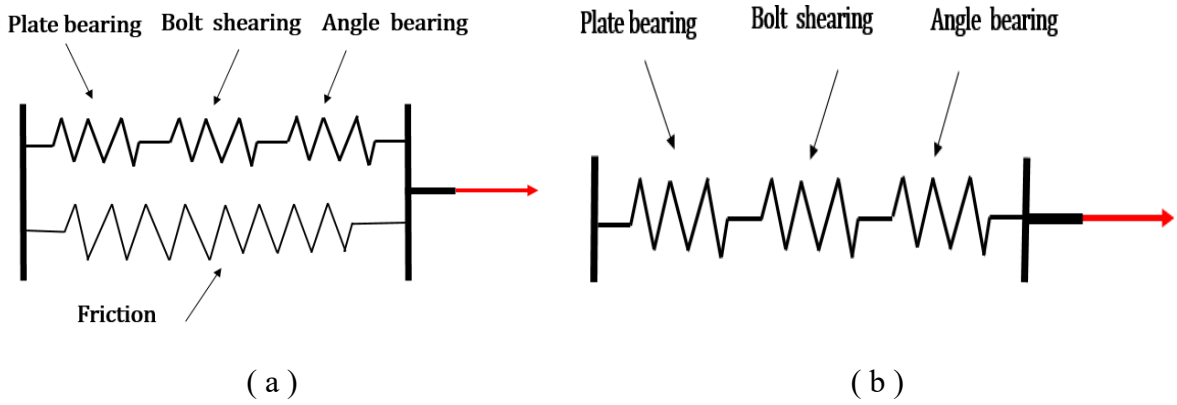

(a) (b)

Figure 4-1. Component spring models for angle-plate connection with:

(a) HR bolt and (b) ordinary bolt

4.3 Methodology for the characterization of the components

4.3.1 Plate in bearing component

Rex et al. [165] introduced bearing stiffness and associated curves that illustrate the relationship between bearing forces and associated displacements based on in-depth experimental and numerical examinations of bolted connections. Furthermore, Sarraj [80] highlighted that the load-bearing capacity of panels exposed to fire is similar to that under normal conditions. They suggest accounting for fire conditions by incorporating reduction factors for material properties. Consequently, the initial bearing stiffness Ki, can be formulated as follows:

$$K_i = \frac{1}{\frac{1}{K_{br}} + \frac{1}{K_b} + \frac{1}{K_v}} \tag{30}$$

$$K_{br} = 120 t f_y (d_b/25.4)^{0.8} \tag{31}$$

$$K_b = 32 E t (e_2/d_b - 0.5)^3 \tag{32}$$

$$K_v = 6.67 G t (e_2/d_b - 0.5) \tag{33}$$

K_{br} represents the bearing stiffness of bolt holes; $K_b$and K_v denote the bending and shear stiffness of the bolt connection plate, respectively. G stands for the shear modulus of the bolt connection plate; E is the Young modulus; f_y the yield stress; d_b indicates the bolt diameter; t is the thickness of the bolt connection plate; e_2 signifies the distance from the center of the bolt to the edge of the plate.

Rex and Easterling [165] provided bearing stiffness and correlation graphs showing the relationship between bearing forces and associated displacement, depending on substantial experimental and numerical investigations on bolt connections. Furthermore, it has been noted by Sarraj [80] that bolt holes exposed to fire exhibit bearing performance that is similar to that of normal settings.

$$\frac{F_b}{F_{b,Rd}} = \frac{\Psi\overline{\Delta}}{(1+\overline{\Delta}^{0.5})^2} - \varphi\overline{\Delta} \tag{34}$$

Where:

$$\overline{\Delta} = {\Delta_b K_i}/{F_{b,Rd}} \tag{35}$$

$$F_{b,Rd} = \min(e_2; 2.76d_b) \times f_u \times t \text{ (for the gusset plate)} \tag{36}$$

As recommended in Eurocode 3 and evident from the numerical results, the maximum tensile strength for a single angle in the connection can be determined as follows:

$$F_b = N_{u,Rd} = 2(e_2 - 0.5d_0)tf_u \quad \text{for angles connected with one bolt} \tag{37}$$

$$F_b = N_{u,Rd} = \beta A_{net} f_u \quad \text{for angles connected with more than one bolt} \tag{38}$$

It should be mentioned that the equations may only be used for joints that are joined by a single row of bolts, up to a maximum of three. This represents the most typical cases in practice and is the subject of the current study.

$F_{b,Rd}$and F_b represent the bearing load and resistance of the plate equation (36) and the net section resistance for the angle in equations (37), (38), respectively. $\overline{\Delta}$ and Δ_b signify the

nominal and total deformation of bolt holes, respectively. Ψ and Φ represent the influential factors of fire temperatures, with their respective values provided in Table 4-1.

The above bearing force-displacement relationship curve describes the development of the bearing pressure to reach its maximum force gradually, as shown in Figure 4-2. The bearing capacity should be set at half the bolt diameter, $0.5d_b$.

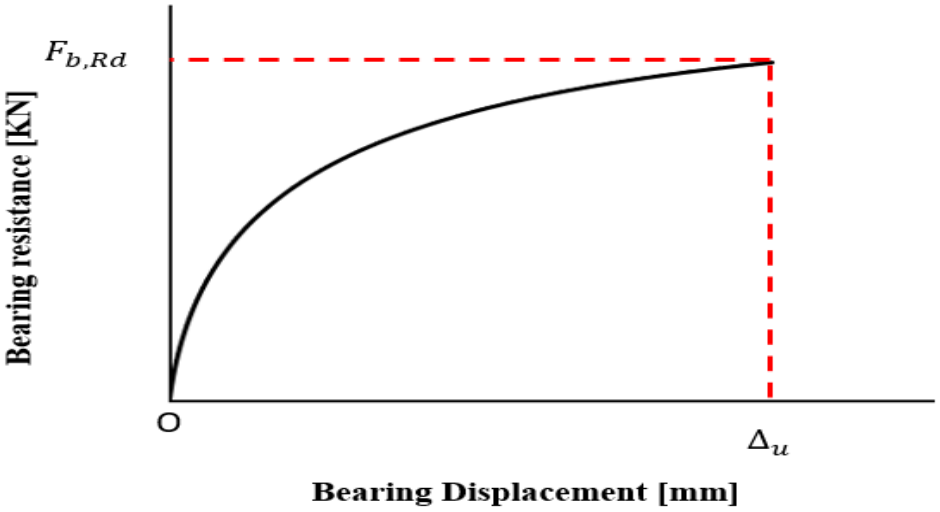

Figure 4-2. Angle and gusset plate behaviour

Table 4-1. Correlation factors with respect to reduction factors at ambient & high temperatures [80]

Fire temperature °C	Correlative factors			Reduction factors
	Ψ	φ	Ω	
20	1.7	0.008	2.5	0.580
500	1.7	0.008	2	0.323
700	1.7	0.007	0.6	0.061

4.3.3 Force-displacement relationship of the bolt in the shear component

Sarraj's [80] approach contended that the adjusted Ramberg-Osgood equation accurately depicts the force-displacement dynamics of a fire-exposed bolt under shear. The stiffness of the bolt is estimated by assuming that the stress distribution is uniform across the shear plane of the bolt. The relationship between the bolt shear deformation Δ_υ and the level of shear force F_v is given by:

$$\Delta_\upsilon = \frac{F_v}{K_{\upsilon,b}} + \Omega \left(\frac{F_v}{F_{\upsilon,Rd}}\right)^n \quad (39)$$

$$F_{\upsilon,Rd} = R_{f,v,b} \times f_{ub} \times A_s \tag{40}$$

$$K_{\upsilon} = \frac{0.15GA_s}{d_b} \tag{41}$$

Δ_{υ} represents the shear deformation of the bolt; F_v and $F_{\upsilon,Rd}$ denote the shear loads and ultimate shear loads of the bolt, respectively; Ω is the temperature-dependent parameter for curve fitting

$K_{\upsilon,b}$ stands for the shear stiffness of the bolt; Ω signifies the influential factors of fire temperatures; n (with n = 6) represents the correlation coefficient of the curve shape; $R_{f,v,b}$ is the reduction factors of shear strength exposed to fire Table 4-2**.** The whole shear force-displacement relationship curve of a typical bolt in considering the shear failure, is illustrated in Figure 4-3.

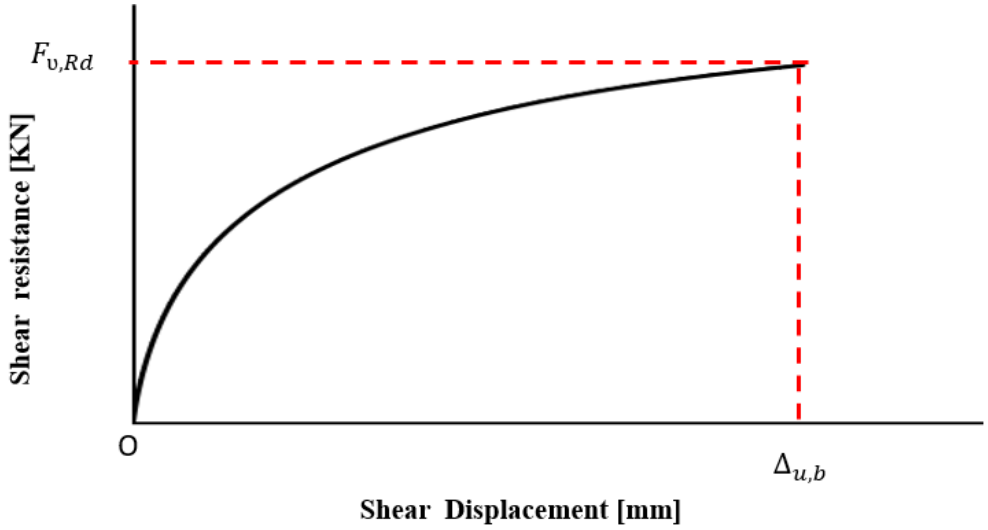

Figure 4-3. Bolt in shear

Table 4-2. Bolt shearing curve fit parameters [80]

Temperature [°C]	20	500	700
$R_{f,v,b}$	0.580	0.323	0.061
Ω	2.5	2	0.6

4.3.4 Angle and plate in slip behaviour

For plate assemblies with bolted angle connections using high-strength bolts, the pre-tension force applied to the bolts generally does not significantly affect the structural response under

conditions of simple shear loading. However, relative sliding between the connected plates can give rise to frictional forces, which may influence the overall connection behaviour, especially in the early stages of loading. Based on the findings from [80] the relationship between slip force and displacement in such configurations can be idealized using a bilinear model, as illustrated in Figure 4-4.This model captures both the initial stiffness and the post-slip behaviour of the connection. The key parameters defining the friction component spring in this model include:

- The initial anti-slip stiffness, which characterizes the elastic resistance before slip occurs.
- The ultimate slip force, representing the maximum frictional resistance generated before sliding begins.
- The degradation stiffness, accounting for the reduction in friction as displacement increases
- The maximum ultimate anti-slip displacement, beyond which the frictional force drops to zero.

This bilinear approach provides a practical and efficient means to simulate the frictional behaviour in component-based connection models, allowing for accurate representation of slip effects in bolted assemblies.

Sarraj [80] proposed a triangular model Figure 4-4 to describe the relationship between frictional force and displacement in bolted connections. In this model, friction increases linearly from zero to a maximum value as slip begins, representing the initial resistance due to bolt clamping. Once the peak frictional force is reached, the resistance decreases linearly back to zero, simulating the reduction in friction with continued slip. This behaviour reflects the stick-slip mechanism commonly observed in real joints. The maximum frictional resistance is defined as:

$$F_{s,Rd} = \frac{K_s . n . \mu . F_{pc}}{\gamma_{M2}} \tag{42}$$

$$F_{pc} = 0.7 . F_{ub} . A_s \tag{43}$$

where

K_s is the groove factor; K_s= 1.0 for the standard hole; n is the number of forces transferring friction surfaces; μ is the anti-slip factor of friction surfaces, and μ = 0.2 is given in EC3; F_{pc} is the bolt pre-tightening forces.

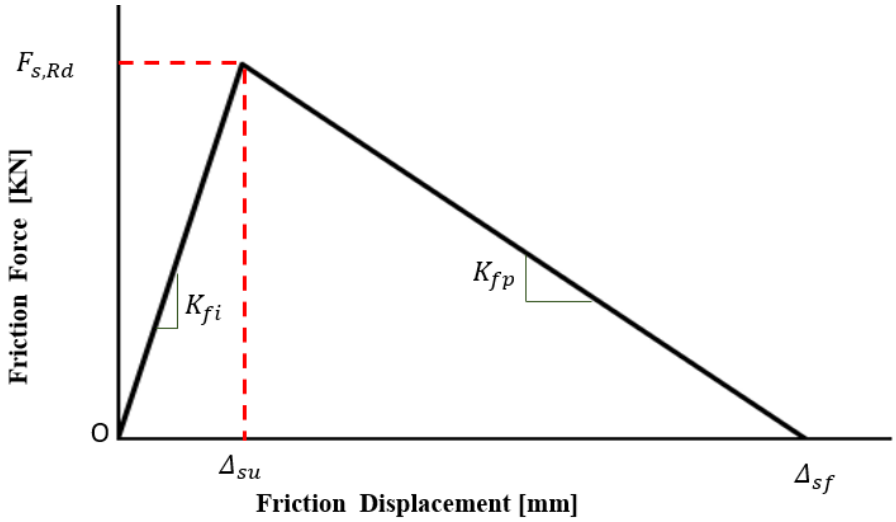

Figure 4-4. Friction component characteristic

The displacements at zero resistance and the maximum resistances are respectively below:

$$\Delta_{sf}= \begin{cases} 16 & (t_1 + t_2) < 20 \\ 16 - 0.3(t_1 + t_2 - 0.5) \leq 38.1 & 20 \leq (t_1 + t_2) \\ 4 & 38.1 \leq (t_1 + t_2) \end{cases} \quad (44)$$

$$\Delta_{su}= 0.18 d_b \quad (45)$$

where t1 and t2 are the thicknesses of the two connected plates and angle respectively.

The initial anti-slip stiffness K_{fi} and degradation stiffnessK_{fp} are given by:

$$K_{fi} = \frac{F_{s,Rd}}{\Delta_{su}} \quad (46)$$

$$K_{fp} = \frac{F_{s,Rd}}{(\Delta_{sf} - \Delta_{su})} \tag{47}$$

4.4 Simplified component model for angle gusset connections

4.4.1 Simplified model with friction effect

After outlining the properties of each component in detail in the previous study, it is now possible to construct the mechanical component model for each angle plate bolted assembly [166]. By simply following the load transfer path through a single-bolt joint under tensile loading, the mechanical component model can be drawn in the form shown in Figure 4-5. For example, for a component consisting of a 15mm thick S235 steel plate and a 10mm thick angle steel fixed with an M16 high-strength bolt, the properties of these components can be generated from the previous parameter expressions and are shown in Figures 4-6, 4-7 and 4-8. The behaviour of the finite element and component models can be compared based on their force-displacement response as shown in Figure 4-9. From this comparison, it can be seen that there is a good correlation between the two models.

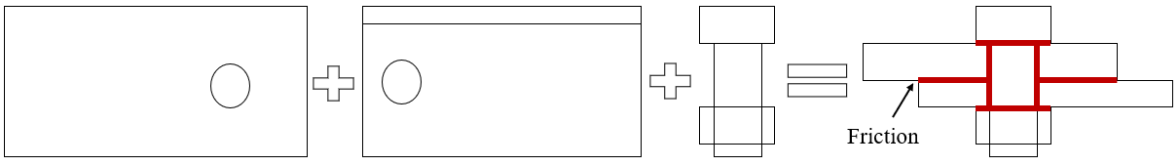

Figure 4-5. Bolted angle-plate component model

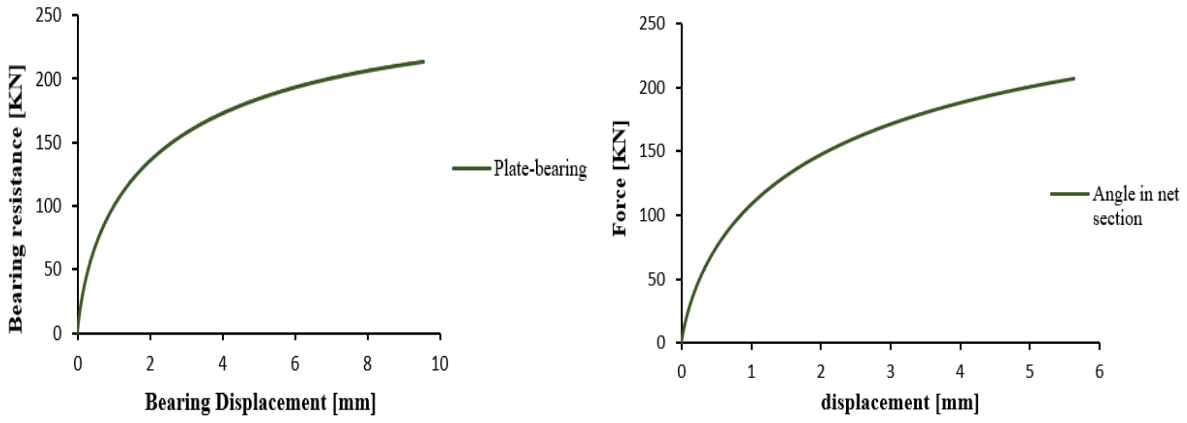

(a) (b)

Figure 4-6. Angle and plate characteristic at 20°C

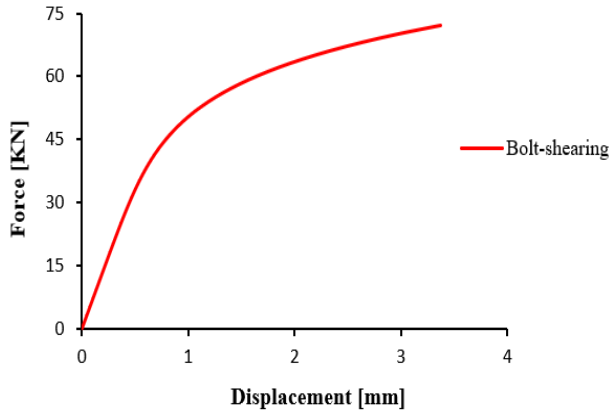

Figure 4-7. Bolt in shear characteristic at 20°C

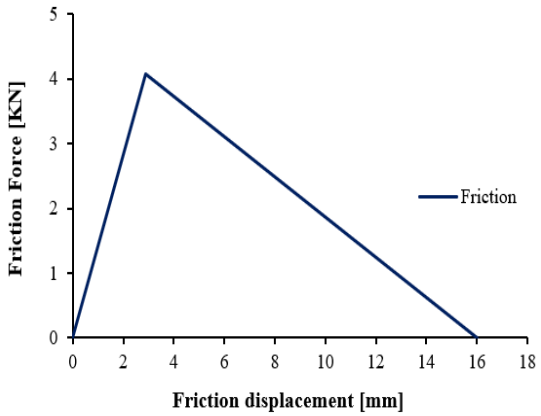

Figure 4-8. Friction component at 20°C

Figure 4-9 illustrates the final behaviour of the assembly as predicted by the Component-Based Model (CBM), incorporating the contribution of the friction component. This representation highlights the capacity of the CBM to capture not only the mechanical interaction of the individual components but also the influence of friction, which plays a significant role in the overall response of the connection. To validate this response, the results obtained from the CBM are subsequently compared with those derived from the finite element (FE) modelling, allowing for a comprehensive assessment of the model's accuracy and reliability.

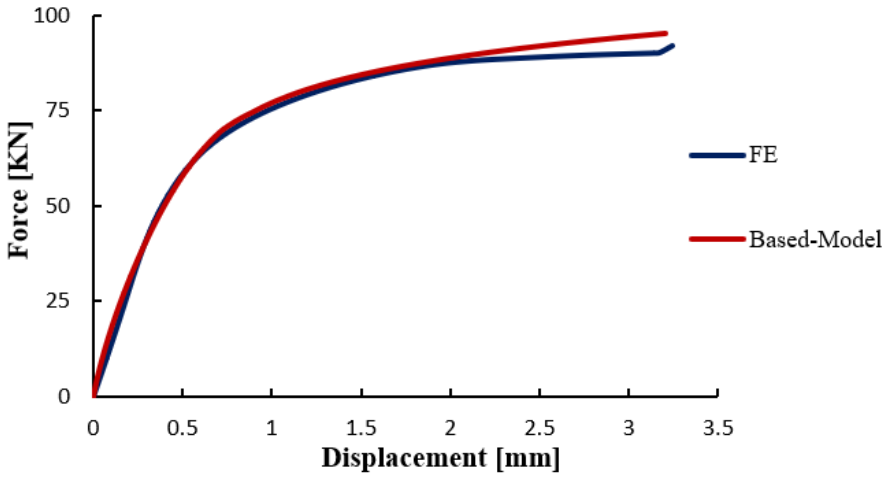

Figure 4-9**.** Comparisons of tensile force curves of the component model and the FE model (Bolt grade 8.8)

4.4.2 Simplified model without friction effect

The Figure 4-10 illustrates the mechanical component-based model of the bolted connection, constructed without accounting for the frictional effects between individual connection components. This simplification focuses purely on the mechanical deformation and load transfer mechanisms, such as bolt shear, plate bearing, and angle deformation, excluding any additional resistance that might arise due to surface friction. In Figures 4-11, and 4-12, this modelling approach is applied specifically to Case 1, which represents a bolted connection using an M16 ordinary bolt. The mechanical properties of the joint components in this case are derived using the previously defined parameters from chapter-2, such as material properties, geometric dimensions, and bolt characteristics. These figures demonstrate how the component-based model can simulate the connection behaviour under load, while isolating the purely mechanical response of the system in the absence of frictional contribution. This approach allows for a clearer understanding of each component's role in the overall joint performance.

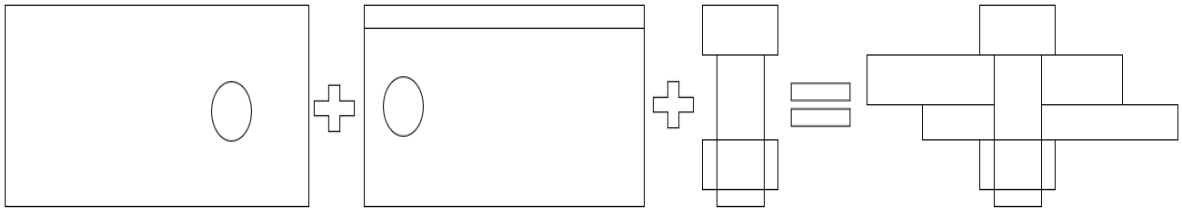

Figure 4-10. Angle-plate component model with ordinary bolt

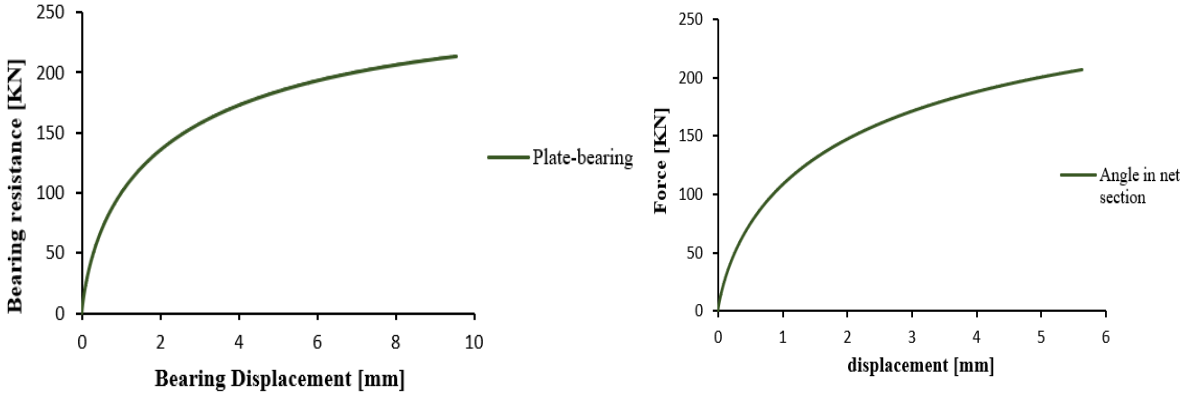

Figure 4-11. Plate in bearing component characteristic at 20°C

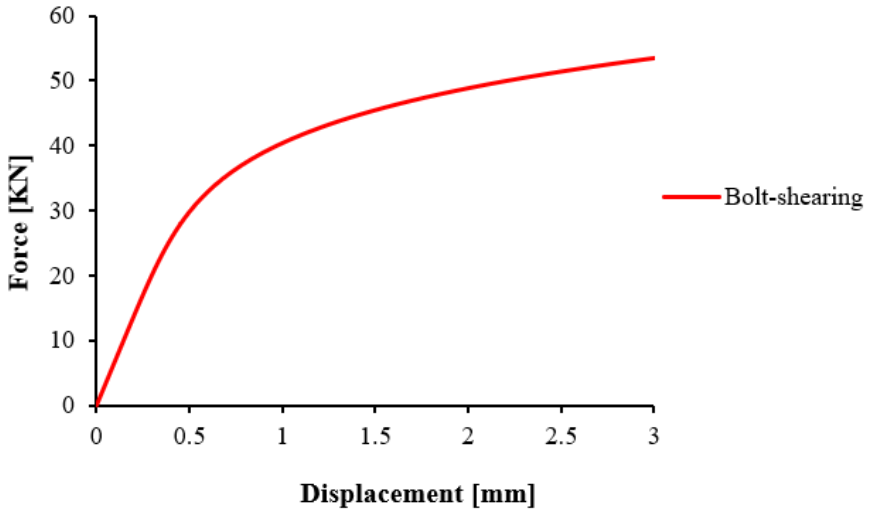

Figure 4-12. Bolt in shear component characteristic at 20°C

Figure 4-13 presents the final behaviour of the assembly when modelled with ordinary bolts and without considering the effect of friction. In this case, the response is governed primarily by the bearing and shear interaction of the bolts, while the absence of friction reduces the overall stiffness and load-carrying capacity of the connection. The predicted behaviour highlights a more direct transfer of forces through bolt deformation and localized bearing, providing a conservative representation of the assembly's structural performance.

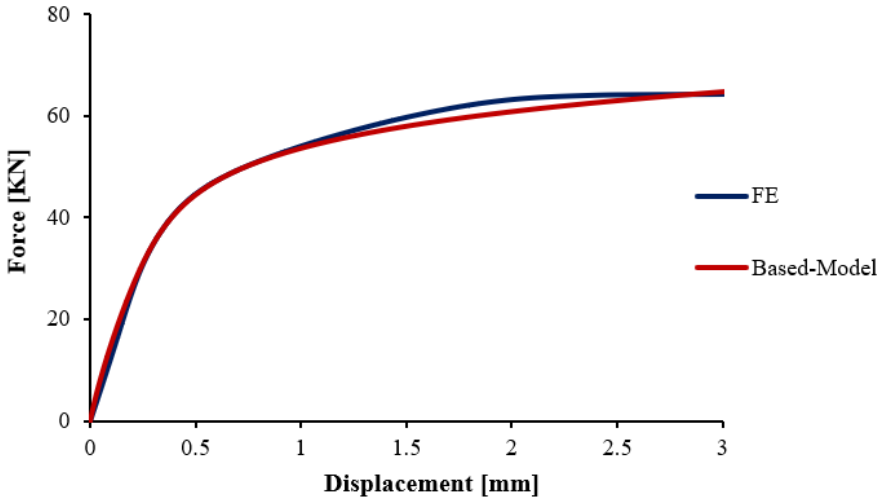

Figure 4-13. Comparisons of tensile force curves of the component and the FE models (bolt grade 6.8)

The previous section explains each angle plate assembly component's stress behaviour and load transfer mechanism. As shown in Figure (4-1), the component model of the bolt assembly spring can be defined with and without taking the friction effect. The model consists of a plate represented by the load-bearing component spring, a bolt represented by the shear component spring, and an angle represented by the bolt assembly spring. In both configurations, these springs are connected in series; however, when high-strength bolts are used, an additional

friction spring is introduced in parallel, as illustrated in Figure 4-1(a), whereas in the case of ordinary bolts, the connection is frictionless, as shown in Figure 4-1(b). In the above model, the maximum displacement can be calculated by superimposing the rows of the spring assembly.

4.5 Performance of the connection through the FE models & the CBM models

As discussed earlier in Chapters 2 & 3, six bolted single-angle connections were introduced as case studies, each modelled using finite element (FE) analysis, with their corresponding force–horizontal displacement curves provided. These FE models form the basis for evaluating the performance and accuracy of the modified component-based model developed in this chapter, particularly in terms of its ability to predict the resistance capacity of various joint configurations. For Cases 1 to 3, which involve angle gusset connections, the study was extended to investigate how varying the number of bolts influences the overall strength and behaviour of the connection. The resulting load-displacement responses for each scenario, using both ordinary bolts and high-strength bolts, were compared and illustrated in Figures 4-14(a) through 4-14 (f). These comparisons focus on the shear failure mode, which is a dominant mechanism in these types of connections.

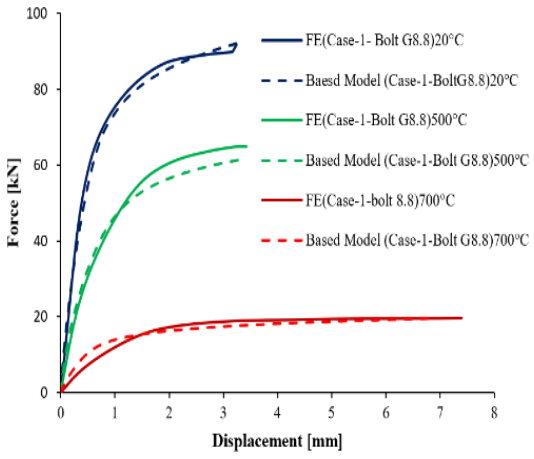

(a) Case 1 (8.8 bolts)

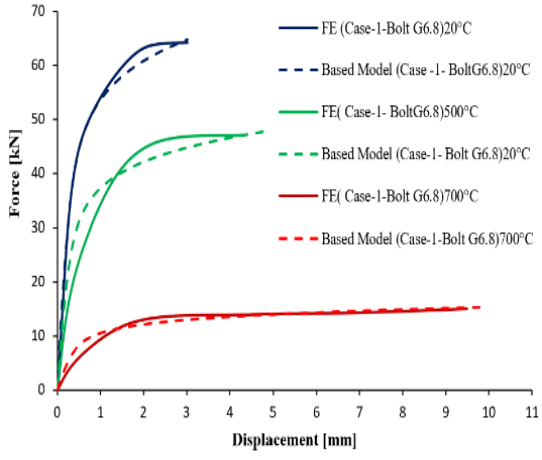

(b) Case 1 (6.8 bolts)

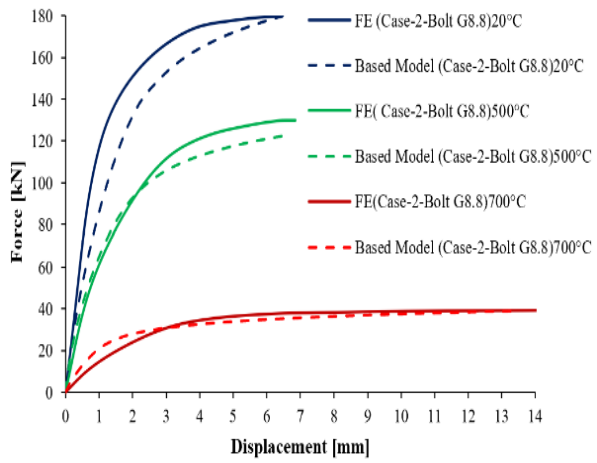

(c) Case 2 (8.8 bolts)

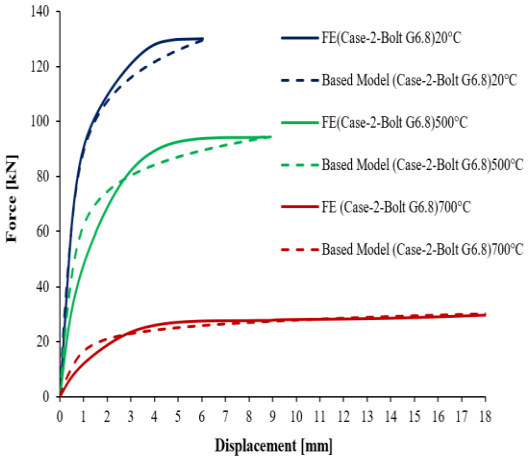

(d) Case 2 (6.8 bolts)

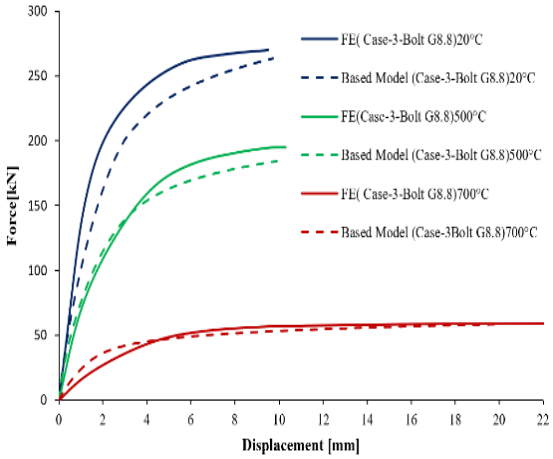

(e) Case 3 (8.8 bolts)

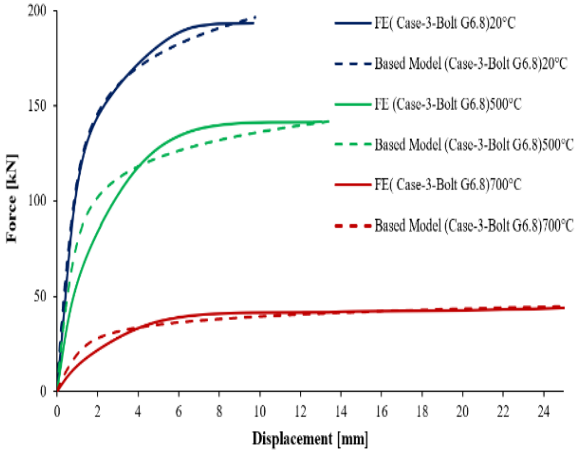

(f) Case 3 (6.8 bolts)

Figure 4-14. Comparisons of tensile force curves from FE and theoretical analysis for assemblies with the same failure mode (Case1, Case2, Case3, Case4)

In Case 4, involving a double-angle bolted connection, the analysis clearly shows in Figures 4-15(a) and 4-15 (b) that the resistance of the assembly approximately doubles compared to Case 1 (a single-angle connection), reflecting the increased number of load paths. Furthermore, it was observed that the connection failed when the bolt displacement reached 3 mm, under the same shear failure mechanism seen in the earlier cases, confirming the consistency in behaviour across different configurations.

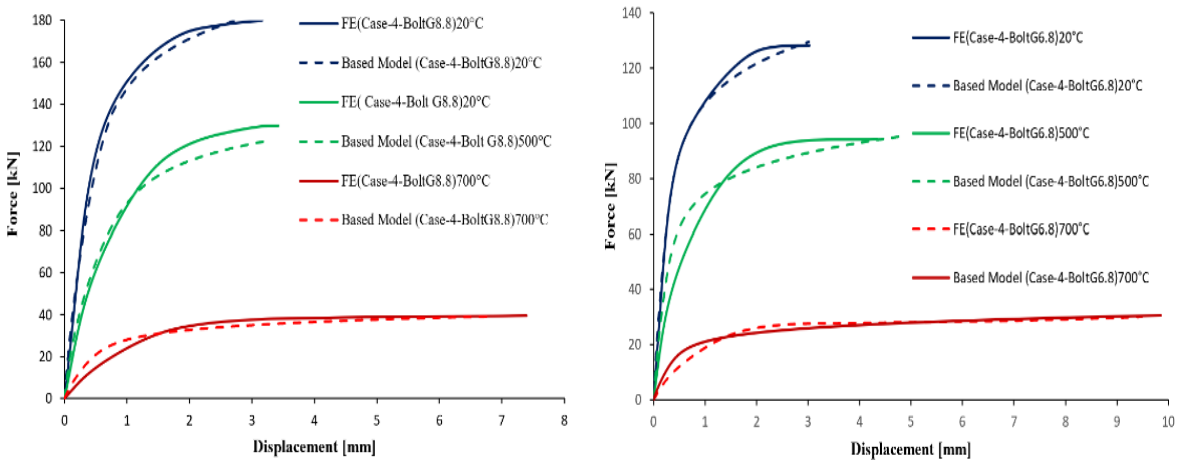

(a) Case 4 (8.8 bolts) (b) Case 4 (6.8 bolts)

Figure 4-15. Comparisons of tensile force curves from FE and theoretical analysis for assemblies with double-shear failure mode (Case4)

Other scenarios of study (Case-5 & Case-6) was conducted involving a connection with two bolts and a small-sized angle, subjected primarily to the tensile failure mode. This configuration was selected to explore the behaviour of compact connections under axial tension, where geometric limitations might influence the overall performance. The resulting force–displacement response is illustrated in Figure 4-16, showing the progression of loading up to the ultimate strength of the assembly. Interestingly, the results indicate that the bolt grade (i.e., whether high-strength or ordinary bolts were used) had a negligible influence on the global behaviour of the connection in this scenario. This suggests that, under pure tensile loading in small-angle connections, the failure is governed more by the angle geometry and material properties than by the bolt strength itself. Therefore, for such configurations, the focus should be placed on angle design and net section capacity, rather than solely on bolt specification.

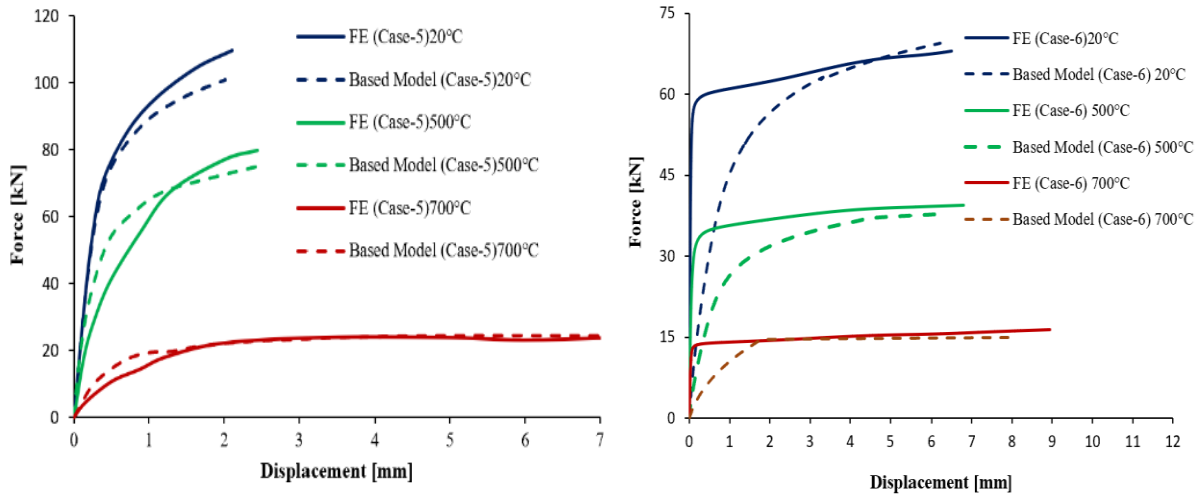

(a) (b)

Figure 4-16. Comparisons of tensile force curves from FE and theoretical analysis for assemblies with the same failure mode (Case 5)

4.6 Initial stiffness analysis

The initial stiffness K_i in the elastic regime, prior to significant plastic deformation, characterizes the tensile load response of the assembly. It was defined as two-thirds of the plastic strength then projecting this point onto the load–displacement curve as illustrated in Figure 4-17, in line with previous studies [167] and the European design code [73], with corresponding values summarized in Table 4-3 for both the component-based model (CBM) and the finite element model (FE). For connections with grade 8.8 bolts (cases 1–3) failing in shear, a marked difference in initial stiffness is observed compared with those using grade 6.8 bolts, while the number of bolts had little influence when the failure mode was the same. A substantial increase in stiffness occurred in the double-shear configuration (case 4), nearly doubling that of single-shear cases. In cases 5 and 6, stiffness was governed mainly by material properties and geometric configuration rather than bolt grade.

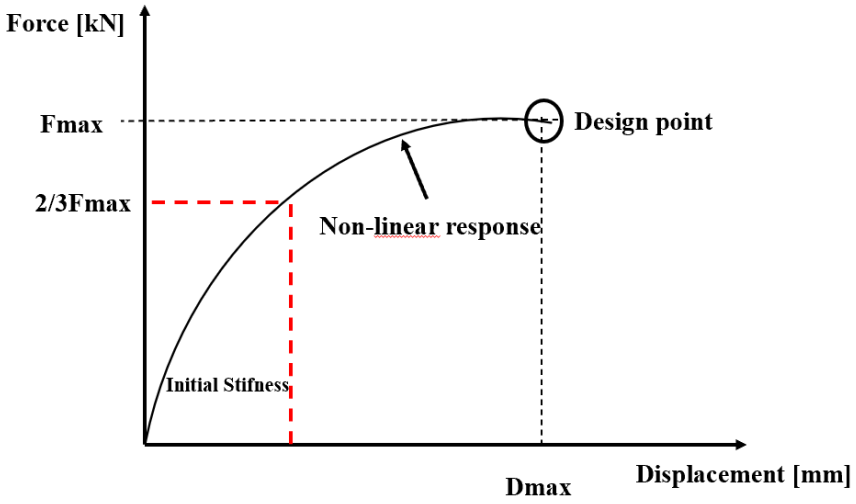

Figure 4-17. Initial stiffness concepts related to the assembly's full non-linear response

Table 4-3. Axial initial stiffness of joints at different temperatures

Studied Scenarios	$K_{ini,CBM}$ (KN/mm)		$K_{ini,FE}$(kN/mm)		$K_{ini,FE}/K_{ini,CBM}$	
	Bolt 8.8	Bolt 6.8	Bolt 8.8	Bolt 6.8	Bolt 8.8	Bolt 6.8
20°C						
Case (1)	96	93	115	95	1.197	1.021
Case (2)	99	96	114	97	1.151	1.010
Case (3)	89	85	124	107	1.393	1.258
Case (4)	211	192	240	194	1.137	1.010
Case (5)	118		126		1.067	
Case (6)	46		52		1.13	
500°C						
Case (1)	46	31	46	32	1.000	1.032
Case (2)	54	60	48	41	0.888	0.683
Case (3)	48	43	51	37	1.062	0.860
Case (4)	88	76	96	78	1.090	1.026
Case (5)	47		51		1.085	
Case (6)	19		21		1.105	
700°C						
Case (1)	13	13	16	13	1.230	1.000
Case (2)	14	13	11	13	0.785	1.000
Case (3)	13	13	17	15	1.307	1.153
Case (4)	19	17	23	17	1.210	1.000
Case (5)	10		11		1.100	
Case (6)	7		9		1.285	

At elevated temperatures, all assemblies exhibited reduced initial stiffness, reflecting lower resistance and greater susceptibility to deformation. At ambient temperature, the force–displacement curves of all studied connections (cases 1–6) showed nonlinear behaviour due to plastic yielding; however, as temperature increased, the response became more linear, reflecting the progressive stiffness degradation of the materials.

4.7 Ultimate strength analysis

Table 4-4 presents the ultimate strengths obtained from both analytical calculations and numerical finite element (FE) simulations, offering a comparative assessment of the performance of the studied bolted connections. For each case, the corresponding failure mode is identified at the point where the connection reaches its ultimate load-carrying capacity, commonly referred to as the threshold of failure. In this study, the ultimate strength is defined as the peak value on the force–displacement curve Figures 4-14 to 4-16, which represents the maximum load the joint can sustain before a marked reduction in capacity or the activation of a distinct failure mechanism.

The comparison between the proposed analytical modified component-based model and numerical predictions demonstrates a strong correlation: the average ratio of FE to component-based analytical results ranges between 0.9 and 1.0. This narrow range indicates that the modified component-based model is capable of reliably reproducing the connection response. Such agreement provides confidence in the modified component-based model for practical design purposes, while the FE model offers deeper insight into localized stresses, deformation patterns, and the progression of failure mechanisms.

Furthermore, the consistency observed across both ambient and elevated temperature conditions reinforces the robustness of the actual modified component-based method in predicting ultimate strength. Nevertheless, the FE analyses reveal additional behavioural details such as stiffness degradation, redistribution of stresses, and the influence of temperature on material properties that are not explicitly accounted for in the simplified formulation. This highlights the complementary value of combining both approaches: the analytical method for efficient design checks and the FE method for advanced investigations into connection performance under complex loading or thermal scenarios.

Table 4-4 Ultimate strength of the assemblies with their failure mode at ambient and elevated temperatures

Studied Scenarios	Component-based model (KN)		FE (KN)		FE/CBM		Failure mode
	Bolt G8.8	BoltG6.8	Bolt G8.8	BoltG6.8			
20°C							
Case (1)	87.1	64.8	87.8	64.1	1.008	0.989	Bolt shear
Case (2)	178.3	128.1	179.8	130.1	1.008	1.015	
Case (3)	259.4	194.4	269.7	193.6	1.038	0.995	
Case (4)	174.2	129.6	175.6	128.2	1.008	0.989	Bolt double shear
Case (5)	102.4		110.5		1.079		Tensile rupture
Case (6)	69.3		67.9		0.979		Block shear
500°C							
Case (1)	62.7	46.6	64.8	46.1	1.033	0.989	Bolt shear
Case (2)	128.3	92.2	129.4	93.6	1.008	1.015	
Case (3)	186.7	139.9	194.1	139.3	1.039	0.995	
Case (4)	122.2	93.3	129.6	92.3	1.060	0.989	Bolt double shear
Case (5)	73.7		79.5		1.083		Tensile rapture
Case (6)	37.7		39.4		1.045		Block shear
700°C							
Case (1)	20.0	14.9	20.1	14.7	1.005	0.986	Bolt shear
Case (2)	41.0	29.4	41.3	29.9	1.007	1.017	
Case (3)	59.6	44.7	62.0	44.5	1.040	0.995	
Case (4)	40.0	29.8	39.6	29.3	0.990	0.983	Bolt double shear
Case (5)	23.5		25.4		1.080		Tensile rapture
Case (6)	21.3		21.1		0.990		Tensile rapture

4.8 Conclusions

In this chapter, the called modified component-based method is developed using an efficient computational spring model adapted for the structural analysis of steel brace connections under both ambient and elevated temperature conditions. The focus is placed on accurately modelling the behaviour of angle-plate shear connections using a component-based approach, which

captures the nonlinear load-deformation response of the joint with reasonable accuracy. This method decomposes the connection into distinct mechanical components, each represented by a spring with mathematically defined behaviour. For the fin-type angle connection, the key components identified include plate bearing, net section failure of the angle, bolt shear, and slip due to bolt-hole clearance. Each of these elements is thoroughly investigated through finite element (FE) parametric studies, which help to calibrate the component model and verify its behaviour under various loading and temperature conditions.

Several significant findings emerged from the simulations and analyses:

- The angle-plate connections can be reliably modelled using the modified component-based method, offering a practical alternative to full-scale FE simulations.
- The influence of the friction component, particularly in high-strength friction bolts, was explicitly evaluated, showing its contribution to connection stiffness and strength.
- The reduction factors for bolts in shear prescribed by Eurocode 3 were found to correlate well with those proposed in Serraj's model, supporting the applicability of code-based simplifications.
- The modified model demonstrated its capability to predict different failure modes, such as bolt shear, plate bearing, and net section fracture, under varying thermal conditions.
- A detailed comparative analysis was conducted using numerical results at each temperature level, revealing that the solid FE model yielded the most accurate predictions, although the component-based model remained acceptably close.
- The developed model proved to be versatile and efficient, showing for the design of braced steel frame. It accommodates various bolt types (including ordinary bolts and high-strength bolts) by accurately defining the characteristics of each connection component across a range of temperatures.

This work confirms the viability of using a modified component-based model as a practical and computationally efficient tool for analysing complex bolted steel connections in both standard and fire-exposed conditions.

CHAPTER5. COMPONENT-BASED FINITE ELEMENT MODEL CBFEM

5.1 Introduction to CBFEM

CBFEM combines the component approach with finite element analysis as illustrated in Figure5-1 and is a method for the design and standard verification of steel connections, anchors, and steel components. CBFEM can be defined as a design-oriented finite element method. In principle, the method can be used for most connections. It is effortless, fast, and provides results in a comparable time to solid models. As described in the Eurocodes, CBFEM decomposes the entire connection into individual components, namely bolt shear, tension, support, and the interaction of tension and shear in the screw connection. Each component has its analysis model: 2D shell elements for the steel plates, nonlinear springs for the bolts, and contact elements between the plates in the connection. The model then checks the calculated forces for each component against standard equations.

In recent years, many studies have been devoted to extending the component-based approach to study the behaviour of connections under various loading conditions, such as fire conditions or sudden support removal. Xie et al. [85], [168] created CBMs of fin-plate joints exposed to fire with and without considering plate friction, respectively, and then verified the accuracy of the model with the results of solid finite element modelling.

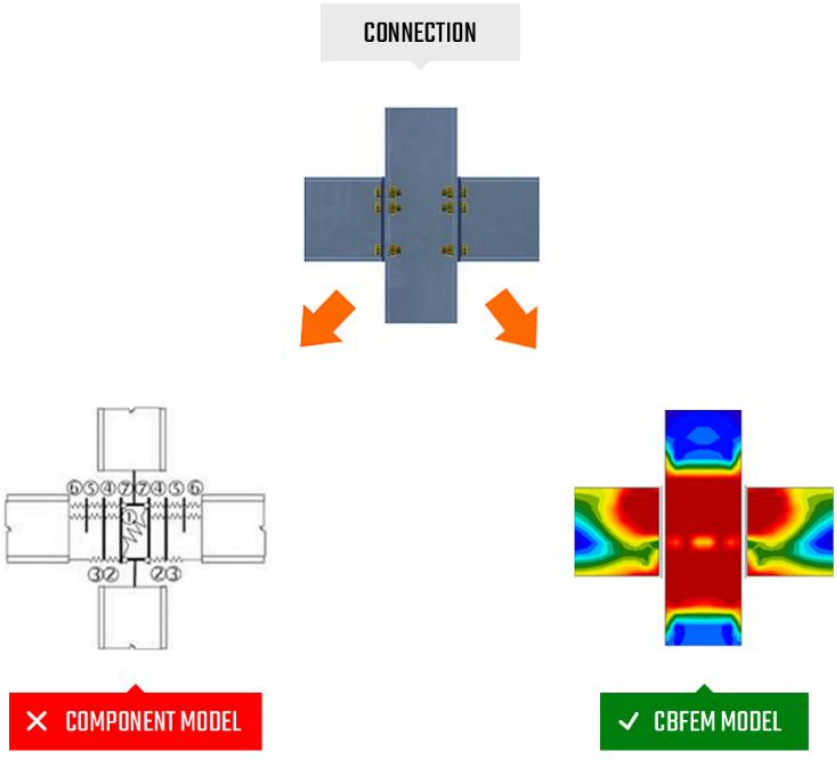

Figure 5-1. CBFEM model description [169]

5.2 CBFEM Model

5.2.1 CBFEM within IDIA StatiCa

The Component-Based Finite Element models (CBFEM) are created using IDEA StatiCa Software [169] to simulate the behaviour of the angle bolted steel connections at elevated temperatures. Additionally, IDEAStatiCa Member [170] is utilized to construct CBFEM models aimed at evaluating the mechanical performance of entire steel members under high-temperature conditions. The design checks are adjusted using the reduction factors specified in EN 1993-1-2 to account for the diminished resistance of steel joints at elevated temperatures. According to EN 1993-5 [171], a 5% strain limit is recommended to define the failure of steel plates at ambient temperature. One the objectives of this thesis is to explore the applicability of using a 5% plastic strain criterion to assess the resistance of steel plates under elevated temperature conditions.

5.2.2 Bolted angle steel joint modelling

The configuration of the bolted lap joints is presented in Figure 5-2. In this setup, the inner plate (M1) was kept fixed, while the outer plate (M2) was designated as the primary member for analysis. During the numerical modelling, convergence issues were encountered, particularly in cases where the analysed member was connected using a single bolt. To overcome these difficulties, the rotation of member M2 was constrained in such cases to ensure stability and reliable simulation results. It is important to note that the influence of heat transfer between the bolts and the adjoining plates was not explicitly modelled in this study. Instead, the prescribed target temperature was directly applied to the individual components of the joint, following the author's assumptions and simplifications.

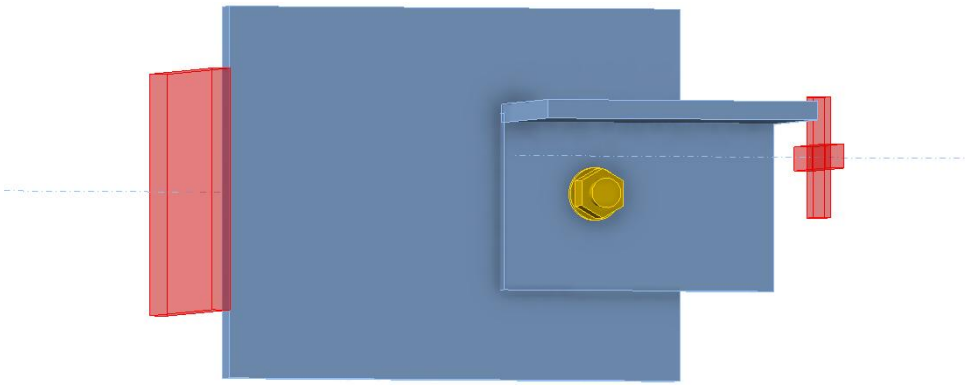

Figure 5-2. Assembly of the studied angle plate connection

5.3 Contact interaction

In CBFEM [169], the contact interactions between assembly components, such as bolts, plates, and angles, are modelled using the standard penalty method. This approach introduces a penalty stiffness when interpenetration is detected between a node and the surface of an opposing component, effectively applying a restoring force to resist further penetration. The magnitude of this penalty stiffness is dynamically adjusted throughout the nonlinear iteration process by a heuristic control algorithm, which is designed to improve numerical stability and ensure convergence of the solution. The solver automatically identifies the regions where penetration occurs and calculates the corresponding contact force distribution across the affected nodes, particularly at the interface with the angle. This treatment allows the model to realistically capture the mechanical behaviour of contact surfaces, including compression, sliding, and potential separation, which is critical for the accurate prediction of joint performance.

5.4 Mesh sensitivity

The relationship between the number of mesh elements used to divide the angle, the plates, and the resulting resistance of the bolted angle plate joint is presented in Figure 5-3. As the mesh is refined, the computed resistance values gradually stabilize, indicating improved numerical accuracy. It was determined that using 14 mesh elements provides sufficient convergence, beyond which further refinement yields minimal change in resistance. To ensure reliable and stable results while maintaining computational efficiency, a mesh size of 16 elements was ultimately selected for the Component-Based Finite Element Method (CBFEM) simulations.

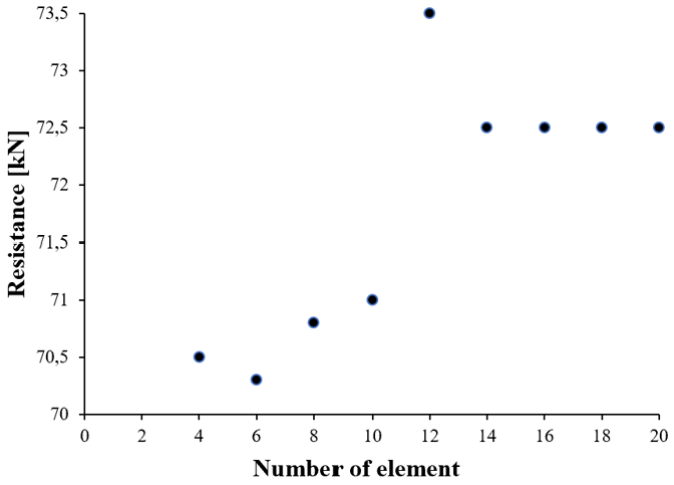

Figure 5-3. Mesh sensitivity study

5.5 Analysis process

The analysis model developed in IDEAStatiCa [169] incorporates the interaction between shear forces and the bi-linear force-deformation behaviour of the bolt under shear loading. This bi-linear model captures the initial elastic response of the bolt, followed by yielding, allowing for a more realistic simulation of bolt performance under load. To account for the effects of elevated temperatures, the material properties of the bolts, specifically the elastic modulus, yield strength, and ultimate strength, are reduced by the temperature-dependent reduction factors specified in EN 1993-1-2. The bolt assembly, which includes the bolt shank, washer, and nut, is modelled using a combination of nonlinear springs, rigid (stiff) body components, and gap elements. This setup enables the model to simulate not only the mechanical response of the individual components but also the complex interaction between them, including potential separation or slipping under load.

The flowchart presented in Figure 5-4 summarizes the essential steps of the Component-Based Finite Model (CBFM) analysis carried out with IDEAStatiCa software [169]. The procedure begins with the definition of project parameters, including design code, material properties, and connection geometry. Subsequently, the connection components such as bolts, plates, and welds are introduced, followed by the application of loads and boundary conditions. Once the model is established, the nonlinear CBFM analysis is performed to evaluate the structural response. The obtained results, such as stresses, deformations, and component utilization, are then verified against the selected design code. If required, the design can be optimized through iterative modifications before generating the final report. This structured process ensures a comprehensive and code-compliant assessment of steel connections under different loading scenarios.

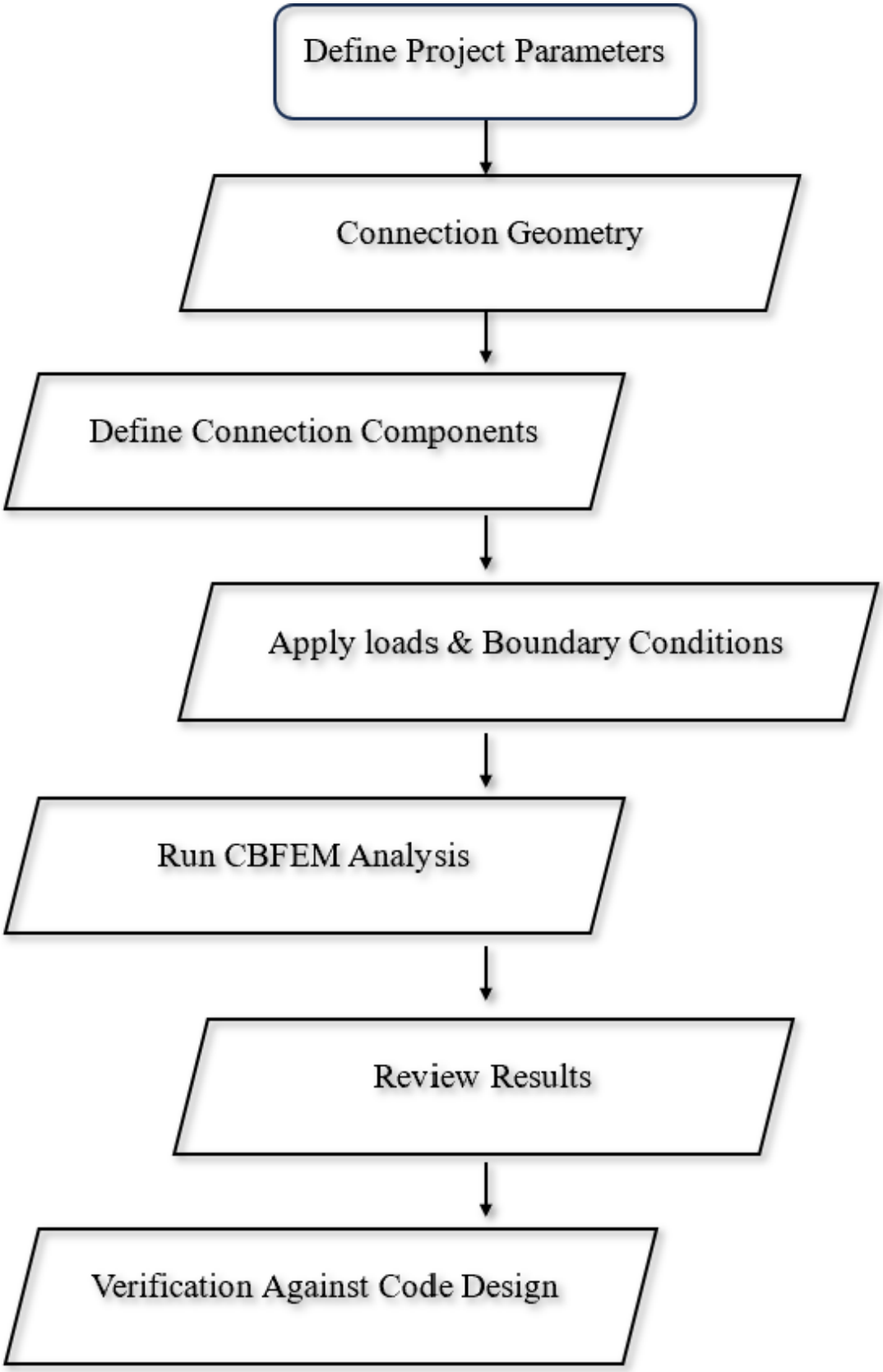

Figure 5-4. Flowchart of the CBFM analysis process in IDEAStatiCa.

5.6 Verification with analytical design

The reliability of the CBFEM model was verified by comparing its results with the analytical calculations presented in Chapter 2. The comparison was carried out at the failure load, for instance the shear load in Case 1 to Case 3, where the CBFEM predictions were found to be in close agreement with the analytical values obtained from Eurocode provisions. A detailed comparison of the results, including the failure loads and corresponding ratios, is presented in Table 5-1, which illustrates the strong correlation between the two methods.

Table 5-1. Comparison of the resistances from the AM and the CBFEM

Studied Scenarios	Analytical Model (EN1993-1-8			CBFEM (IDEAStatiCa)			CBFEM/ AM	
	Resistance [kN]		Critical failure	Resistance [kN]		Critical failure		
	G8.8	G6.8		G8.8	G6.8			
20°C								
Case (1)	75	64	Bolt shear	76.1	51.6	Bolt shear	1.01	0.80
Case (2)	150	128	Bolt shear	154.4	105.2	Bolt shear	1.02	0.82
Case (3)	225	191	Bolt shear	232.6	158.8	Bolt shear	1.03	0.83
Case (4)	150	128	Double-shear	154.4	105.2	Double-shear	1.02	0.82
Case (5)	93		Tension	78		Tension	0.83	
Case (6)	56		Block shear	61.5		Block shear	1.09	
500°C								
Case (1)	41	35	Bolt shear	52.7	35.5	Bolt shear	1.28	1.01
Case (2)	83	70	Bolt shear	109.4	73.5	Bolt shear	1.31	1.05
Case (3)	124	105	Bolt shear	162.8	111.2	Bolt shear	1.31	1.05
Case (4)	83	70	Double-shear	109.4	73.5	Double-shear	1.31	1.05
Case (5)	73		Tension	60.8		Tension	0.83	
Case (6)	37		Block shear	47.9		Block shear	0.65	
700°C								
Case (1)	8	6	Bolt shear	16.2	10.2	Bolt shear	2.02	1.7
Case (2)	15	13	Bolt shear	31.2	24.1	Bolt shear	2.08	1.85
Case (3)	23	19	Bolt shear	53.4	36.4	Bolt shear	2.32	1.91
Case (4)	15	13	Double-shear	31.2	24.1	Double-shear	2.07	1.85
Case (5)	21		Tension	17.9		Tension	0.85	
Case (6)	12		Tension	12.3		Tension	1.02	

The ratios of CBFEM to Eurocode results were consistently close to unity, indicating that the numerical model successfully reproduces the connection capacity defined by the analytical approach [172]. The slight deviations observed can be attributed to the simplified assumptions inherent in the Eurocode method, which neglect nonlinear effects such as contact, friction, and large deformations, while the CBFEM model explicitly incorporates these aspects. This closer representation of the real structural behaviour provides the CBFEM model with an advantage in capturing not only the ultimate resistance but also the detailed interaction mechanisms within the connection. The overall consistency between both approaches demonstrates that the CBFEM model is a reliable tool for validating the global behaviour of steel connections.

5.7 Deformation and failure modes

At the failure load, the deformation state obtained from the CBFEM model using IDEAStatiCa illustrates the overall behaviour of the studied connections and provides a clear indication of the zones most affected by loading. The numerical results show that deformations become increasingly localized around the connection region as the load approaches the ultimate value, with visible stress concentrations and plasticization developing in critical areas. This global deformation pattern highlights the combined influence of shear transfer, bolt interaction, and angle deformation, which collectively govern the structural response. For the sake of a better understanding more details using deformation states will be further discussed in the following sections according to the studied scenarios, allowing a closer examination of the differences in connection behaviour under varying load cases.

In Case (1), the CBFEM analysis indicated that the governing failure mechanism was bolt shear. This outcome suggests that the connection geometry and configuration are such that the shear resistance of the bolts controls the overall capacity, regardless of thermal effects. The CBFEM results also confirmed that the same shear failure mode was predicted for all models (Case 1 to 4), reflecting the method's reliance on component behaviour and standard code-based design checks. Despite this simplification, the predicted deformation state is consistent with the expected structural response, validating the accuracy of the model in reproducing the bolt shear mechanism. Figure 5-4 illustrates the shear failure mode at ambient temperature (20°C) as predicted by the CBFEM model.

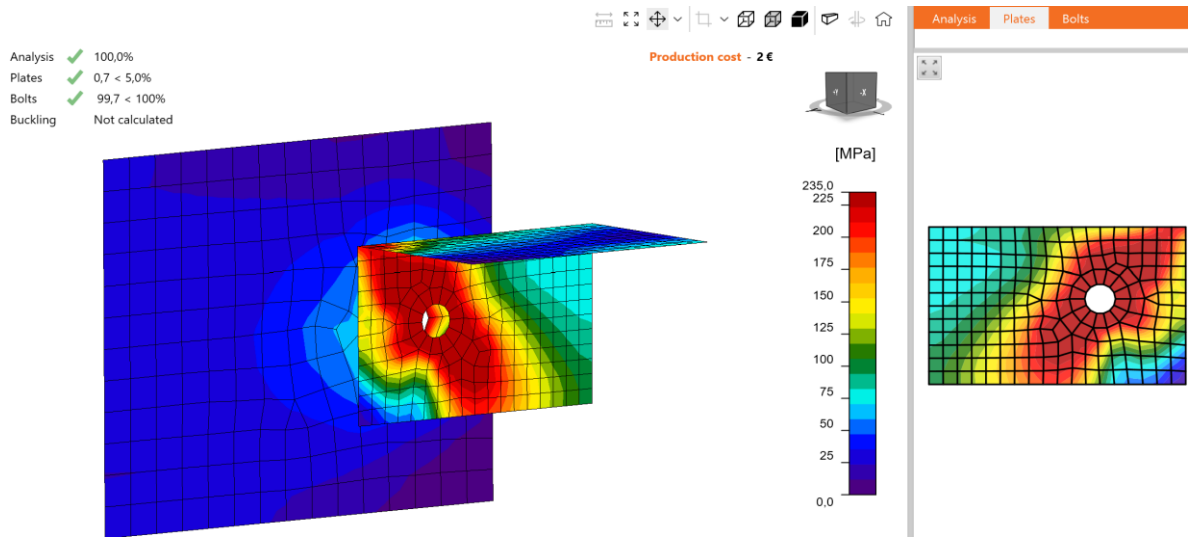

Figure 5-4. Bolt in shear at 20°C in CBFEM

At elevated temperatures, the CBFEM analysis indicates that the shear failure load of Case 1 remains constant across all investigated temperature levels. Figure 5-5 illustrates the shear failure mechanism of Case 1 at 700 °C. These results confirm that, despite the considerable reduction in steel strength at such a high temperature, the CBFEM prediction of the shear resistance remains unchanged compared to room temperature.

For Cases 2, 3 and 4, the CBFEM analysis also predicts the same shear failure mode as observed in Case 1. This consistency across all cases indicates that the governing failure mechanism is primarily shear-driven and is not significantly influenced by variations in connection configuration within the studied range of parameters.

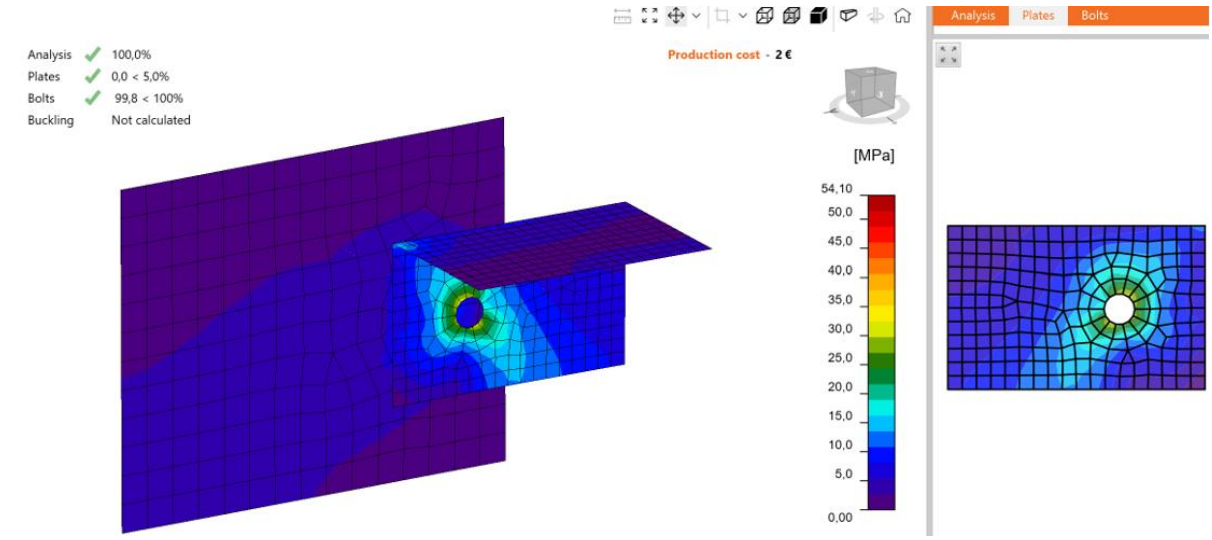

Figure 5-5. Bolt in shear at 700°C in CBFEM

In Case (5), the governing failure mode was tension, which is consistent with the FE model. Moreover, the CBFEM results indicate that this failure mode is not influenced by changes in the bolt grade. This outcome suggests that the overall resistance of the connection is primarily governed by the tensile capacity of the angle rather than the strength of the bolts. Consequently, increasing the bolt grade does not enhance the ultimate resistance in this case. Figure 5-6 illustrates the tension failure of the angle at 20 °C.

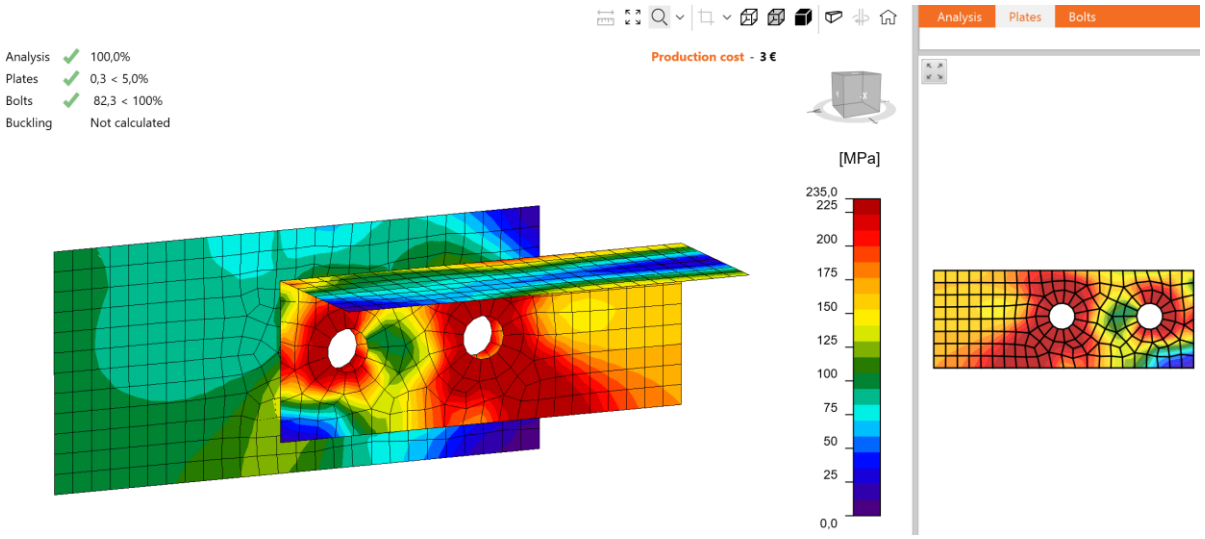

Figure 5-6. Angle tension failure at 20°C in CBFEM

At elevated temperatures, the failure in Case 5 occurs in the leg of the angle at 700 °C, as illustrated in Figure 5-7. The result highlights that, under fire conditions, the angle leg becomes the most vulnerable component of the connection, thereby controlling the ultimate failure mode.

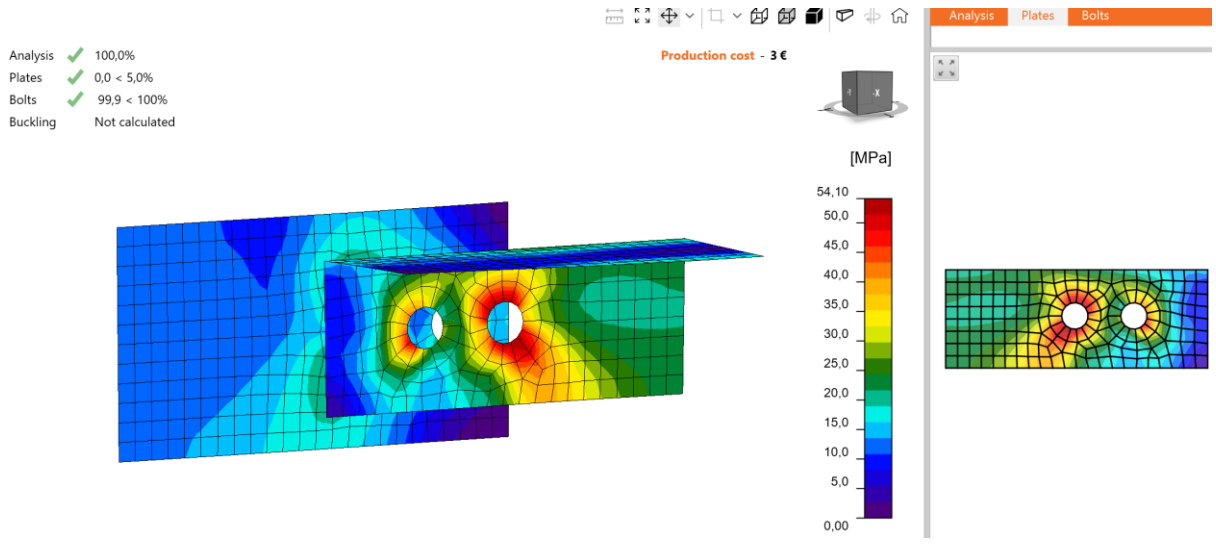

Figure 5-7. Tension failure (Case-5) at 700°C in CBFEM

In Case 6, where the predominant failure mode is block shear, the CBFEM successfully captures this behaviour with good agreement to the expected structural response. Figure 5-8 illustrates the block shear failure at 20 °C. This outcome confirms that the model is capable of reproducing complex failure mechanisms involving the interaction of shear and tensile stresses in the connection. The prediction also demonstrates that block shear resistance is governed mainly by the net section of the angle around the bolt line, rather than by the bolt grade or other parameters. Hence, CBFEM proves reliable in identifying and simulating this combined failure mode.

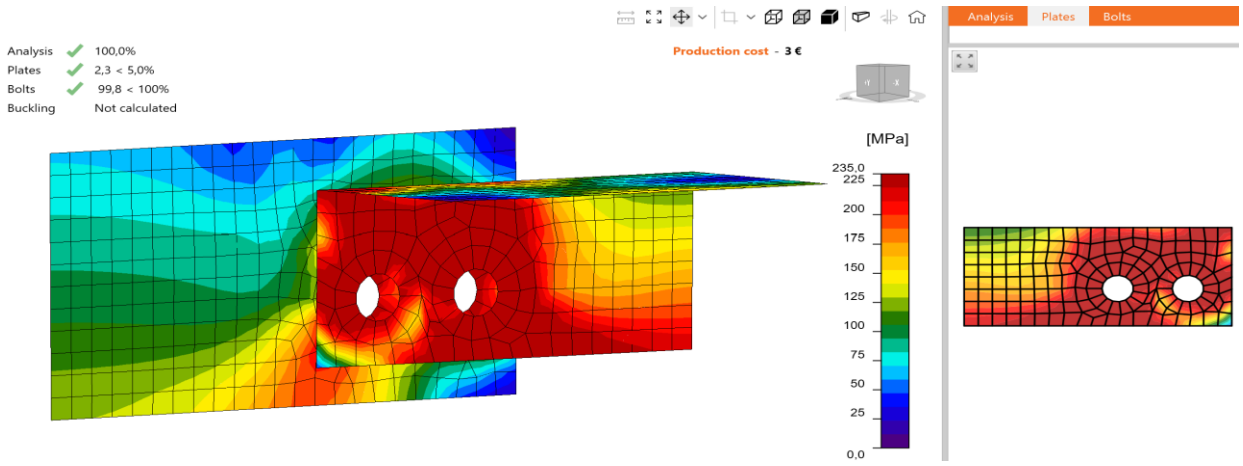

Figure 5-8. Block-shear at 20°C in CBFEM (Case-6)

At 500 °C, the failure mode in Case 6 begins to shift from block shear toward tension, and at 700 °C it fully develops into a tensile failure, as indicated in Figure 5-9. This transition can be explained by the progressive degradation of steel strength and stiffness at elevated temperatures, which reduces the shear resistance of the net section and promotes tensile rupture as the dominant mechanism.

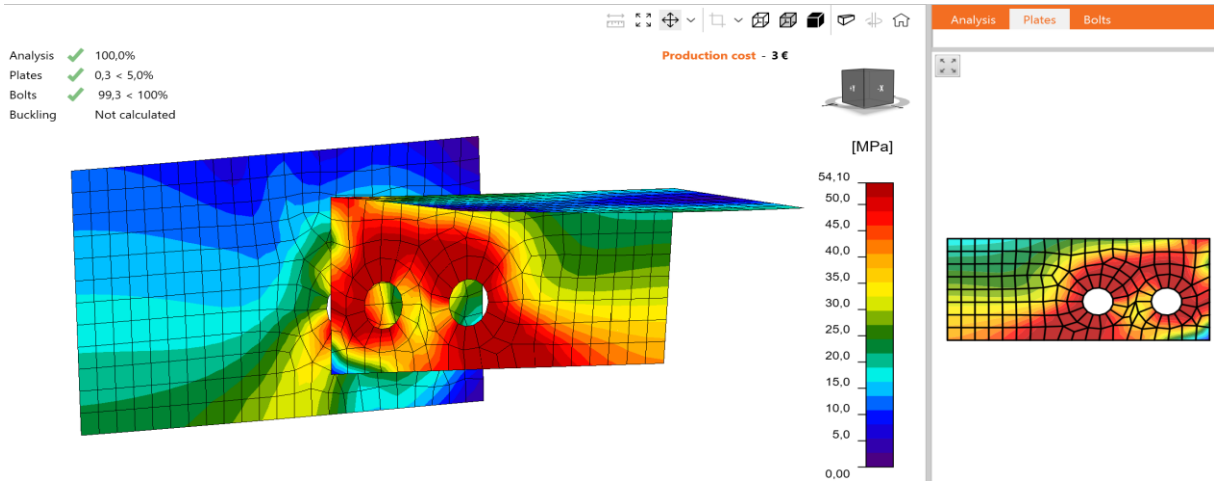

Figure 5-9. Tension failure (Case-6) at 700°C in CBFEM (Case-6)

5.8 Accuracy of the modified component-based model

In order to evaluate the accuracy and reliability of the proposed Modified Component-Based Model developed in Chapter 4, a verification study was conducted using the Component-Based Finite Element Method (CBFEM). The CBFEM framework has been widely recognized as a robust numerical approach for capturing the nonlinear response of steel connections, and therefore it serves as a suitable benchmark for validating simplified analytical formulation.

The comparison was carried out by assessing the global force-displacement response, stiffness characteristics and the ultimate resistance obtained from the FE model, The proposed model against those derived from the CBFEM simulations.

5.8.1 Comparative Evaluation of Global Response

The global response of the studied bolted connections (Cases 1–4), illustrated by the force–displacement curves in Figure 5-10, where the failure mode remained consistent across all investigated temperatures, demonstrates a close agreement between the proposed CBM predictions and the reference CBFEM simulations across different bolt configurations and temperature levels. Across all bolt configurations and temperatures, the CBFEM response is systematically conservative when compared with both the CBM predictions and the reference FEM results. At 20 °C, CBFEM reproduces the initial stiffness reasonably well but underestimates the peak resistance and the associated displacement at peak, leading to a lower envelope of the force–displacement curve. This conservative bias becomes more pronounced at elevated temperatures (500 °C and 700 °C), where CBFEM predicts a steeper stiffness degradation and earlier onset of nonlinearity, resulting in reduced ultimate load and greater post-peak softening relative to CBM and FEM. In contrast, the CBM closely tracks the FEM curves in both the elastic and peak regions, with only minor deviations in the softening branch. These trends indicate that while CBFEM provides a safe-side estimate suitable for design, the proposed CBM offers a more accurate reproduction of the global behaviour with substantially lower modelling effort, particularly valuable for parametric or preliminary assessments.

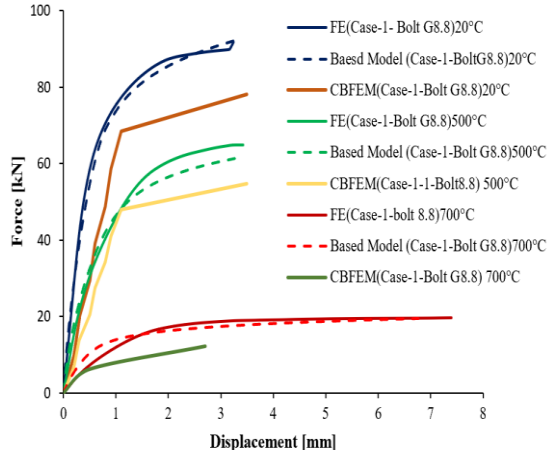

(a) Case 1 (8.8 bolts)

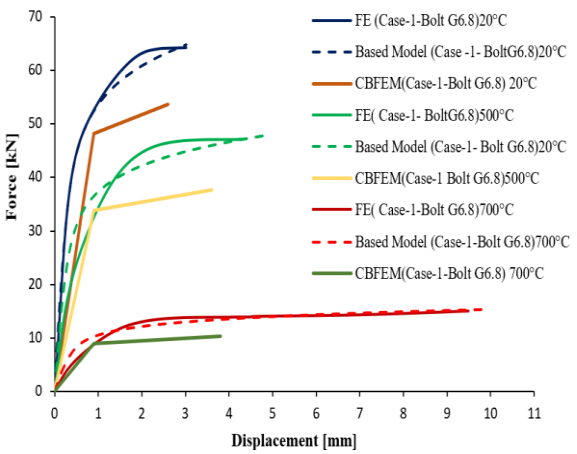

(b) Case 1 (6.8 bolts)

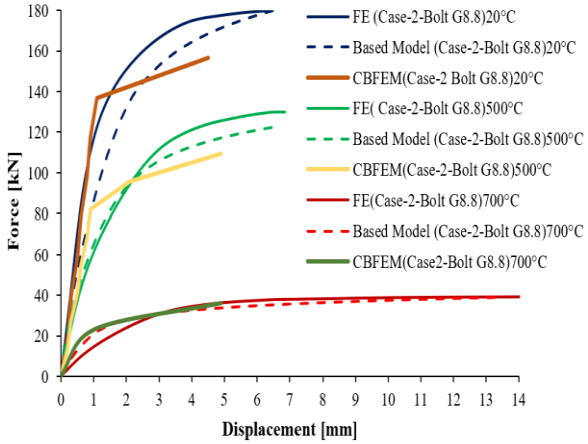

(c) Case 2 (8.8 bolts)

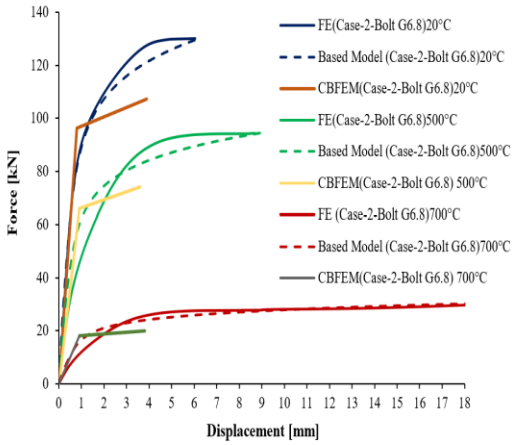

(d) Case 2 (6.8 bolts)

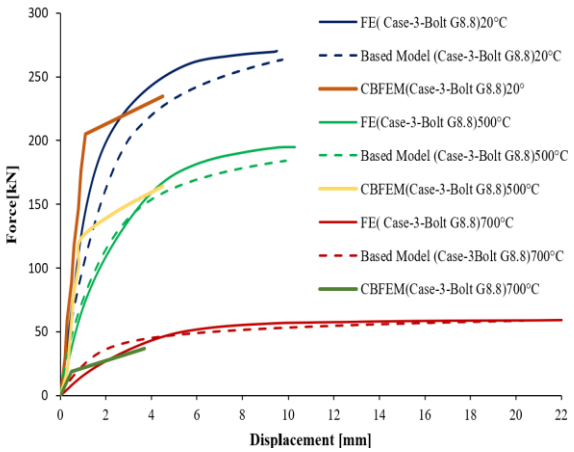

(e) Case 3 (8.8 bolts)

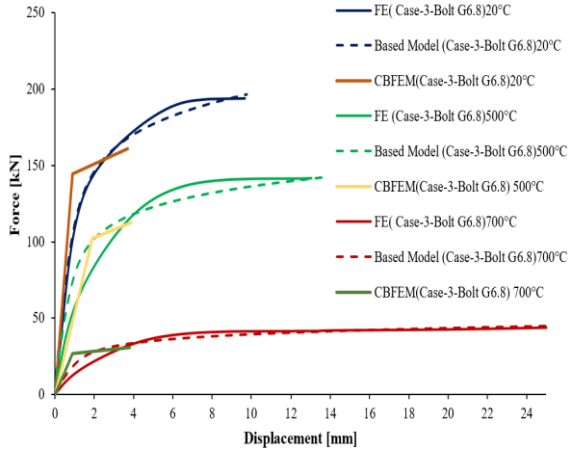

(f) Case 3 (6.8 bolts)

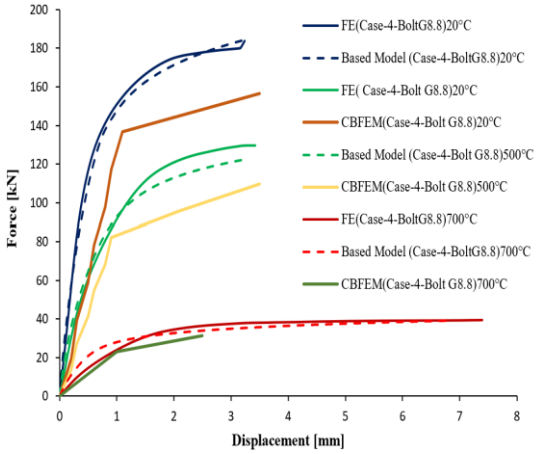

(g) Case 4 (8.8 bolts)

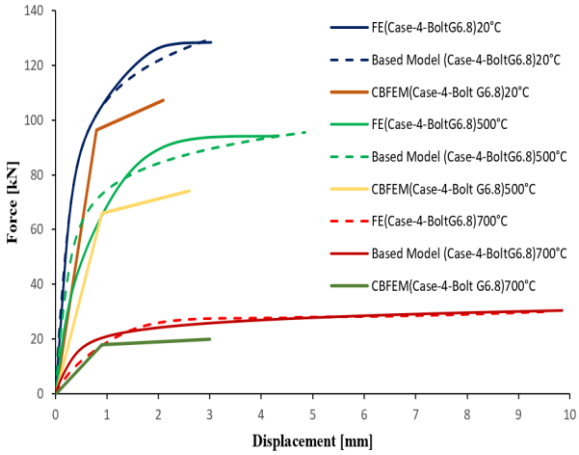

(h) Case 4 (6.8 bolts)

Figure 5-10. Comparisons of FE and component-based model for assemblies with the same failure mode (Case1, Case2, Case3, Case4)

The global responses of Cases 5 and 6 in Figure 5-11. The global force–displacement responses of Cases 5 and 6 reveal a progressive reduction in stiffness and strength with increasing temperature, with Case 6 showing a more pronounced degradation compared to Case 5. At ambient conditions, the CBM reproduces the FEM curves accurately in both stiffness and peak load, while the CBFEM remains systematically conservative. At elevated temperatures (500 °C and 700 °C), both cases exhibit downward shifts of the curves, yet the reduction is more severe in Case 6, resulting in lower peak forces and flatter post-peak behaviour. Across all cases, the CBM provides a closer approximation of the FEM response, whereas the CBFEM consistently underestimates the global capacity.

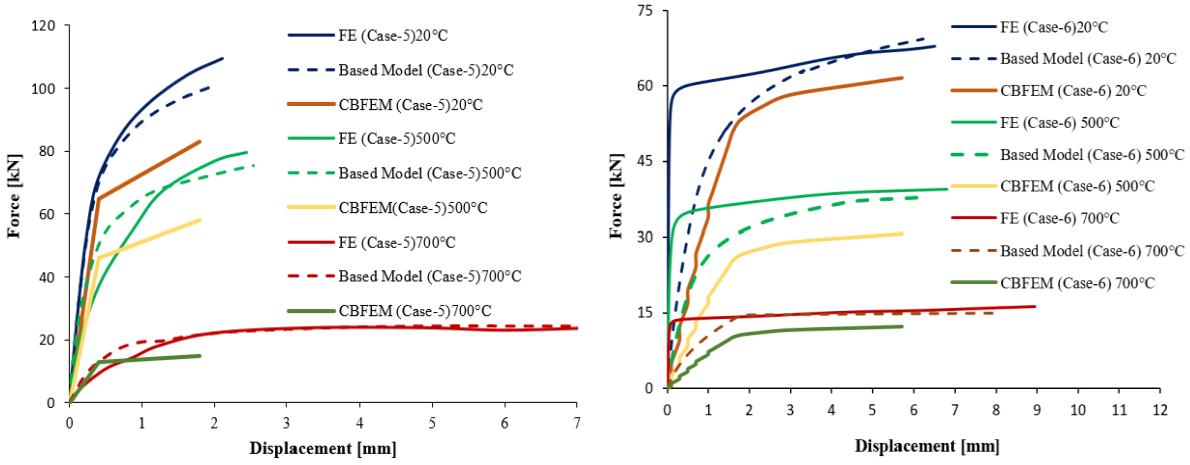

Figure 5-11. Comparisons of FE and component-based model for Cases 5 & 6

5.8.2 Comparaison of the ultimate force predictions

Table 5-2 illustrates the ultimate force results for the investigated cases together with their corresponding failure modes at both ambient and elevated temperatures. Verification against the FEM reference shows that the CBM provides a very close estimation of the ultimate resistance, with only minor deviations across cases. This confirms the ability of the CBM to capture not only the peak capacity but also the governing failure modes of the connections. By comparison, the CBFEM consistently produces lower ultimate force values for the same failure modes, reflecting its conservative nature. This conservative bias becomes more pronounced at elevated temperatures, where material degradation reduces strength. Overall, the results demonstrate that the CBM offers reliable and accurate predictions of ultimate resistance, while the CBFEM remains safe-sided in its estimates.

Table 5-2. Ultimate Force of the connections with their failure mode at ambient and elevated temperatures

	Component-based model (KN)		FE (KN)		CBFEM (kN)		Failure mode
	Bolt G8.8	BoltG6.8	Bolt G8.8	BoltG6.8	Bolt G8.8	Bolt G6.8	
20°C							
Case (1)	87.1	64.8	87.8	64.1	76.1	51.6	Bolt shear
Case (2)	178.3	128.1	179.8	130.1	154.4	105.2	
Case (3)	259.4	194.4	269.7	193.6	232.6	158.8	
Case (4)	174.2	129.6	175.6	128.2	154.4	105.2	Bolt double shear
Case (5)	102.4		110.5		78		Tensile rapture
Case (6)	37.7		39.4		61.5		Block shear
500°C							
Case (1)	62.7	46.6	64.8	46.1	52.7	35.5	Bolt shear
Case (2)	128.3	92.2	129.4	93.6	109.4	73.5	
Case (3)	186.7	139.9	194.1	139.3	162.8	111.2	
Case (4)	122.2	93.3	129.6	92.3	109.4	73.5	Bolt double shear
Case (5)	73.7		79.5		60.8		Tensile rapture
Case (6)	69.3		67.9		47.9		Block Shear
700°C							
Case (1)	20.0	14.9	20.1	14.7	16.2	10.2	Bolt shear
Case (2)	41.0	29.4	41.3	29.9	31.2	24.1	
Case (3)	59.6	44.7	62.0	44.5	53.4	36.4	
Case (4)	40.0	29.8	39.6	29.3	31.2	24.1	Bolt double shear
Case (5)	23.5		25.4		17.9		Tensile rapture
Case (6)	21.3		21.1		12.3		Tensile rapture

5.8.3 Verification of the initial stiffness predictions

Table 5-3 presents the comparison of initial stiffness values for the studied assemblies. For connections with high-strength bolts (Cases 1 to 3) governed by shear failure, a clear difference in initial stiffness is observed when compared with ordinary bolt assemblies. Within these cases, which fail by the same mode, the number of bolts does not appear to significantly influence the stiffness, indicating that bolt strength plays a more dominant role than bolt quantity in the elastic range.

Table 5-3. Axial initial stiffness of joints at different temperatures

	$K_{ini,CBM}$ (kN/mm)		$K_{ini,FE}$ (kN/mm)		$K_{ini,CBFEM}$ (kN/mm)	
	Bolt 8.8	Bolt 6.8	Bolt 8.8	Bolt 6.8	Bolt 8.8	Bolt 6.8
20°C						
Case (1)	96	93	115	95	25	17
Case (2)	99	96	114	97	51	35
Case (3)	89	85	124	107	77	53
Case (4)	211	192	240	194	51	35
Case (5)	118		126		58	
Case (6)	46		52		24	
500°C						
Case (1)	46	31	46	45	17	12
Case (2)	54	60	48	41	35	24
Case (3)	48	43	51	37	63	37
Case (4)	88	76	96	78	35	24
Case (5)	47		51		19	
Case (6)	19		21		12	
700°C						
Case (1)	13	13	16	13	6	4
Case (2)	14	13	11	13	11	8
Case (3)	13	13	17	15	15	12
Case (4)	19	17	23	17	11	8
Case (5)	10		11		6	
Case (6)	7		9		5	

A distinct behaviour is noted in Case 4, where the assembly subjected to double shear exhibits approximately twice the initial stiffness of those in single shear, reflecting the higher load transfer efficiency of this configuration. In Cases 5 and 6, the initial stiffness is primarily governed by the material properties and the overall connection geometry, with negligible influence from bolt grade. As expected, increasing the temperature leads to a progressive reduction in initial stiffness across all cases, demonstrating the degradation of material properties and the reduced ability of bolted joints to resist deformation. While all connections at ambient temperature display nonlinear force–displacement responses with yielding initiated by plastic deformation, the behaviour becomes progressively more linear with increasing temperature due to the loss of material stiffness and the consequent reduction in overall joint rigidity.

5.9 Conclusion

In this chapter, the CBFEM modelling approach was identified and implemented using the IDEAStatiCa software. The modelling process included a detailed mesh sensitivity study and the definition of the analysis procedures, ensuring reliable representation of the connection behaviour. The results obtained from the CBFEM were first verified against analytical predictions derived from Eurocode provisions, which provided a solid reference for evaluating the accuracy of the software.

Subsequently, the proposed MCBM model was validated in terms of its ability to reproduce the global behaviour of the connections. Force–displacement curves demonstrated a close correspondence between the CBM and the FEM reference results, with the CBFEM consistently showing more conservative predictions. Furthermore, the verification of the ultimate resistance confirmed that the CBM is capable of accurately estimating peak load values across different cases and temperature levels, while the CBFEM remained safe-sided by systematically underestimating capacity. Finally, the evaluation of the initial stiffness revealed that the CBM effectively captures the elastic response of the connections, reflecting the influence of bolt strength, connection geometry, and temperature.

Overall, the findings presented in this chapter demonstrate that the proposed CBM is a robust and reliable tool for predicting the mechanical performance of angle bolted connections under

both ambient and elevated temperatures, while the CBFEM offers conservative predictions that are suitable for design applications.

GENERAL CONCLUSION

6.1 General Conclusion

This thesis investigated the structural behaviour of single- and double-leg bolted steel angle connections subjected to tension, using bolts of grades 8.8 and 6.8. Finite element models were developed and validated in ANSYS to perform a comprehensive parametric study, addressing the influence of angle dimensions, number of legs, bolt grade, and bolt arrangement, all designed in accordance with Eurocode 3. The results demonstrate that variations in these parameters significantly affect the ultimate resistance of the connections, leading to different failure modes such as bolt shear fracture or angle tensile rupture. The finite element models, which accounted for geometric and material nonlinearities as well as contact interactions between components, showed strong agreement with experimental data reported in the literature. Furthermore, a modified component-based model was proposed, capable of capturing the interaction among all connection elements while incorporating the influence of material properties under elevated temperature conditions.

The following main conclusions can be set:

- Initially, the design was performed in accordance with Eurocode provisions. A comparison with the finite element (FE) results revealed that the Eurocode approach provides conservative predictions, underestimating the resistance of the connection at both ambient and elevated temperatures.

- The finite element (FE) analysis offered a comprehensive understanding of the structural response of the angle steel connections under both ambient and elevated temperatures. It successfully captured the nonlinear behaviour, including stiffness degradation, stress redistribution, and the evolution of failure modes with increasing temperature.

- The results show that shear governs the failure mode consistently across all temperatures, indicating its dominance over thermal effects. This underlines the importance of accounting for shear in connection design and evaluation.

- With a thick angle, the failure is localized within the angle itself across all temperatures, remaining unaffected by bolt variations. This confirms the dominance of the angle’s behaviour in governing the connection response.

- The model exhibits block shear failure at ambient temperature but shifts to tension failure at elevated temperatures, independent of bolt changes. This highlights the governing role of temperature in altering the failure mechanism.

- The Component-Based Model (CBM) was assessed against the finite element (FE) results in order to evaluate its capability to accurately predict the global behaviour of bolted single-angle connections.

- A good agreement was observed between the CBM and FE results in terms of the force displacement response, confirming that the CBM is able to capture the essential mechanical behaviour of the connection. This validates the applicability of the component-based approach for representing the nonlinear response of such connections under both ambient and elevated temperatures.

-Regarding the initial stiffness, the CBM predictions were found to be in close agreement with those obtained from the FE analysis. In most cases, the initial elastic slope derived from the CBM matches well with the FE results, indicating that the model appropriately represents the elastic response of the connection. Minor discrepancies observed in some configurations where the FE model predicts slightly higher stiffness can be attributed to local effects and simplifications inherent in the CBM formulation.

-In terms of ultimate capacity, the CBM generally provides reasonable predictions compared to the FE results. However, a tendency to underestimate the ultimate strength was observed in certain cases. This underestimation suggests that while the CBM is conservative, it may require refinement or calibration particularly in the definition of component resistances or interaction effects to improve its accuracy at higher load levels.

-The Component-Based Finite Element Method (CBFEM) was implemented to provide a more advanced representation of the structural behaviour of bolted single-angle connections. Its formulation combines the advantages of the component-based approach with the accuracy of finite element modelling, allowing for a detailed yet design-oriented analysis.

-The preparation of the CBFEM model involved defining the connection components (angle, bolts, and gusset plate) using nonlinear material behaviour, appropriate boundary conditions, and interaction properties. Particular attention was given to the modelling of contacts and load

transfer mechanisms, ensuring consistency with the physical behaviour observed in the FE simulations.

-The design according to the Eurocode (EC3) was first performed to establish a reference resistance and stiffness using standard analytical expressions. As observed previously, the Eurocode provides safe and conservative estimates, particularly in terms of resistance, due to simplified assumptions and partial safety factors.

-When comparing the CBFEM results with the FE analysis, a good agreement was observed in terms of global response. The CBFEM was able to capture both the initial stiffness and the nonlinear behaviour up to failure with reasonable accuracy. However, in some cases, slight deviations were noted, particularly near the ultimate load, where the CBFEM may underestimate the resistance due to embedded safety assumptions and simplifications in component formulations.

-In comparison with the Component-Based Model (CBM), the CBFEM shows improved accuracy, especially in representing the interaction between components and the redistribution of stresses. While the CBM provides a simplified and efficient prediction, the CBFEM offers a more refined description of the structural response.

- The CBM model shows good agreement with the CBFEM model in terms of global behaviour and predicted resistance. This consistency confirms the reliability of both approaches for connection evaluation.

- The IDEAStatiCa software consistently predicts the same failure modes across all temperatures, even when the actual behaviour changes or begins to shift. This reflects its reliance on simplified component assumptions rather than temperature-dependent effects.

Finally, the above methods and especially the proposed modified component based-method is highly recommended for the assessment of the fire resistance present for braced steel connections.

6.2 Recommendations for future research

The recommendations for potential future research are outlined below:

- Expand the investigation by simply modifying one geometric parameter, such as analysing the behaviour of steel braced frames for U profile sections.

- Inverstigate the effect of inclined load conditions of this connection type.
- Expand the analysis to include thermo-mechanical considering non-uniform temperature fields.
- Performing an experimental study on angle steel members under fire conditions.
- Extend the study for the case of post-earthquake fire scenario.
- Extend the study for welded and hybrid connections when subjected to fire.

BIBLIOGRAPHY

[1] Andrade, J. B., Bragança, L., Camões, A. 2016. *Steel sustainability assessment — Do BSA tools really assess steel properties? ,* Journal of Constructional Steel Research, 120, pp. 106–116. https://doi.org/10.1016/j.jcsr.2016.01.011

[2] Kosanović, S., Fikfak, A., Novaković, N., Klein, T.2018. *Reviews of Sustainability and Resilience of the Built Environment for Education, Research and Design*, TU Delft OPEN Publishing, Available from: https://books.bk.tudelft.nl/index.php/press/catalog/series/KLABS

[3] Mayar, K., Carmichael, D. G., Shen, X. 2022. *Resilience and Systems—A Review. ,* Sustainability, 14(14), pp. 8327. https://doi.org/10.3390/su14148327

[4] Buchanan, A. H., Abu, A. K.2017. *Structural design for fire safety*, John Wiley & Sons,

[5] Abidelah, A., Bouchaïr,A., Kerdal,D. E. 2012. *Experimental and analytical behavior of bolted end-plate connections with or without stiffeners,* Journal of Constructional Steel Research, 76, pp. 13–27. https://doi.org/10.1016/j.jcsr.2012.04.004

[6] Simões da Silva, L.,Santiago A.,Vila Real P. 2001. *A component model for the behaviour of steel joints at elevated temperatures,* Journal of Constructional Steel Research, 57(11), pp. 1169-1195. https://doi.org/10.1016/S0143-974X(01)00039-6

[7] ANSYS.2023. *ANSYS Student® Academic research, R 2.*, 2023. [cited Access; Available from: https://www.ansys.com/academic/students/ansys-student [Accessed: 20 December 2023]

[8] EN_1993-1-8. 2005. Eurocode3:design of steel structures-part 1-8: Design of Joints,European Committee for Standarization: Brussel, Belgium.

[9] EN_1993-1-1. 2005. Eurocode 3: Design of steel structures - Part 1-1: General rules and rules for buildings,European Committee for Standarization: Brussel, Belgium.

[10] EN_1993-1-2. 2005. Eurocode 3: Design of steel structures - Part 1-2: General rules - Structural fire design,European Committee for standarization: Brussels, Belgium.

[11] G, W.2024. *MODERN STEEL CONSTRUCTION*, American Institute of Steel Construction (AISC), Available from: https://www.aisc.org/globalassets/modern-steel/archives/2024/december2024.pdf

[12] Buchanan, A. H.,Abu A. K.2017. *Structural Design for Fire Safety*, Wiley

[13] Der, B., Raszková, S., Wald, F., Bihina, G., Gaigl, C., Rus, V., & Malaska, M. . 2022. *Emissivity of hot-dip galvanized surfaces in future development of EN 1993-1-2,* Journal of Structural Fire Engineering, 13.4 pp. 535-557. https://www.emerald.com/insight/content/doi/10.1108/jsfe-11-2021-0070/full/html

[14] Hassoune, M.,Kada A.,Menadi B.,Lamri B.,Yessad O.,Piloto P. A.,Jiang L. J. E. S. 2025. *Performance of single and built-up I-shaped cold formed steel stud under double sided walls fire exposure,* 335, pp. 120392. https://doi.org/10.1016/j.engstruct.2025.120392

[15] Gernay, T. 2024. *Performance-based design for structures in fire: Advances, challenges, and perspectives,* Fire Safety Journal, 142, pp. 104036. https://doi.org/10.1016/j.firesaf.2023.104036

[16] Simms, W. I.2012. *Fire resistance design of steel framed buildings* SCI, Silwood Park, Ascot, Berkshire. SL5 7QN UK, Available from: https://www.steelconstruction.info/images/5/5e/SCI_P375.pdf

[17] Franssen, J.-M.,Real P. V.2015. *Fire Design of Steel Structures*. 2nd EDITION, Wilhelm Ernst & Sohn,

[18] CEN. 2005. EN-1993-1-2,Eurocode 3: Design of steel structures - Part 1-2: General rules - Structural fire design,European Committee for standarization: Brussels, Belgium.

[19] Merouani, M. R.,Kada A.,Lamri B.,Piloto P. A. J. A. J. o. C. E. 2023. *Finite-element analysis for the performance of steel frames under fire after earthquake,* 24(2), pp. 593-606. https://doi.org/10.1007/s42107-022-00520-1

[20] Oribi, S. B.,Kada A.,Lamri B.,Mesquita L. 2023. *Behaviour of cellular steel beams at ambient and high-temperature conditions,* Journal of Constructional Steel Research, 207, pp. 107969. https://doi.org/10.1016/j.jcsr.2023.107969

[21] Sakumoto, Y.,Keira K.,Furumura F.,Ave T. 1993. *Tests of Fire-Resistant Bolts and Joints,* Journal of Structural Engineering, 119(11). https://doi.org/10.1061/(ASCE)0733-9445(1993)119:11(3131)

[22] Li, G. Q.,Yin Y. Z.,Li M. F. 2002. *Experimental studies on the material properties of high-strength bolt connection at elevated temperatures.,* Steel and Composite Structures, An International Journal,, 2(4), pp. 247-258. https://doi:10.12989/scs.2002.2.4.247

[23] L. Yu. "*Behavior of bolted connections during and after a fire* ", 2006. Available from: http://search.ebscohost.com/login.aspx?direct=true&db=edsndl&AN=edsndl.oai.union.ndltd.or

[24] Hu, J. B., Davison, I. W. Burgess, and R. J. Plank, . *Comparative study of the behaviour of BS 4190 and BS EN ISO 4014 bolts in fire. The 3rd International Conference on Steel and Composite Structures* Manchester: Francis,

[25] Kodur. V,Kand. S,Khaliq.W. 2012. *fect of Temperature on Thermal and Mechanical Properties of Steel Bolts,* Journal of Materials in Civil Engineering, 24, pp. 765 774,. https://doi.org/10.1061/(ASCE)MT.1943-5533.0000445

[26] Peixoto, R. M.,Seif M. S.,Vieira L. C. M. 2017. *Double-shear tests of high-strength structural bolts at elevated temperatures,* Fire Safety Journal, 94, pp. 8-21. https://doi.org/10.1016/j.firesaf.2017.09.003

[27] Cai, W.-Y.,Jiang J.,Li G.-Q.,Wang Y.-B. 2021. *Fracture behavior of high-strength bolted steel connections at elevated temperatures,* Engineering Structures, 245, pp. 112817. https://doi.org/10.1016/j.engstruct.2021.112817

[28] Rezaeian, A.,Keshavarz M.,Hajjari E. 2020. *Mechanical properties of steel welds at elevated temperatures,* Journal of Constructional Steel Research, 167, pp. 105853. https://doi.org/10.1016/j.jcsr.2019.105853

[29] Ban, H.,Yang Q.,Shi Y.,Luo Z. 2021. *Constitutive model of high-performance bolts at elevated temperatures,* Engineering Structures, 233, pp. 111889. https://doi.org/10.1016/j.engstruct.2021.111889

[30] Shaheen, M. A.,Foster A. S. J.,Cunningham L. S.,Afshan S. 2020. *A numerical investigation into stripping failure of bolt assemblies at elevated temperatures,* Structures, 27, pp. 1458-1466. https://doi.org/10.1016/j.istruc.2020.07.042

[31] Yu, H. 2011. *Experimental investigation of structural steel welds at high temperature,* Advanced Materials Research. https://www.scientific.net/AMR.250-253.3350

[32] Kada, A.,Lamri B.,Mesquita L.,Bouchair A. J. A. J. o. C. E. 2016. *Finite element analysis of steel beams with web apertures under fire condition,* 17(8), pp. 1035-1054. https://scholar.google.com/scholar?hl=ar&as_sdt=0%2C5&q=+Finite+element+anaysis+of+steel+beams+with+web+apertures+under+fire+condition+&btnG=

[33] Kada, A.,Lamri B. J. A. J. o. C. E. 2019. *Numerical analysis of non-restrained long-span steel beams at high temperatures due to fire,* 20(2), pp. 261-267. https://doi.org/10.4081/fire.2017.27

[34] Simões da Silva, L.,Girão Coelho A. M. 2001. *An analytical evaluation of the response of steel joints under bending and axial force,* Computers & Structures, 79(8), pp. 873-881. https://doi.org/10.1016/S0045-7949(00)00179-6

[35] Wald, F.,da Silva L. S.,Moore D.,Santiago A. "*Experimental behaviour of steel joints under natural fire* ", in, 2004,

[36] Shyam-Sunder, S.,Gann R. G.,Grosshandler W. L.,Lew H. S.,Bukowski R. W.,Sadek F.,Gayle F. W.,Gross J. L.,McAllister T. P.,Averill J. D. 2005. *Federal building and fire safety investigation of the world trade center disaster: final report of the national construction safety team on the collapses of the world trade center towers (NIST NCSTAR 1)*.

[37] Newman, G. J. F. S. E., Vol. 2000. *New Approach to Multi-Storey Steel Framed Buildings,* 7(6), pp. 14-16.

[38] Leston-Jones, L. C. "*THE INFLUENCE OF SEMI-RIGID CONNECTIONS ON THE PERFORMANCE OF STEEL FRAMED* ",University of Sheffield, 1997. Available from:

[39] Al-Jabri, K. S. "*The behaviour of steel and composite beam-to-column connections in fire* ",University of Sheffield, 1999. Available from: https://etheses.whiterose.ac.uk/id/eprint/2997/

[40] Burgess, I.,Davison J. B.,Dong G.,Shan-Shan Huang. 2012. *The Role of Connections in the Response of Steel Frames to Fire,* Structural Engineering International. https://doi.org/10.2749/101686612X13363929517811

[41] Kruppa, J. 1976. Resistance en feu des assemblages par boulons haute resistance,Centre Technique Industriel de la Construction Metallique,

[42] Steel, B., *The performance of beam/column/beam connections in the BS476: art 8 fire test*. 1982, Reports T/RS/1380/33/82D and T/RS/1380/34.

[43] Lawson, R. J. S. e. 1990. *Behaviour of steel beam-to-column connections in fire,* 68, pp. 263-71.

[44] Yu, H.,Burgess I.,Davison J.,Plank R. J. E. s. 2009. *Tying capacity of web cleat connections in fire, Part 1: Test and finite element simulation,* 31(3), pp. 651-663.

[45] Hu, Y.,Davison J.,Burgess I.,Plank R. "*Experimental study on flexible end plate connections in fire* ", in, 2008, pp. 1007-1012,

[46] Yu, H.,Burgess I.,Davison J.,Plank R. "*Experimental investigation of the behaviour of flush endplate connections in fire* ", in, 2008,

[47] Yu, H.,Burgess I. W.,Davison J. B.,Plank R. J. 2009. *Experimental investigation of the behaviour of fin plate connections in fire,* Journal of Constructional Steel Research, 65(3), pp. 723-736. https://doi.org/10.1016/j.jcsr.2008.02.015

[48] Yu, H.,Burgess I.,Davison J.,Plank R. J. P. o. t. I. 2007. *Experimental investigation of the robustness of fin plate connections in fire*.

[49] Yu, H.,Burgess I. W.,Davison J. B.,Plank R. J. 2009. *Tying capacity of web cleat connections in fire, Part 1: Test and finite element simulation,* Engineering Structures, 31(3), pp. 651-663. https://doi.org/10.1016/j.engstruct.2008.11.005

[50] Al-Jabri, K. S.,Burgess I. W.,Lennon T.,Plank R. J. 2005. *Moment–rotation–temperature curves for semi-rigid joints,* Journal of Constructional Steel Research, 61(3), pp. 281-303. https://doi.org/10.1016/j.jcsr.2004.09.001

[51] Leston-Jones LC, L. T., Plank RJ, and Burgess IW 1997. *Elevated Temperature Moment Rotation Tests on Steelwork Connections,* Proc. Instn. Civ. Engrs Structs. & Bldgs, 122, pp. 410-419. https://doi.org/10.1680/istbu.1997.29830

[52] Liu, T. C. H.,Fahad M. K.,Davies J. M. 2002. *Experimental investigation of behaviour of axially restrained steel beams in fire,* Journal of Constructional Steel Research, 58(9), pp. 1211-1230. https://doi.org/10.1016/S0143-974X(01)00062-1

[53] ISO. 2014. Fire resistance tests — Elements of building construction — Part 11: Specific requirements for the assessment of fire protection to structural steel elements (ISO 834-11:2014),International Organization for Standardization, Geneva, Switzerland.

[54] Hu, G.,Engelhardt M. 2011. *Investigations on the Behavior of Steel Single Plate Beam End Framing Connections in Fire,* Journal of Structural Fire Engineering, 2(3), pp. 195-204. https://doi.org/10.1260/2040-2317.2.3.195

[55] Selden, K.,Fischer E.,Varma A. 2016. *Experimental investigation of composite beams with shear connections subjected to fire loading,* Journal of Structural Engineering

142(2), pp. 04015118. https://doi.org/10.1061/(ASCE)ST.1943-541X.000138

[56] Faralli, A. C.,Latour M.,Tan P. J.,Rizzano G.,Wrobel P. 2021. *Experimental investigation and modelling of T-stubs undergoing large displacements,* Journal of Constructional Steel Research, 180, pp. 106580. https://doi.org/10.1016/j.jcsr.2021.106580

[57] Qiang, X.,Bijlaard F. S. K.,Kolstein H.,Jiang X. 2014. *Behaviour of beam-to-column high strength steel endplate connections under fire conditions – Part 1: Experimental study,* Engineering Structures, 64, pp. 23-38. https://doi.org/10.1016/j.engstruct.2014.01.028

[58] Wang, W.,Fang H.,Zhang L. 2023. *Experimental and numerical studies on the behavior of high strength steel shear connections at elevated temperatures,* Fire Safety Journal, 139, pp. 103820. https://doi.org/10.1016/j.firesaf.2023.103820

[59] Qiang, X.,Shu Y.,Jiang X. 2023. *Mechanical behaviour of high strength steel T-stubs at elevated temperatures: Experimental study,* Thin-Walled Structures, 182, pp. 110314. https://doi.org/10.1016/j.tws.2022.110314

[60] Abdoh, D. A. 2024. *Failure analysis of bolted steel plate connections with three-dimensional flexibilities,* International Journal of Mechanical Sciences, 272, pp. 109313. https://doi.org/10.1016/j.ijmecsci.2024.109313

[61] Khonsari, S. V.,Bazli M.,Jafari A.,Mohammadi M. 2024. *Effect of ductility of flush end-plate connections on the behaviour of MRFs under fire conditions: An experimental study,* Engineering Structures, 311, pp. 117977. https://doi.org/10.1016/j.engstruct.2024.117977

[62] Wang, H.,Nie S.,Liu M.,Zhang L.,Elchalakani. M. 2025. *Enhanced Fire Resistance of Double Web Angle Cleat Connections with Austenitic High-Strength Bolts during Furnace Fires,* Journal of Structural Engineering, 151(5). https://doi.org/10.1061/JSENDH.STENG-1367

[63] Institute, S. C., *investigation of Broadgate Phase 8 fire*, Structural fire engineering :Steel Construction Institute, Editor. 1991.

[64] Wang, Y. C. E. 2002. *Behaviour and Design for Fire Safety (1st ed.).* Steel and Composite Structures, (CRC Press.). https://doi.org/10.1201/9781482267693

[65] Bailey, C. G. J. A. i. S. E. 2005. *Fire engineering design of steel structures,* 8(3), pp. 185-202.

[66] Lennon, T.,Moore D.,Bailey C. J. T. S. E. 1999. *The behaviour of full-scale steel-framed buildings subjected to compartment fires,* 77(8), pp. 15-21.

[67] Usmani, A. S.,Chung Y.,Torero J. L. J. F. S. J. 2003. *How did the WTC towers collapse: a new theory,* 38(6), pp. 501-533.

[68] Orabi, M. A.,Jiang L.,Usmani A.,Torero J. 2024. *The Collapse of World Trade Center 7: Revisited,* Fire Technology, 60(5), pp. 2963-2990. 10.1007/s10694-022-01225-2

[69] Wald, F.,Simões da Silva L.,Moore D. B.,Lennon T.,Chladná M.,Santiago A.,Beneš M.,Borges L. 2006. *Experimental behaviour of a steel structure under natural fire,* Fire Safety Journal, 41(7), pp. 509-522. https://doi.org/10.1016/j.firesaf.2006.05.006

[70] Wang, Y. C. 2000. *An analysis of the global structural behaviour of the Cardington steel-framed building during the two BRE fire tests,* Engineering Structures, 22(5), pp. 401-412. https://doi.org/10.1016/S0141-0296(98)00127-8

[71] Wang, W.-Y.,Li G.-Q.,Dong Y.-L. 2007. *Experimental study and spring-component modelling of extended end-plate joints in fire,* Journal of Constructional Steel Research, 63(8), pp. 1127-1137. https://doi.org/10.1016/j.jcsr.2006.10.006

[72] Torero, J. L. *Fire-induced structural failure: the world trade center, New York. Proceedings of the Institution of Civil Engineers-Forensic Engineering.* DOI: https://doi.org/10.1680/feng.2011.164.2.69

[73] CEN. 2005. EN-1993-1-8, Eurocode3:design of steel structures-part 1-8: Design of Joints. ,European Committee for Standarization: Brussel, , Belgium.

[74] Jaspart, J. P. 2000. *General report: session on connections,* Journal of Constructional Steel Research, 55(1), pp. 69-89. https://doi.org/10.1016/S0143-974X(99)00078-4

[75] Al-Jabri, K. S. "*The behaviour of steel and composite beam-to-column connections in fire* ",PhD thesis,University of Sheffield, 199. Available from: https://etheses.whiterose.ac.uk/id/eprint/2997/

[76] Spyrou, S. "*Development of a component based model of steel beam-to-column joints at elevated temperatures.* ",PhD thesis,University of Sheffield, 2002. Available from: https://etheses.whiterose.ac.uk/id/eprint/12830/

[77] Weigand, J. M.,Peixoto R.,Marcos Vieira L. C.,Main J. A.,Seif M. 2018. *An empirical component-based model for high-strength bolts at elevated temperatures,* Journal of Constructional Steel Research, 147, pp. 87-102. https://doi.org/10.1016/j.jcsr.2018.03.034

[78] Yu, H.,Burgess I. W.,Davison J. B.,Plank R. J. 2009. *Tying capacity of web cleat connections in fire, Part 2: Development of component-based model,* Engineering Structures, 31(3), pp. 697-708. https://doi.org/10.1016/j.engstruct.2008.11.006

[79] Block, F. M.,Burgess I. W.,Davison J. B.,Plank R. J. 2007. *The development of a component-based connection element for endplate connections in fire,* Fire Safety Journal, 42(6), pp. 498-506. https://doi.org/10.1016/j.firesaf.2007.01.008

[80] Sarraj, M. "*The behaviour of steel fin plate connections in fire.* ",PhD thesis,University of Sheffield, 2007. Available from: https://etheses.whiterose.ac.uk/id/eprint/3035/

[81] Santiago, A. M. d. C. "*Behaviour of beam-to-column steel joints under natural fire* ",Universidade de Coimbra, 2008. Available from: https://hdl.handle.net/10316/7543

[82] Taib, M. "*The performance of steel framed structures with fin-plate connections in fire* ",Doctoral dissertation,University of Sheffield 2012. Available from:

[83] Sana, E. K.,Elie H. 2017. *Mechanical modeling for predicting the axial restraint forces and rotations of steel top and seat angle connections at elevated temperatures,* Journal of Structural Fire Engineering, 8(3), pp. 258-286. https://doi.org/10.1108/JSFE-05-2017-0033

[84] Quan, G.,Huang S.-S.,Burgess I. 2016. *Component-based model of buckling panels of steel beams at elevated temperatures,* Journal of Constructional Steel Research, 118, pp. 91-104. https://doi.org/10.1016/j.jcsr.2015.10.024

[85] Xie, B.,Hou J.,Xu Z.,Dan M. 2018. *Component-based model of fin plate connections exposed to fire-part I: Plate in bearing component,* Journal of Constructional Steel Research, 149, pp. 1-13. https://doi.org/10.1016/j.jcsr.2018.07.011

[86] Liu, Y.,Huang S.-S.,Burgess I. 2020. *Component-based modelling of a novel ductile steel connection,* Engineering Structures, 208, pp. 110320. https://doi.org/10.1016/j.engstruct.2020.110320

[87] Quan, G.,Dai X.,Ye J.,Huang S.-S.,Burgess I. 2022. *Modelling of composite fin-plate connections under fire conditions using component-based method,* Engineering Structures, 264, pp. 114451. https://doi.org/10.1016/j.engstruct.2022.114451

[88] Zhao, H.,Liu X.-G.,Tao M.-X. 2022. *Component-based model of semi-rigid connections for nonlinear analysis of composite structures,* Engineering Structures, 266, pp. 114542. https://doi.org/10.1016/j.engstruct.2022.114542

[89] Guo, Z.,Li G.,Nie Z.,Chen Y. 2024. *Component-based models of beam-column joints exposed to fire in steel framed structures against progressive collapse,* Engineering Structures, 304, pp. 117645. https://doi.org/10.1016/j.engstruct.2024.117645

[90] Wang, B.,Jiang J.,Li H.,Chen W.,Ye J. 2025. *Development of high-temperature component-based models for TSWA connections in fire,* Engineering Structures, 325, pp. 119489. https://doi.org/10.1016/j.engstruct.2024.119489

[91] Guo, Z.,Li G.,Chen Y.,Zhang X. 2025. *The development of a component-based model for extended endplate joints in fire-induced progressive collapse scenarios,* Journal of Constructional Steel Research, 225, pp. 109182. https://doi.org/10.1016/j.jcsr.2024.109182

[92] Zhan, G.,Guokeng L.,Ying C.,Xiaoyong Z. 2025. *The development of a component-based model for extended endplate joints in fire-induced progressive collapse scenarios,* Journal of Constructional Steel Research, 225, pp. 109182. https://doi.org/10.1016/j.jcsr.2024.109182

[93] Aquino, B.,Jesus G.,Amador A. M. G.,Miranda J. H. A.,Fonfría J. J. J. d. C. 2021. *A Review of the T-Stub Components for the Analysis of Bolted Moment Joints,* Applied Sciences, 11. https://doi.org/10.3390/app112210731

[94] Anwar, G. A. "*Ultimate deformation and resistance capacity of bolted T-Stub connections under different loading conditions* ", 2017. Available from:

[95] Heidarpour, A.,Bradford M. A. 2008. *Behaviour of a T-stub assembly in steel beam-to-column connections at elevated temperatures,* Engineering Structures, 30(10), pp. 2893-2899. https://doi.org/10.1016/j.engstruct.2008.04.007

[96] Ribeiro, J.,Santiago A.,Rigueiro C.,da Silva L. S. 2015. *Analytical model for the response of T-stub joint component under impact loading,* Journal of Constructional Steel Research, 106, pp. 23-34. https://doi.org/10.1016/j.jcsr.2014.11.013

[97] Saberi, V.,Gerami M.,Kheyroddin A. 2014. *Comparison of bolted end plate and T-stub connection sensitivity to component thickness,* Journal of Constructional Steel Research, 98, pp. 134-145. https://doi.org/10.1016/j.jcsr.2014.02.012

[98] Lyu, J.,Yan S.,He S.,Zhao X.,Rasmussen K. 2023. *Mechanical model for the full range behaviour of bolted T-stubs,* Journal of Constructional Steel Research, 200, pp. 107652. https://doi.org/10.1016/j.jcsr.2022.107652

[99] Zhang, Y.,Gao S.,Guo L.,Fu F.,Wang S. 2022. *Ultimate tensile behavior of bolted stiffened T-stub connections in progressive collapse resistance,* Journal of Constructional Steel Research, 189, pp. 107111. https://doi.org/10.1016/j.jcsr.2021.107111

[100] Barata, P.,Ribeiro J.,Rigueiro C.,Santiago A.,Rodrigues J. P. 2014. *Assessment of the T-stub joint component at ambient and elevated temperatures,* Fire Safety Journal, 70, pp. 1-13. https://doi.org/10.1016/j.firesaf.2014.08.009

[101] Li, Y.,Zhao J. 2018 *Analytical Investigation of Beam-to-Column Endplate Connections at Elevated Temperatures,* International Journal of Steel Structures 19. https://doi.org/10.1007/s13296-018-0127-6

[102] Johan, M.,Matteis. G. D. 2016. *Structural response of aluminium T-stub connections at elevated temperatures and fire,* Key Engineering Materials. https://doi.org/10.4028/www.scientific.net/KEM.710.127

[103] Li, Y.,Zhao J. 2017. *Mechanical model and finite element analyses of the T-stub joint component in fire,* Advances in Structural Engineering, 20(12). https://doi.org/10.1177/1369433217695621

[104] Gao, F.,Liu Z.,Guan X. 2021. *Fire resistance behavior of T-stub joint components under transient heat transfer conditions,* Engineering Structures, 237, pp. 112164. https://doi.org/10.1016/j.engstruct.2021.112164

[105] Roy, K.,Rezaeian H.,Lakshmanan D.,Fang Z.,Beulah Gnana Ananthi G.,Lim J. B. P. 2023. *Structural behaviour of cold-formed steel T-Stub connections with HRC and screws subjected to tension force,* Engineering Structures, 283, pp. 115922. https://doi.org/10.1016/j.engstruct.2023.115922

[106] Wang, W.,Fang H.,Wang Z. 2023. *Comprehensive studies on the behaviors of high strength steel T-stubs with thin-walled flange at elevated temperatures,* Thin-Walled Structures, 190, pp. 110998. https://doi.org/10.1016/j.tws.2023.110998

[107] Krishnamurthy, N. 1980. *Modelling and prediction of steel bolted connection behavior,* Computers & Structures, 11(1), pp. 75-82. https://doi.org/10.1016/0045-7949(80)90148-0

[108] Al Jabri, K. J. W. T. o. T. B. E. 2004. *Modelling of the behaviour of beam-to-column connections at elevated temperature,* 76.

[109] Al-Jabri, K. S.,Seibi A.,Karrech A. 2006. *Modelling of unstiffened flush end-plate bolted connections in fire,* Journal of Constructional Steel Research, 62(1), pp. 151-159. https://doi.org/10.1016/j.jcsr.2005.04.016

[110] Kevin, L.,Jonathan B.,Donald D. 2009. *Failure analysis of the World Trade Center 5 building,* Journal of Fire Protection Engineering, 19(4), pp. 261-274. https://doi.org/10.1177/1042391509105596

[111] Schaumann, P.,Kirsch T. 2013. *Simulation of a Flush Endplate Connection at Elevated Temperatures Including Fracture Simulation,* Journal of Structural Fire Engineering, 4(2), pp. 103-112. https://doi.org/10.1260/2040-2317.4.2.103

[112] Sarraj, M.,Burgess I. W.,Davison J. B.,Plank R. J. 2007. *Finite element modelling of steel fin plate connections in fire,* Fire Safety Journal, 42(6), pp. 408-415. https://doi.org/10.1016/j.firesaf.2007.01.007

[113] Qiang, X.,Bijlaard F. S. K.,Kolstein H.,Jiang X. 2014. *Behaviour of beam-to-column high strength steel endplate connections under fire conditions – Part 2: Numerical study,* Engineering Structures, 64, pp. 39-51. https://doi.org/10.1016/j.engstruct.2014.01.034

[114] Selamet, S.,Garlock M. E. 2014. *Fire resistance of steel shear connections,* Fire Safety Journal, 68, pp. 52-60. https://doi.org/10.1016/j.firesaf.2014.05.016

[115] Seif, M.,Main J.,Weigand J.,McAllister T. P.,Luecke W. 2016. *Finite element modeling of structural steel component failure at elevated temperatures,* Structures, 6, pp. 134-145. https://doi.org/10.1016/j.istruc.2016.03.002

[116] Hantouche, E. G.,Abboud N. H.,Morovat M. A.,Engelhardt M. D. 2016. *Analysis of steel bolted double angle connections at elevated temperatures,* Fire Safety Journal, 83, pp. 79-89. https://doi.org/10.1016/j.firesaf.2016.05.002

[117] Fischer, E. C.,Varma A. H. 2015. *Fire behavior of composite beams with simple connections: Benchmarking of numerical models,* Journal of Constructional Steel Research, 111, pp. 112-125. https://doi.org/10.1016/j.jcsr.2015.03.013

[118] Fischer, E. C.,Varma A. H. 2017. *Fire resilience of composite beams with simple connections: Parametric studies and design,* Journal of Constructional Steel Research, 128, pp. 119-135. https://doi.org/10.1016/j.jcsr.2016.08.004

[119] Gernay, T.,Franssen J.-M. 2020. *The introduction and the influence of semi-rigid connections in framed structures subjected to fire,* Fire Safety Journal, 114, pp. 103007. https://doi.org/10.1016/j.firesaf.2020.103007

[120] Akagwu, P. "*Experimental and Numerical Study on Bolted Web-Flange Steel Connections in Fire* ",DOCTORAL THESIS,Ulster University, 2020. Available from: https://pure.ulster.ac.uk/ws/portalfiles/portal/104163652/2021AkagwuPOPhD.pdf

[121] Zheng, Y.-h.,Zhong W.-h.,Zhang Y.,Tan Z.,Duan S.-C.,Meng B.,Gao Y.,Wang H.-c. 2024. *Failure mechanism of steel frames with angle steel-bolted connections exposed to fire under progressive collapse condition,* Engineering Failure Analysis, 155, pp. 107744. https://doi.org/10.1016/j.engfailanal.2023.107744

[122] Natesh, P. S.,Agarwal A.,Choe L. 2022. *Behaviour and design of double angle beam-column connection in fire conditions,* Fire Safety Journal, 134, pp. 103707. https://doi.org/10.1016/j.firesaf.2022.103707

[123] Huseyin, S.,Airong C.,Rujin M. 2023. *Simulation of bolted connections under fire: optimization and model validation,* Journal of Structural Fire Engineering, 14(4), pp. 481-500. https://doi.org/10.1108/JSFE-06-2022-0024

[124] Rezaeian, A.,Mansoori M.,Khajehdezfuly A. 2024. *Performance of steel beam with welded top-seat angle connections at elevated temperatures,* Journal of Structural Fire Engineering, 15(1), pp. 113-146. 10.1108/JSFE-07-2022-0026

[125] Gödrich, L.,Wald F.,Kabeláč J.,Kuříková M. 2019. *Design finite element model of a bolted T-stub connection component,* Journal of Constructional Steel Research, 157, pp. 198-206. https://doi.org/10.1016/j.jcsr.2019.02.031

[126] Kuříková, M.,Sekal D.,Wald F.,Maier N. 2021. *Advanced Design of Block Shear Failure,* Metals, 11, no. 7: 1088. https://doi.org/10.3390/met11071088

[127] Der, B. "*NUMERICAL CALCULATION OF MEMBERS AND JOINTS AT ELEVATED TEMPERATURE* ",PhD Thiesis,Czech Technical University, 2024. Available from: https://www.proquest.com/openview/9eaa869377e796e84e96b41f3dabf738/1?cbl=2026366&diss=y&pq-origsite=gscholar

[128] Batuhan, D.,Wald F.,Vild M. 2024. *Numerical Design Calculation of T-Stubs at Elevated Temperatures.,* Fire Technology, 1-22. https://doi.org/10.1007/s10694-024-01626-5

[129] Der, B.,Wald F. 2024. *Numerical design calculation of bolted lap joints at elevated temperatures,* Fire Safety Journal, 147, pp. 104202. https://doi.org/10.1016/j.firesaf.2024.104202

[130] Alfredo, B.2018. *Design and analysis of connections in steel structures: fundamentals and examples*, John Wiley & Sons,

[131] Zhang, A.-L.,Liu X.-C.,Wang Y.,Yu C.,Bai Z.-X.,Tran H. 2021. *Static performance of slidable bolt-assembly truss-to-column connection with oversized bolt holes,* Journal of Constructional Steel Research, 176, pp. 106374. https://doi.org/10.1016/j.jcsr.2020.106374

[132] Gong, Y. 2008. *Double-angle shear connections with small hollow structural section columns,* Journal of Constructional Steel Research, 64(5), pp. 539-549. https://doi.org/10.1016/j.jcsr.2007.11.006

[133] Gong, Y. 2009. *Design moment of shear connections at the ultimate limit state,* Journal of Constructional Steel Research, 65(10), pp. 1921-1930. https://doi.org/10.1016/j.jcsr.2009.06.004

[134] Bursi, O. S.,Gerstle K. H.,Sigfusdottir A.,Zitur J. L. 1994. *Behavior and analysis of bracing connections for steel frames,* Journal of Constructional Steel Research, 30(1), pp. 39-60. https://doi.org/10.1016/0143-974X(94)90076-0

[135] Oliveira, J. C. d.,Willibald S.,Packer J. A.,Christopoulos C.,Verhey T., *Cast steel nodes in tubular construction – Canadian experience*, in *Tubular Structures XI*. 2017

[136] Sukhen, C.2008. *The design of modern steel bridges.*, John Wiley & Sons,

[137] *Fabrication de pont métallique*, [cited Access; Available from: https://www.canametal.fr/ouvrage-art-et-ouvrages-complexes/fabrication-pont-metallique/

[138] Songzhao, Q.,Zhou Y.,Yin P.,Li X.,Wu H.,Wang W.,Huo S.,An W.,Tian Q.,Wu Y. 2025. *Staggered Two-Bolt Connections in Transmission Towers: A Comprehensive Study on Failure Mechanisms and Design Codes,* Buildings 15(4). https://doi.org/10.3390/buildings15040629

[139] EN_10056-1:2017. 2017. Structural steel equal and unequal leg angles; Part 1: Dimensions BSI Standards Limited 2017,

[140] *Hebei Changtong Steel Structure Co., Ltd.*, [cited Access; Available from: https://www.anglesteeltower.com/quality-13566667-oem-self-supporting-lattice-tower

[141] *Images libres de droits de Braced steel frame*, [cited Access; Available from: https://www.shutterstock.com/fr/search/braced-steel-frame

[142] Abedin, M.,Maleki S.,Kiani N.,Shahrokhinasab E. 2019. *Shear Lag Effects in Angles Welded at Both Legs,* Advances in Civil Engineering, 2019(1), 8041767. https://doi.org/10.1155/2019/8041767

[143] P, D. R.,P B. G. 1934. *Tensile tests of welded and riveted structural members,* Journal of the American Welding Society, 13(4),, pp. 21-27.

[144] T, G. G.,T W. B. 1942. *An investigation of welded connections for angle tension members. ,* The Welding Journal,, 44.

[145] Eugene, C. J.,Munse W. H. 1963. *Riveted and bolted joints: Truss-type tensile connections,* Journal of the Structural Division 89.1, pp. 67-106. https://doi.org/10.1061/JSDEAG.000089

[146] Samuel, E. W.,Giroux L. G. 1993. *Shear lag effects in steel tension members.,* Engineering Journal 30.3, pp. 77-89. https://doi.org/10.62913/engj.v30i3.618

[147] Georges, A.-S.,Bauer D. 2006. *Analytical approach for shear lag in welded tension members,* Canadian Journal of Civil Engineering, 33.4, pp. 384-394.. https://doi.org/10.1139/l06-058

[148] Zhu, H. T.,Yam M. C. H.,Lam A. C. C.,Iu V. P. 2009. *The shear lag effects on welded steel single angle tension members,* Journal of Constructional Steel Research, 65(5), pp. 1171-1186. https://doi.org/10.1016/j.jcsr.2008.10.004

[149] Fang, C.,Lam A. C. C.,Yam M. C. H. 2013. *Influence of shear lag on ultimate tensile capacity of angles and tees,* Journal of Constructional Steel Research, 84, pp. 49-61. https://doi.org/10.1016/j.jcsr.2013.02.006

[150] Ke, K.,Xiong Y. H.,Yam M. C. H.,Lam A. C. C.,Chung K. F. 2018. *Shear lag effect on ultimate tensile capacity of high strength steel angles,* Journal of Constructional Steel Research, 145, pp. 300-314. https://doi.org/10.1016/j.jcsr.2018.02.015

[151] Prabha, P.,Arul Jayachandran S.,Saravanan M.,Marimuthu V. 2011. *Prediction of the tensile capacity of cold formed angles experiencing shear lag,* Thin-Walled Structures, 49(11), pp. 1348-1358. https://doi.org/10.1016/j.tws.2011.06.003

[152] Kim Roddis, A., Bhargava, , *Tension capacity of bolted single angle shear connection*, AISC Research Report, Editor.

[153] Chandrakar, B., Gupta, M. K., Jaiswal, S. 2023. *Study of block shear failure on steel angle tension members through finite element modelling,* International Journal of Sustainable Building Technology and Urban Development, 14(3), pp. 389-404. https://doi.org/10.22712/susb.20230029

[154] Teh, L. H., & Gilbert, B. P. 2014. *Net section tension capacity of equal angle braces bolted at different legs,* Journal of Structural Engineering, 140(6). https://doi.org/10.1061/(ASCE)ST.1943-541X.0000964

[155] Construction, A. I. o. S. 2016. Specification for Structural Steel Buildings,ANSI/AISC, AISC, Chicago, Illinois,

[156] Construction, A. I. o. S. 2022. Specification for Structural Steel Buildings, ANSI/AISC, AISC, Chicago, Illinois.

[157] Yessad, O.,Kada A.,Lamri B. 2-7 July 2023. *Behaviour of Shear Bolted Connections in Bracing Steel Frames at Elevated Temperature*. *20th International Conference on Experimental Mechanics Applications in Materials Science, Engineering and Biomechanics*. Porto, Portugal, https://www.up.pt/arquivoweb/paginas.fe.up.pt/_icem20/proceedings_icem20/data/papers/20177.pdf

[158] Virdi, K. S.1999. *Guidance on good practice in simulation of semi-rigid connections by the finite element method. Numerical Simulation of Semi-Rigid Connections by the Finite Element Method, COST C1, Rep. of Working Group 6—Numerical Simulation, 1-12.*,

[159] Ungkurapinan, N. "*A study of joint slip in galvanized bolted angle connections* ",MSc Thesis,University of Manitoba, 2000. Available from: http://hdl.handle.net/1993/6

[160] Fischer, E. C.,Varma A. H.,Zhu Q. 2018. *Experimental evaluation of single-bolted lap joints at elevated temperatures,* Journal of Structural Engineering, 144(1), pp. 04017176. https://doi.org/10.1061/(ASCE)ST.1943-541X.0001911.

[161] EN_ISO898-1. 2013. Mechanical Properties of Fasteners Made of Carbon Steel and Alloy Steel, Part 1, Bolts, Screws and Studs with Specified, Property Classes, Coarse Thread and Fine Pitch Thread,Geneva,

[162] 2011. *ANSYS Mechanical APDL Element Reference*, ed. ANSYS,

[163] Jiang, B., Yam, M. C., Ke, K., Lam, A. C., Zhao, Q. 2020. *Block shear failure of S275 and S690 steel angles with single-line bolted connections,* Journal of Constructional Steel Research, 170, pp. 106068. https://doi.org/10.1016/j.jcsr.2020.106068

[164] Zoetemeijer, P. J. S. r.-.-. *Summary of the research on bolted beam-to-column connections (period 1978-1983)*. 1983, Delft: Stevin II Laboratory.

[165] Rex, C. O.,Easterling W. S. 2003. *Behavior and modeling of a bolt bearing on a single plate,* Journal of Structural Engineering, 129(6), pp. 792–800. https://doi.org/10.1061/(ASCE)0733-9445(2003)129:6(792)

[166] Yessad, O., Kada,A.,Lamri,B., Al-Jabri,K.,Waris,M,B.,Bouchair,A. 2025. *Modified Component-based Model for Single and Double-angle Bolted Connections Used in Braced Steel Frames at Elevated Temperature,* Periodica Polytechnica Civil Engineering, 69(3), pp. 1046–1061. https://doi.org/10.3311/PPci.40269

[167] Wald, F., Sokol, Z., Moal, M., Mazura, V., Muzeau, J. P. 2004. *Stiffness of cover plate connections with slotted holes,* Journal of Constructional Steel Research, 60(3), pp. 621-634. https://doi.org/10.1016/S0143-974X(03)00133-0

[168] Xie, B.,Hou J.,Xu Z.,Dan M. 2018. *Component-based model of fin plate connections exposed to fire-part II: Establishing of the component-based model,* Journal of Constructional Steel Research, 145, pp. 218-231. https://doi.org/10.1016/j.jcsr.2018.02.018

[169] 24.1, I. S. C.2024. *Product documentation*, 2024. [cited Access; Available from: https://www.ideastatica.com/support-center/release-notes-idea-statica-24-1

[170] 24.1, I. S. C.2024. *Member*, 2024. [cited Access; Available from: https://www.ideastatica.com/support-center/release-notes-idea-statica-24-1

[171] EN_1993-1-5. 2005. Eurocode3:design of steel structures- Part 1-5: Plated structural elements,European Committee for Standarization: Brussel, Belgium.

[172] Yessad, O., Kada,A.,Lamri,B.,Wald,F. 25-27 June 2025. *Fire design of bolted braced steel connections using component-based finite element method*. *International Fire Safety Symposium (IFireSS 2025) - 5TH Edition*. Ulster University Belfast,Northern Ireland,UK : https://doi.org/10.21251/03828a0d-6ceb-4fce-ba02-e93ccb60d4fc

ANNEX. Von mises stress distribution

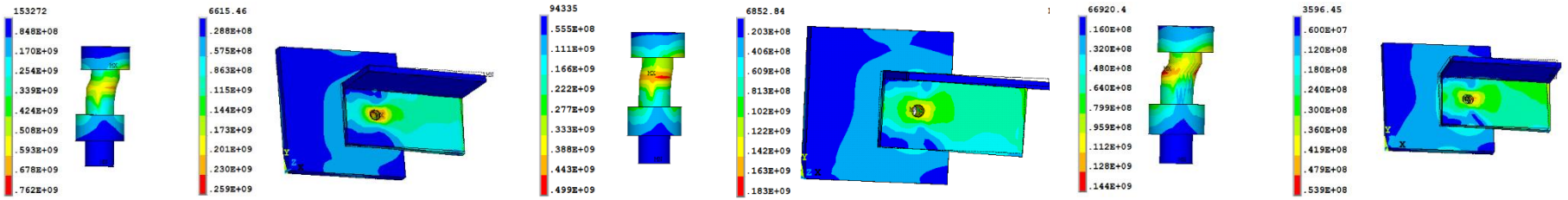

(a) Case 1 (8.8 bolts) for 20°C, 500°C and 700°C

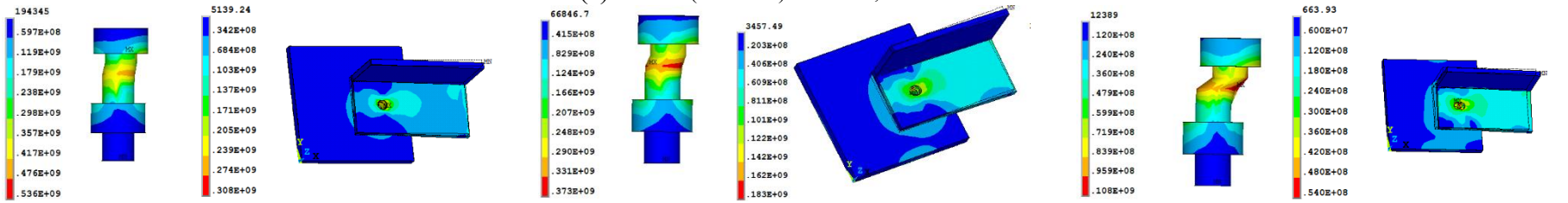

(b) Case 1 (6.8 bolts) for 20°C, 500°C and 700°C

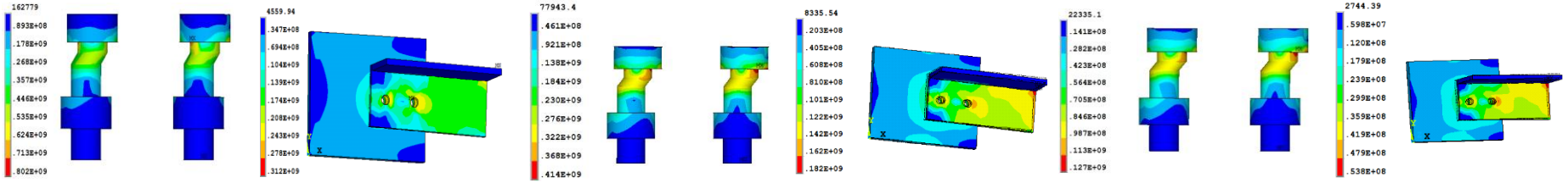

(c) Case 2 (8.8 bolts) for 20°C, 500°C and 700°C

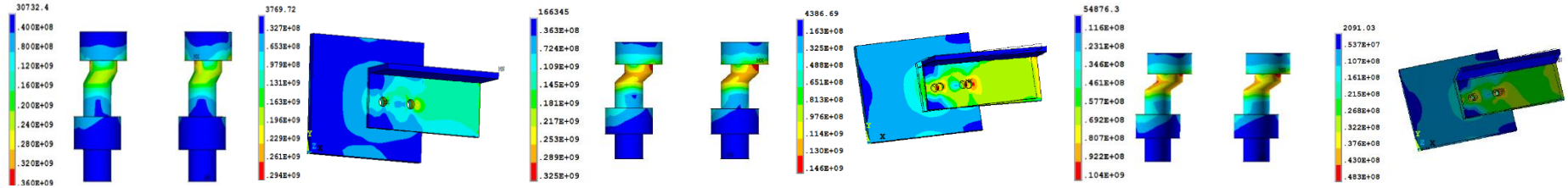

(d) Case 2 (6.8 bolts) for 20°C, 500°C and 700°C

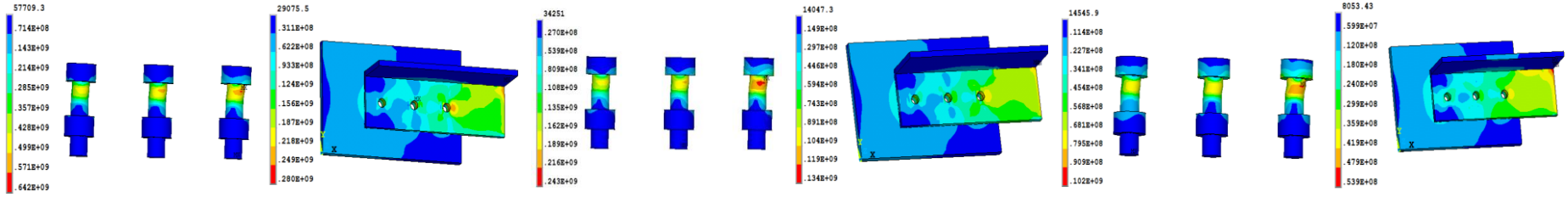

(e) Case 3 (8.8 bolts) for 20°C, 500°C and 700°C

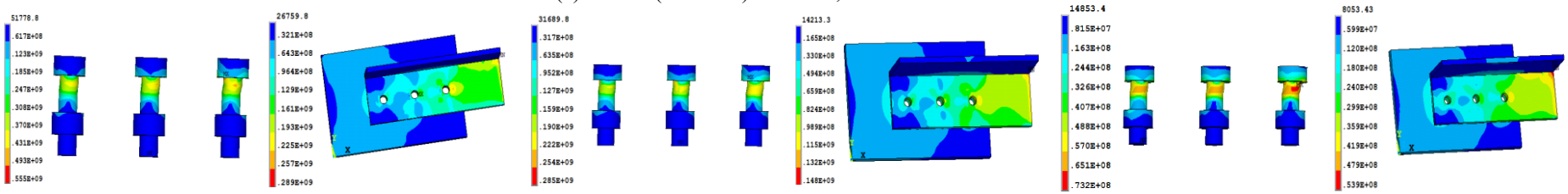

(f) Case 3 (6.8 bolts) for 20°C, 500°C and 700°C

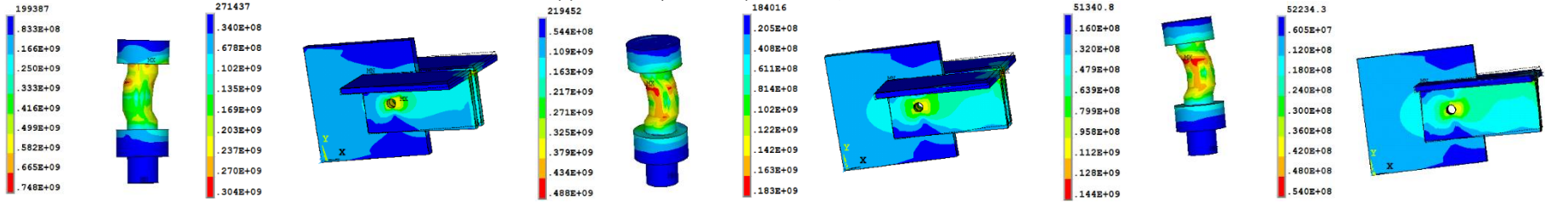

(g) Case 4 (8.8 bolts) for 20°C, 500°C and 700°C

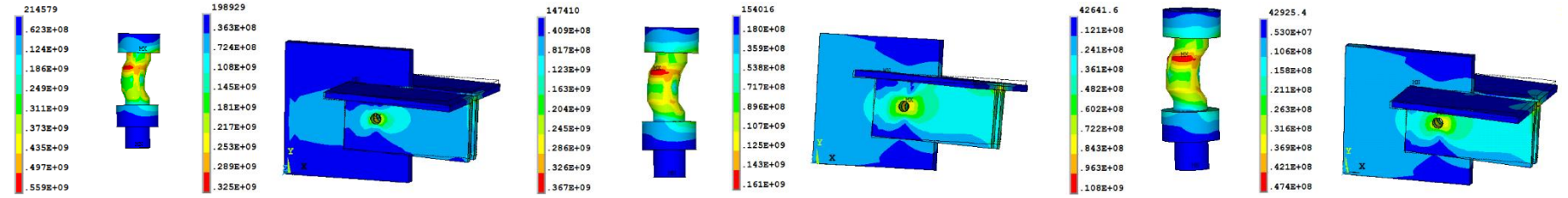

(h) Case 4 (6.8 bolts) for 20°C, 500°C and 700°C

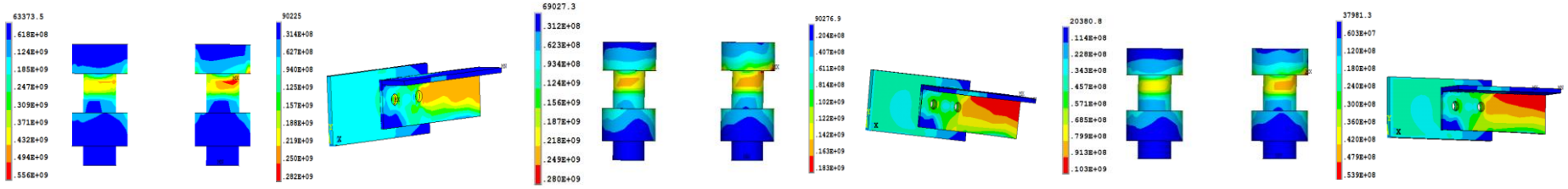

Case 5 (8.8 bolts) for 20°C, 500°C and 700°C

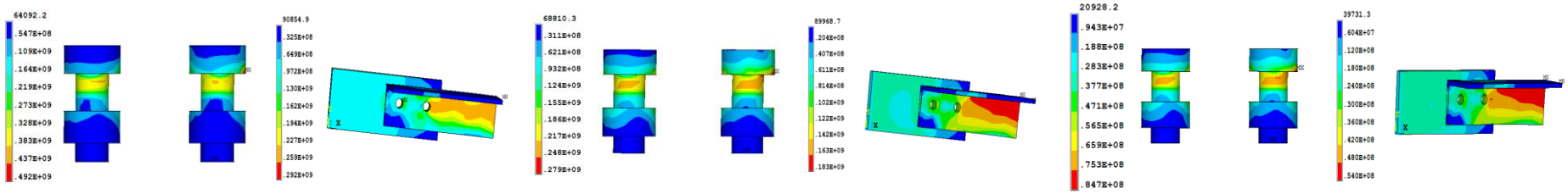

Case 5 (6.8 bolts) for 20°C, 500°C and 700°C

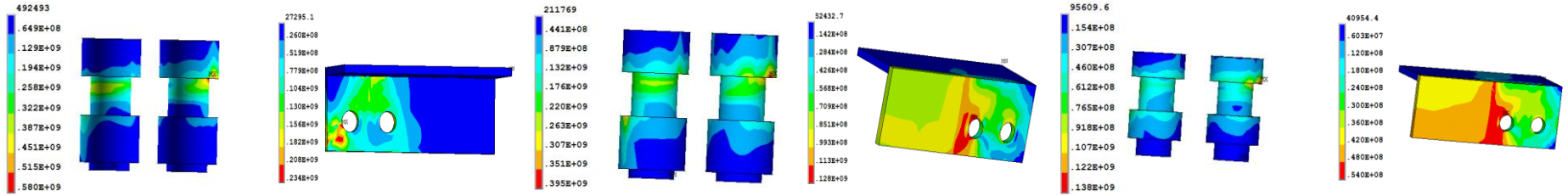

Case 6 (8.8 bolts) for 20°C, 500°C and 700°C

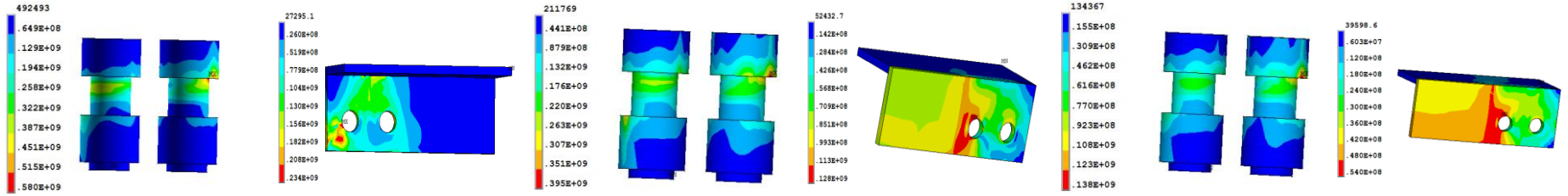

Case 5 (6.8 bolts) for 20°C, 500°C and 700°C